The Dissertation Committee for Archit Bharat Sanghvi certifies that this is the approved version of the following dissertation:

Phage Display Technology for Surface Functionalization of a Synthetic Biomaterial

Committee:

_____
Christine E. Schmidt, Supervisor

_____
George Georgiou

_____
Krishnendu Roy

_____
Wolfgang Frey

_____
Angela Belcher

Phage Display Technology for Surface Functionalization of a Synthetic Biomaterial

by

Archit Bharat Sanghvi, B.S.E.;M.S.E

Dissertation

Presented to the Faculty of the Graduate School of

The University of Texas at Austin

in Partial Fulfillment

of the Requirements

for the Degree of

Doctor of Philosophy

The University of Texas at Austin

August, 2005

Dedication

This dissertation is dedicated to my wife, Meera and my families

Swadhyay Parivar, Sanghvi, and Kothari.

Acknowledgements

The purpose of graduate school was a purpose full of discovery. Through this experience I was able to not only understand science, but more importantly myself. The years spent in graduate school were most important because of the many essential relationships I was able to build. Although not necessary, as he is always a part of me and within me, I want to thank God for giving me this wonderful life that is always full of happiness and challenges. I want to thank my Swadhyay Parivar in Austin, Texas given to me by Revered Pandurang Shastri Athavale for providing invaluable support above and beyond imagination. I want to thank my wife Meera for providing the most essential guidance and strength throughout the hardest part of the graduate work, writing and preparing for the dissertation. As she knows better than anyone else, these years in graduate school have provided experiences above and beyond research and education. I have been able to grow and develop many positive qualities during graduate school because of my experiences with her. I also want to thank both of my families, Sanghvi and Kothari. My parents, Bharat, Kanchan, Harkant and Panna, instilled in me the much strength and courage necessary throughout graduate school along with guidance to maintain my sanity. I also want to thank my sister, Mitali, who provided much needed laughter to help in diverting my stress as it occurred quite often.

Each and everyday my interactions in the Schmidt Laboratory were full of new understanding and learning about science and research. I would like to thank Dr. Christine Schmidt for giving this opportunity and providing the needed guidance for completion of various projects. Additionally, I would like to thank numerous people in the Schmidt lab including, Hyma, Terry, Jennie, Jessica, Curt, Kate, Kiko, Natalia, and Scott. It was because of the numerous interactions and discussions with the various lab members, the experience of graduate school was invaluable. Kiley P-H Miller, who co-authored in the Nat Mat manuscript was an intricate part of the project and contributed equally during the initial phase of the work. I want to also thank my committee members including Dr. Wolfgang Frey, Dr. Krishnendu Roy, Dr. George Georgiou, and Dr. Angela Belcher.

Phage Display Technology for Surface Functionalization of a Synthetic Biomaterial

Publication No._____

Archit Bharat Sanghvi, Ph.D.

The University of Texas at Austin, 2005

Supervisor: Christine E. Schmidt

The rapid growth in the use of synthetic polymers in medicine and biotechnology has prompted the development of advanced biomaterials that present unique surface properties to control cellular activity. To control the surface properties of biomaterials numerous methods have been developed for immobilization of biomolecules. The goal of this work was to develop a new method for surface functionalization of synthetic biopolymers using phage display technology. This approach has traditionally been utilized for both biological and non-biological materials to select peptides expressed on the bacteriophage using a combinatorial approach. As presented in this thesis chloride-doped polypyrrole (PPyCl) was used as a model biopolymer to screen for a peptide insert

selected from a combinatorial library with diversity of 10^9. A PPyCl-binding peptide (T59) was successfully identified using this phage display approach.

As a biomaterial, polypyrrole presents many unique opportunities in the field of biomedicine, specifically in tissue engineering, drug delivery and biosensor development. A peptide-expressing phage (ϕT59) that binds to PPyCl, when compared to other selected materials, was identified. Furthermore, the T59 peptide, independent of the phage, was synthesized and its binding ability and characteristics were analyzed using both qualitative and pseudo-quantitative analysis. Furthermore, the stability of the peptides in the presence of serum proteins was explored using indirect methods to compare to a control condition. Finally, we explored a potential application of the selected T59 peptides by attaching a cell-adhesion promoting sequence that permitted cell attachment on PPyCl surface without the presence of serum proteins. Although not directly shown here, this approach, which is highly versatile, simple and imparts not changes to the material's bulk properties, can potentially be applied to various biopolymers.

Table of Contents

List of Tables……xi

List of Figures……xii

Chapter 1: Introduction……...1

1.1 Tissue Engineering – Peripheral Nerve Regeneration……...1

1.2 Role of Polymeric Biomaterials in Tissue Engineering……4

1.3 Development of Bioactive and Biofunctional Materials……5

1.4 Conducting Polymers in Biomedicine – Polypyrrole……6

1.5 Phage Display……8

1.6 Overview of Dissertation……....10

1.7 References……21

Chapter 2: Characterization of Conducting Polymer – Polypyrrole……...……...29

2.1 Introduction……..29

2.2 Materials and Methods……34

2.2.1 Electrochemical synthesis of polypyrrole……..34

2.2.2 PPyCl surface morphology and chemistry characterization ……35

2.3 Results……..36

2.3.1 Evaluation of surface morphology using SEM and AFM……36

2.3.2 Evaluation of surface chemistry using XPS……...37

2.4 Discussion……38

2.5 References……47

Chapter 3: PPyCl-Specific Peptide Selection Using Phage Display……51

3.1 Introduction – Phage display technology …….52

3.2 Materials and Methods…….53

3.3 Results……..56

3.3.1 Peptide sequences identified via biopanning…….56

3.3.2 Phage amplification analysis……..…57

3.4 Discussion…….58

3.5 References…….67

Chapter 4: PPyCl-Specific Phage and Peptide Binding Analysis……..70

4.1 Introduction……..71

4.1.1 Characterization of ϕT59 and T59 peptide binding to PPyCl……71

4.1.2 Determining essential amino acids in T59 peptide in binding PPyCl…...72

4.1.3 Binding strength of T59 peptides to PPyCl using AFM……73

4.2 Materials and Methods…….75

4.2.1 Titer count analysis to study binding of ϕT59……...75

4.2.2 Immunofluorescence study of ϕT59/T59 peptide binding PPyCl…….76

4.2.3 Fluorescamine assay and XPS to study T59 peptide binding to PPyCl… 78

4.2.4 Atomic force microscopy analysis of T59 peptide and PPyCl……..81

4.3 Results……..84

4.3.1 Titer count analysis to evaluate specificity of ϕT59 to PPyCl……...84

4.3.2 Immunfluorescence evaluation of ϕT59 and T59 peptide binding……...85

4.3.3 The role of key amino acids in T59 peptide binding to PPyCl……..86

4.3.4 Atomic force microscopy to evaluate strength of interaction……88

4.4 Discussion……....90

4.5 References……..120

Chapter 5: Surface functionalization of PPyCl using T59 peptide……..125

5.1 Introduction……126

5.2 Materials and Methods……...128

5.2.1 T59 modification and PPyCl surface functionalization……...128

5.2.2 T59 peptide stability in the presence of serum proteins……..130

5.3 Results……....131

5.4 Discussion……..133

5.5 References……..141

Chapter 6: Conclusions and Recommendations……..144

6.1 Summary……144

6.2 Limitations……..145

6.3 Recommendations for Future Research……148

6.3.1 Developing a method to determine the mechanism of peptide interaction……148

6.3.2 Evaluate the *in vivo* stability and functionality of PPyCl-T59 peptide……..149

6.3.3 Use of phage display against other polymeric biomaterials……150

Bibliography……151

Vita……...168

List of Tables

Table 1.1 Synthetic polymeric biomaterials researched for bioengineering applications.12

Table 1.2 Surface modification methods for promoting bioactivity…….13

Table 1.3 Use of conductive polymers in biomedicine…….14

Table 3.1 Non-biological materials studied for phage-displayed peptide selection…..…59

Table 3.2 Amino acid distribution in native Ph.D.12^{TM} phage library……..…60

Table 4.1 T59 peptide variants……...92

Table 4.2 Properties of the charged amino acids in T59 peptide……...93

Table 4.3 AFM measurements on biomolecular forces with varying binding partners….94

Table 4.4 Amino acid distribution in native Ph.D. 12 phage library……..…95

List of Figures

Figure 1.1 Commonly studied paradigm for tissue engineering……15

Figure 1.2 The Nervous System……16

Figure 1.3 Nerve Tissue Degeneration……..17

Figure 1.4 Various properties of a nerve conduit……..18

Figure 1.5 Chemical structure of polypyrrole……...19

Figure 2.1 Mechanism of polypyrrole polymerization……..….39

Figure 2.2 PPyCl electrochemical synthesis apparatus ……40

Figure 2.3 SEM micrographs of PPyCl…….41

Figure 2.4 Atomic force microscopy image of PPyCl……...…42

Figure 2.5 XPS survey spectrum of PPyCl……...….43

Figure 2.6 Variable carbon linkages in PPy…….……..44

Figure 2.7 XPS C1s Spectrum of PPyCl……45

Figure 3.1 Biopanning with Ph.D.-12 peptide library……...61

Figure 3.2 Peptide sequences acquired from biopan rounds 3-5……...…62

Figure 3.3 A peptide sequence binding to PPyCl determined from analysis…….....63

Figure 3.4 Amplification rates of T59 phage compared to WT phage……..64

Figure 4.1 Illustration of the Au-coated Si_3N_4 cantilever and functionalized tips…….96

Figure 4.2 ϕT59 binding to PPyCl compared to the binding of random phage.……97

Figure 4.3 ϕT59 binding is relatively specific to PPyCl……98

Figure 4.4 T59 phage, compared to a random phage, uniquely binds to PPyCl……....99

Figure 4.5 T59 binds to PPyCl and not to PPyPSS or to polystyrene (PS)……...100

Figure 4.6 Relative binding of T59 and variants using fluorescamine assay……101

Figure 4.7 Relative binding of T59 variants to PPyCl with respect to T59 peptides…..102

Figure 4.8 Role of Asp confirmed by varying pH study of T59 peptide……...…..103

Figure 4.9 pH 2 elution of T59 peptides from PPyCl…….104

Figure 4.10 XPS surface scan analysis of PPyCl to detect binding of T59 peptides….105

Figure 4.11 Relative binding strength evaluation of T59 peptides to PPyCl…….106

Figure 4.12 Illustration of a typical force plot of T59-PPyCl……..107

Figure 4.13 Illustration of a typical force plot of streptavidin-biotin interactions…..…108

Figure 4.14 Illustration of a typical force plot of a blank tip and PPyCl surface……109

Figure 4.15 Illustration of a typical force plot of a streptavidin-coated tip and PPyCl...110

Figure 4.16 Illustration of a typical force plot of GRGDS peptide-coated tip and PPyCl……111

Figure 4.17 Illustration of a typical force plot of T59-GRGDS peptide-coated tip and PPyCl……112

Figure 4.18 Dynamic force spectroscopy loading rate variation study of PPyCl-T59 interactions……..……...……113

Figure 4.19 Plot of F vs.ln r, loading rate dependenc e on T59-PPyCl interactions……114

Figure 5.1 T59 peptide modified with GRGDS promotes PC12 cell adhesion in serum-free environment…….……...128

Figure 5.2 Functionalization study of PPyCl surface using T59 peptide complexed with GRGDS and the stability of T59 peptide binding to PPyCl……..129

Figure 5.3 Qualitative images of PPyCl-bound T59 peptides after serum incubation for various time points, suggesting stability in binding……...130

Figure 5.4 T59 peptide binding to PPyCl is stable in the presence of serum proteins with an approximate lost of 15% after 21 days……..…131

Chapter 1: Introduction

1.1 TISSUE ENGINEERING – PERIPHERAL NERVE REGENERATION

The potential and ability to treat tissue loss or end-stage organ failure is a primary focus of medical research today. There have been many strategies developed over the years to repair or regenerate tissues including organ transplantation, autologous tissue replacement, and replacement using external and internally implanted mechanical devices. Although these strategies have been implemented for many years, the results have been partially successful as the failure of these therapeutic options still remains. To address the growing need for developing treatments for tissue loss and organ failure, tissue engineering has provided new solutions to these problems, where a group of interdisciplinary researchers ranging from molecular biologists and physicists to engineers and clinicians are working to produce new technologies.

Typically, tissue engineering involves the use of cells seeded on or within a scaffold for cell proliferation and differentiation [1,2] (**Figure 1.1**). Additional components present in many strategies include cell adhesion promoting molecules (e.g., laminin, RGD peptides, etc.), growth factors, drugs, and other signaling molecules specific to the tissue being studied [4]. This strategy for tissue repair and regeneration has been researched since the 1960s for applications in the skeletal system, cardiovascular system, organs such as heart, skin, and sensory organs cochlea and nerves. There are numerous devices (e.g., coronary stents, hip and knee prostheses, dental implants, catheters, vascular grafts, etc.) available today, but this is till a nascent field with

significant needs for development of new materials and strategies for solving many of the complex issues with tissue regeneration. As highlighted by Ratner, et al., the holy grail of tissue engineering is to design a way to replace function to damaged tissue with similar tissue components that contain the appropriate functionality including cells and extra-cellular matrix [5].

This has prompted research efforts in developing novel methods to use biomaterials tailored for controlling and guiding new tissue growth. One particular tissue being researched in our lab is peripheral nerve. The ultimate goal is to develop a device that has the necessary material properties for guided neurite growth and subsequent reinnervation resulting in complete functionality.

The current strategies for peripheral nerve (**Figure 1.2**) tissue engineering rely primarily on either end-to-end anastomosis or grafts (e.g., autologous nerve or vein grafts) to bridge the severed nerve ends [6]. Short gap repair has shown success with end-to-end reconstruction. However, this technique is limited by the tension introduced into the nerve cable when the nerve ends are reconnected, which can inhibit nerve regeneration. The use of autologous nerve grafts addresses the problems associated with end-to-end reconstruction, but there exist some limitations including incomplete regeneration and the possibility of irreversible damage [7]. In addition, there are other disadvantages associated with the use of autologous grafts, including loss of function at the donor site, the inability to directly match the size of the donor nerve to the injured nerve, and the need for multiple surgeries. The shortcomings of the current clinical

methods have resulted in the search for engineering methods to regenerate and repair peripheral nerve defects. One such technique is the development of a synthetic guide that provides an optimal physical and chemical environment to enhance peripheral nerve repair. As depicted in **Figure 1.3**, when the nerve damaged the two nerve ends, distal and proximal (near the cell body), separate and degeneration of the distal part occurs along with demyelination [6]. By using a nerve guide with specific and controlled properties, reinnervation of the two ends can occur with the ultimate goal of achieving complete recovery and functionality.

Several physical properties of the guidance channel appear to dramatically affect the extent and quality of regeneration. Some of these properties, depicted in **Figure 1.4**, include porosity, biodegradability, cell encapsulation and oriented extracellular matrix components in inner luminal compartment, and inherent electrical properties [8]. Conduits may swell *in vivo*, thus the conduit dimensions need to be large enough to allow for swelling without inhibiting axonal growth. The walls of the conduit should be sufficiently porous to allow nutrients to freely flow, but the pores should be small enough to exclude inflammatory cells. The ideal guidance channel would be composed of a material that maintains its physical integrity long enough for the nerve to fully regenerate, but eventually degrades leaving only natural tissue. It is believed that regeneration distance can be increased by the optimum combination of guidance channel materials and growth factors and/or support cells in the conduit lumen [8].

1.2 ROLE OF POLYMERIC BIOMATERIALS IN TISSUE ENGINEERING

One of the most important components of tissue engineered devices is the material, specifically its properties including biocompatibility, degradability, and mechanical strength for particular applications. After numerous years of research, there have been many biocompatible materials identified that are divided into metals, ceramics, polymers and natural materials (derived from both plants and animals) [9]. In the selection and subsequent development of tissue engineered devices using scaffolds, biocompatibility and biodegradability have been given initial preference. For this reason, recently biomaterials scientists and engineers have focused more in natural tissues and synthetic polymeric materials for engineering therapies (**Table 1.1**).

The rapid growth in the use of synthetic polymers in medicine and biotechnology has prompted the development of advanced biomaterials that display both biocompatible and bioactive properties. A large variety of biological functions could be programmed into materials including ligands that bind cellular receptors, drugs for targeted delivery, enzymes to catalyze reactions, vectors for gene therapy, and antibodies for detection or binding. Materials modified with these factors could be used in tissue regeneration applications, biosensors, diagnostic assays, drug delivery devices, bioreactors and separation systems, and medical implants [10]. In particular, we are interested in new classes of materials that can be designed to control cell behavior and to direct tissue formation via desired biomolecular recognition events.

Many existing biomaterials possess inadequate properties such as nonspecific interactions, which yield unpredictable outcomes [11]. The choice of a biomaterial for a particular application is often dictated by bulk properties such as strength, wear resistance, flexibility, porosity, and compliance. It is equally important to select biomaterials for specific surface properties because surface chemistry and structure are directly responsible for cell and tissue responses. Thus, the goal in surface modification is to retain bulk properties while modifying only the surface to possess desired functional groups that impart recognition and specificity.

1.3 DEVELOPMENT OF BIOACTIVE AND BIOFUNCTIONAL MATERIALS

Surface modification techniques are classified into two general categories: (1) chemical or physical alteration of the existing surface layer and (2) coating of existing surfaces to present a new component [11]. For both categories there are basic principles that must be followed for a successful modification of a desired surface. These principles include controlled thickness of components modifying the surface to maintain the mechanical and functional properties of the material. Additionally, surface-modified layers should not be prone to delamination in solution, they should resist drifting due to diffusion of surface atoms in response to external environment. The ideal modification method should enable control over functional groups presented on the surface with uniform organization [12].

Ultimately, surface modification techniques should provide an inherent flexibility to permit changes in molecular design for a broad range of applications and should be simple and straightforward to implement. There have been many techniques used to modify the surfaces of biomaterials, including protein adsorption and self-assembly [13], synthesis of novel graft-copolymers with desired functional groups [14,15], and direct covalent surface modifications [16-18] (**Table 1.2**). However, these approaches have limitations associated with them. Covalent surface modification and the synthesis of new materials both require extensive chemical reactions and processing. Protein adsorption, on the other hand, does not require chemical processing, but unfortunately is largely dependent upon nonspecific interactions between the protein and the surface, and therefore, is difficult to control [13]. Additionally, other techniques have promoted cellular interactions using covalently immobilized peptides, thereby promoting neurite extension [19]. PEG modification and silanization of surfaces, such as titanium oxide, have provided active surfaces for extracellular matrix binding domain Arg-Gly-Asp (RGD) immobilization to design biomimetic materials [14,20]. However, these approaches require complicated and multi-step pathways and peptide attachment is often limited by the lack of control over biomolecule density.

1.4 CONDUCTING POLYMERS IN BIOMEDICINE – POLYPYRROLE

Originally when conducting polymers were first discovered in 1976 the primary use was in the fields of chemistry and electronics. These materials permitted the

advantageous electrical and optical properties associated with metals and semiconductors to be combined with the attractive properties of polymers, such as control over processibility and mechanical properties. As their unique electrical and optical properties were researched and characterized, their use began to diversify and researchers in the field of biomedicine began to test out these materials [21-29] (**Table 1.3**).

The use of polymeric biomaterials in the field of tissue engineering has advanced rapidly over the past decade. One synthetic polymer, polypyrrole (PPy), has shown great promise, especially for enhancing nerve regeneration because of its electrical properties [28]. Previous work with oxidized PPy (**Figure 1.4**), which is a polycationic conducting polymer, demonstrated the ability to synthesize thin films using electrochemical synthesis for *in vitro* studies in controlling cell behavior [28,30]. These studies demonstrate that electroconductive PPy can support the growth and differentiation of neurons and endothelial cells [28,30]. PPy, when electrically stimulated, results in nearly a two-fold enhancement of neurite outgrowth from PC-12 cells (i.e., a neuron-like cell line) compared to unstimulated controls. *In vivo* studies have also demonstrated that PPy is not cytotoxic and that this material, when formed into conduits, can support the regeneration of damaged peripheral nerves in rats [31]. The ability to translate the *in vitro* results into *in vivo* applications has required numerous efforts in developing methods to incorporate PPy material into conduit systems.

Recent efforts have focused on developing nerve conduits from biomaterials that not only provide a physical guide, but also actively enhance nerve growth. Polypyrrole

has been highlighted as one of the more suitable materials for this application because of its biocompatibility and flexibility in processing [31]. The focus of this recent work in Christine Schmidt's Laboratory (University of Texas at Austin) for the development of nerve regeneration therapies has successfully shown enhanced neurite outgrowth of cells on polypyrrole under electrical stimulation [28].

1.5 PHAGE DISPLAY

Bacteriophage display of peptides, or phage display, consists of a library of viruses (or bacteriophages) that are genetically engineered so that each virus displays a random single peptide, of specific length, on a portion of the virus' protein coat. In creating bacteriophage libraries, researchers have used genetic engineering techniques to incorporate a random amino acid sequence on the minor coat protein (pIII) or on the major coat protein (pVIII) of a filamentous virus or bacteriophage. There exist commercially-available libraries (New England Biolabs, Inc.) that express linear peptides of different lengths (e.g., 12 amino acids, 7 amino acids) on the pIII of the M13 bacteriophage that can be used for the screening of numerous non-biological materials ranging from semiconductor materials to metals [32-37]. In addition, there also exist "constrained" amino acid libraries, in which the peptides are presented or displayed as "loop" structures (i.e., cysteines are found at the 1st and 9th positions on the peptide to create a loop by a disulfide linkage).

Phage display libraries can be used to screen tens of millions of different peptide inserts against a substrate of interest, in a process referred to as "biopanning". Application of phage display for peptide selection has ranged from antibody-antigen binding studies, mapping of protein-protein contacts, and the identification of receptor ligands [38,39]. This approach has also been used to select for bioactive peptides for the immobilization of purified thrombin receptors as well as for intact cells [40,41]. Smith et al. used phage display to identify protease substrates by attaching an affinity insert prior to the randomized region to separate cleaved from the uncleaved phage [42]. Conversely, other investigators have used phage display to isolate antibodies, hormones, and DNA binding proteins from their variants with altered affinity or specificity from libraries of random mutants [43]. Another use of peptide phage display is to determine a peptide binding motif for a synthetic material to which nature has presumably not had a chance to evolve such an interaction. These types of attachments are being investigated for semiconductor crystalline materials such as InP, ZnS, CdS and GaAs [32,33].

In the work presented here, we have used phage display to select for a unique peptide sequence against polypyrrole. A peptide was selected against PPyCl and its binding was demonstrated. To our knowledge, phage display has never been used for direct applications in developing biofunctional polymers, and would provide a significant contribution to the biomaterials field. Although this approach can be applied to other polymers, this was not directly demonstrated in this thesis. As a candidate, polypyrrole presents two important criteria including the lack of a functional group (e.g., COOH,

NH_2) for direct surface modification and its versatile use in biomedicine and tissue engineering. Using a commercially available phage display library, as material-specific peptides are identified, any biomolecule or cell can potentially be immobilized in order to functionalize biomaterials. Although tissue engineering is our primary focus, this technology can potentially be applied to multiple areas including drug delivery and biosensor development.

1.6 OVERVIEW OF DISSERTATION

This dissertation is organized into five chapters. The overall focus of this work is to develop a novel method for surface functionalizing a synthetic biopolymer, polypyrrole, using phage display-selected peptides. In **Chapter 2**, the use and characterization of polypyrrole is described with focus on synthesis and surface analysis. PPy is a versatile biopolymer that has numerous applications in fields such as drug delivery [23] and nerve regeneration [28], and has been used in biosensors and coatings for neural probes [29]. General electrochemical synthesis method, for chlorine-doped polypyrrole (PPyCl), was used to synthesize thin films for phage display screening. The thin films were characterized in terms of thickness, surface morphology, and surface chemistry. PPyCl characterization results were used for comparison to previously published results and enabled us to develop controlled synthesis conditions for quality control.

In **Chapter 3**, we describe the phage display selection process for peptide selection against PPyCl. A unique phage-displayed peptide (ϕT59) against PPyCl was selected. Detailed characterization of the phage binding is presented. Specifically, amplification and competitive studies along with immunolabeling results are illustrated. The selected phage demonstrated selective binding to PPyCl when compared to other phage and substrates.

These results were expanded and researched further in **Chapter 4**, where the binding of the corresponding peptide ('T59') without the presence of the phage was assessed. Both qualitative and quantitative analysis were performed to assess the actual binding and surface coverage. A pseudo-quantitative assay for relative surface coverage analysis was established and used in detailed studies for determining the mechanism of interaction between T59 and PPyCl. By synthesizing variants of T59 peptide, an initial mechanism of interaction between T59 and PPyCl is determined. The results suggested involvement of the C-terminal end as the active site for PPyCl recognition. Furthermore, strength of interaction using dynamic force spectroscopy techniques are also described in which T59-PPyCl binding strength was compared to relatively weak antigen-antibody interactions.

In **Chapter 5**, steps towards application were established where T59 synthesized with RGD peptides (integrin-binding cell adhesion promoting peptides) resulted in nerve cell adhesion and differentiation. PPyCl surface was modified with T59 peptides synthesized with RGD at the C-terminus, followed by cell incubation. We found that

when RGD is presented on PPyCl through T59 peptides, PC12 cell adhesion was promoted when compared to controls. These initial studies indicated that T59 peptides can be used as bi-functional linkers for surface modification in tissue engineering applications.

In **Chapter 6**, a summary of the results from the highlighted studies is presented. Furthermore, we have summarized the analysis and conclusion of the results along with limitations and recommendations for future work.

Table 1.1 Synthetic polymeric biomaterials researched for bioengineering applications

Material	**Application**	**Reference**
Poly(glycolide-lactide) (PLGA)	Drug delivery Sutures	[44,45]
Poly(ethylene glycol) (PEG)	Orthopedic Drug Delivery	[46,47]
Polyanhydrides	Drug delivery	[48]
Poly(propylene fumarate) (PPF)	Orthopedic	[49]
Polycaprolactone (PCL)	Drug delivery, Stents	[50,51]
Poly(methyl methacrylate) (PMMA)	Bone	[52]

* This list is illustrative rather than exhaustive adapted from [9].

Table 1.2 Surface modification methods for promoting bioactivity

Modification method	**Example of materials**	**Reference**
Chemical reaction - oxidation	Titanium	[53]
Plasma-treatment	Poly(ethylene glycol)	[54]
Silanization	Glass surface	[55]
Langmuir-blodgett deposition	Polyurethane	[56]
Self-assembled monolayer	Gold	[57]
Laser treatment	Hydroxyapatite	[58]
Lithographic patterning	Poly(ethylene glycol)	[59]

* This is an illustrative rather than exhaustive list.

Table 1.3 Use of conductive polymers in biomedicine

Application	**Reference**
Biosensing devices	[21-22]
Drug delivery	[23]
Prosthetics	[24]
Cell manipulation	[25-28]
Neural Probes	[29]

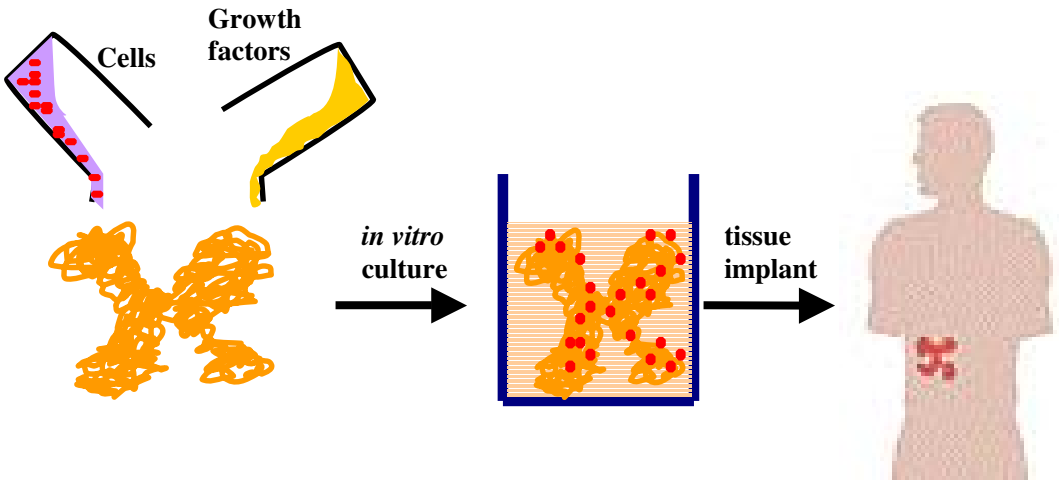

Figure 1.1 Commonly studied paradigm for tissue engineering. Development of engineered organs and tissues using the principles of tissue engineering. A scaffolding material is seeded with specific cells related to the tissue being engineered. Additionally, growth factors and biomolecules are incorporated for signaling and growth. The cells attach to the matrix and through cellular processes extracellular matrix is deposited with the simultaneous degradation of the scaffolding material. A key property of the scaffolding material is the surface characteristic as it is the determining factor in cellular activity. For most tissues the biological complexity and mechanical properties are achieved prior to implanting into a patient (*in vitro*) to mimic the naturally occurring tissues. Adapted from [3].

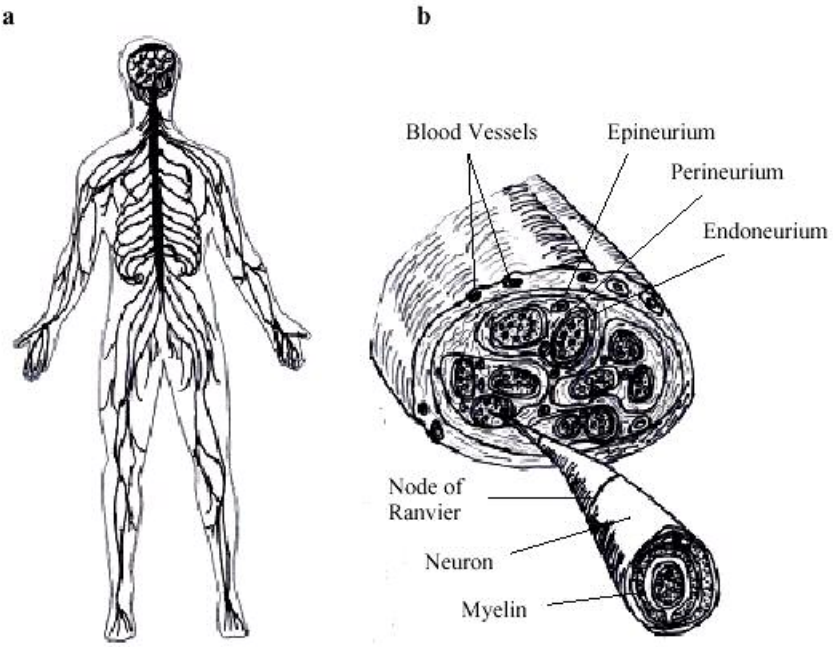

Figure 1.2 The Nervous System a) The central nervous system (CNS) includes the brain and spinal cord. The peripheral nervous system (PNS) contains two main pathways (afferent and efferent) and connects the CNS to other parts of the body. b) Shows enlarged segment of a nerve bundle that is arranged to present the relationship of the axons to the Schwann cells and connective tissue organization. Drawings from [6].

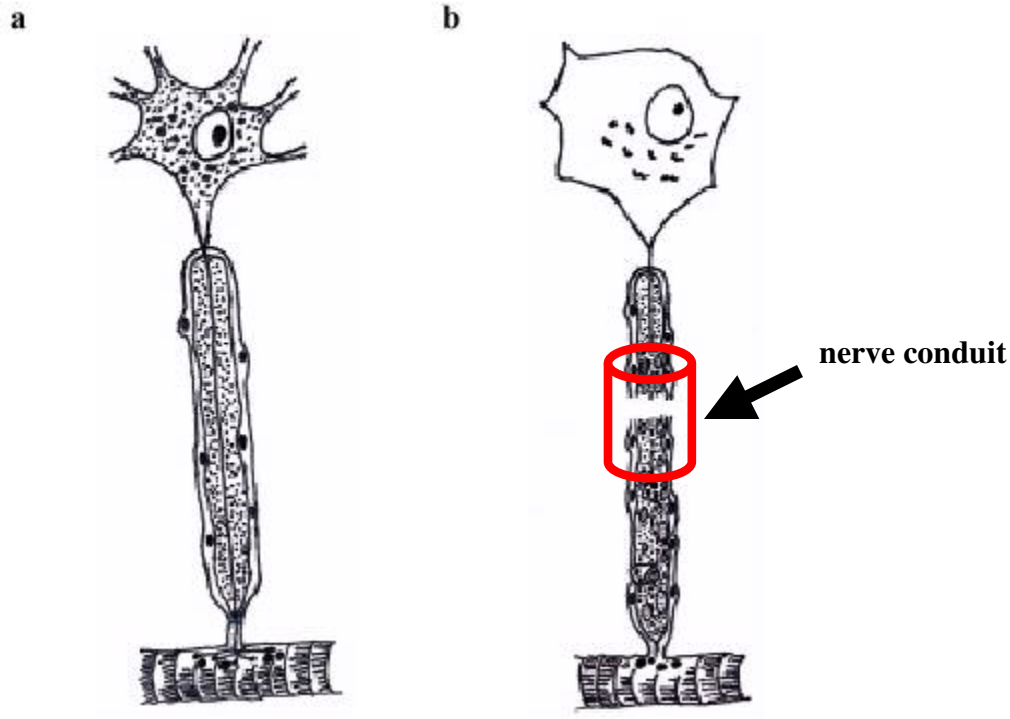

Figure 1.3 Nerve Tissue Degeneration (a) An intact nerve fiber that innervates skeletal muscle cell showing the position of the nucleus within the cell's body. b) The distal end of the axon becomes injured leading to fragmented segments. After injury, the nucleus moves to the cell periphery and degeneration of the distal part occurs along with demyelination. As indicated regeneration can be achieved if a guidance tube is inserted to reconnect the two ends with an optimal growth environment. Drawing from [6].

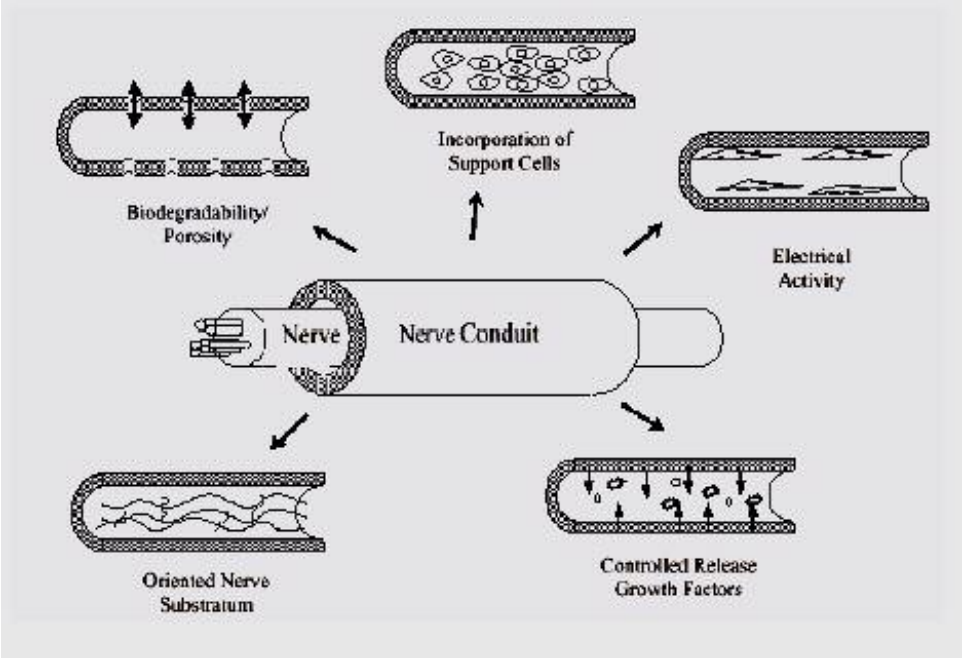

Figure 1.4 Various properties of a nerve conduit. Areas of active research involving a nerve conduit include (clockwise from top left): (1) biodegradability or a porous channel wall, or both; (2) the inclusion of support cells; (3) electric activity; (4) the release of growth promoting molecules; (5) the inclusion of internally oriented matrices. Drawing adapted fro m [8].

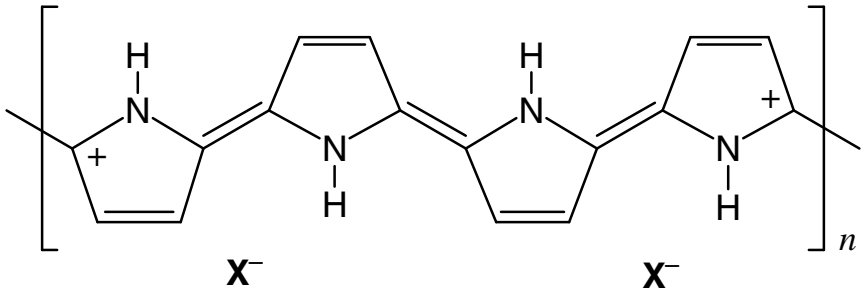

Figure 1.5 Chemical structure of polypyrrole. Structural representation of polypyrrole (PPy). X^- represents the specific dopant ion (e.g., Cl^-, ClO^{-4}, NO^{3-}, PSS^-) and *n* is the number of repeat units in the polymer.

1.7 REFERENCES

1. Saltzman MW. *Tissue engineering: principles for the design of replacement organs and tissues*. 2004, Oxford University Press: New York.
2. Lanza RP. *Principles of tissue engineering.* 2000, Academic Press: San Diego.
3. http://www.ptei.org/techniques.asp. (*accessed* March 2005).
4. Langer R, Vacanti JP. Tissue engineering. *Science* 1993; 260:920-6.
5. Ratner BD, Bryant SJ. Biomaterials: where we have been and where we are going. *Annu Rev Biomed Eng* 2004;6:41-75.
6. Sanghvi AB, Murray JL, Schmidt CE. Tissue engineering of peripheral nerve. In: Wnek GE, Bowlin, GL., editors. *Encyclopedia of biomaterials and biomedical engineering*: New York: 2004.
7. Furnish EJ, Schmidt, CE. Tissue engineering of the peripheral nervous system. In: Patrick CW Jr., editor. *Frontiers in Tissue Engineerin*g: New York; 1998.
8. Hudson T, Evans GR, Schmidt C. Engineering strategies for peripheral nerve repair. *Clinics in Plastic Surgery* 1999;*26*(4):617-28.
9. Ratner BD, Hoffman AS, Schoen FJ, Lemons JE. *Biomaterials science: an introduction to materials science in medicine*. 2004, Academic Press: Boston.
10. Healy K. Molecular engineering of materials for bioeactivity. *Curr. Opn. Sol. Sta. & Mater. Sci*. 1999;4:381-387.
11. Ratner BD. Surface modification of polymers: chemical, biological and surface analytical challenges. *Biosensors & Bioelectronics* 1995;10:797-804.

12. Healy KE, Rezania A, Stile RA. Designing biomaterials to direct biological responses. *Ann N Y Acad Sci* 1999;875:24-35.
13. Zhang S, Altman M. Peptide self-assembly in functional polymer science and engineering. *Reac & Func Polym* 1999;41:91-102.
14. Quirk R, Chan W, Davies M, Tendler S, Shakesheff K. Poly(L-lysine)- GRGDS as a biomimetic surface modifier for poly(lactic acid). *Biomaterials* 2001;22:865-72.
15. Hrkach J, Ou J, Lotan N, Langer R. Poly (L-lactic acid-co-amino acid) graft copolymers. *J Mater Sci Res* 1999;78:92-102.
16. Cook AD, Pajvani UB, Hrkach JS, Cannizzaro SM, Langer R. Colorimetric analysis of surface reactive amino groups on poly(lactic acid-co-lysine):poly(lactic acid) blends. *Biomaterials* 1997;18(21):1417-24.
17. Kubies D, Rypacek F, Kovarova J, Lednicky F. Microdomain structure in polylactide-block-poly(ethylene oxide) copolymer films. *Biomaterials* 2000;21(5):529-36.
18. Hirano BY, Mooney DJ. Peptide and protein presenting materials for tissue engineering. *Advanced Materials* 2004;16(1):17-25.
19. Tong YW, Shoichet MS. Peptide surface modification of poly(tetrafluoroethylene-co-hexafluoropropylene) enhances its interaction with central nervous system neurons. *J Biomed Mat Res* 1998;42(1):85-95.
20. Xiao SJ, Textor M, Spencer N. Covalent attachment of cell-adhesive, (Arg-Gly Asp)- containing peptides to titanium surfaces. *Langmui*r 2000;14(19):5507-16.

21. Vidal JC, Garcia E, Castillo JR. In situ preparation of a cholesterol biosensor: entrapment of cholesterol oxidase in an overoxidized polypyrrole film electrodeposited in a flow system: Determination of total cholesterol in serum. *Anal. Chim. Acta.* 1999;385:213-222.

22. Campbell TE, Hodgson AJ, Wallace GG. Incorporation of Erythrocytes into Polypyrrole to Form the Basis of a Biosensor to Screen for Rhesus (D) Blood Groups and Rhesus (D) Antibodies. *Electroanalysis* 1999;11:215-222.

23. Konturri K, Pentti P, Sundholm G. Polypyrrole as a model membrane for drug delivery. *J Electroanal Chem* 1998;453:231-38.

24. George PM, Lyckman AW, LaVan DA, Hedge A, Leung, Y, Avasare R, et al. Fabrication and biocompatibility of polypyrrole implants suitable for neural prosthetics. *Biomaterials* 2005; 26:3511-19.

25. Valentini RF, Vargo TG, Gardella JA, Aebischer P. Electrically conductive polymeric susbtrates enhance nerve fibre outgrowth in vitro. *Biomaterials* 1992;13:183-190.

26. Garner B, Georgevich B, Hodgson AJ, Liu L, Wallace GG. Polypyrrole-heparin composites as stimulus-responsive substrates for endothelial cell growth. *J Biomed Mater Res* 1999;44:121-29.

27. Castano H, O'Rear EA, McFetridge PS, Sikavitsas VI. Polypyrrole thin films formed by admicellar polymerization support the osteogenic differentiation of mesenchymal stem cells. *Macromol Biosci* 2004;4:785-94.

28. Schmidt CE, Shastri VR, Vacanti JP, Langer R. Stimulation of neurite outgrowth using an electrically conducting polymer. *Proc Nat Acad Sci USA* 1997;94(17):8948-53.

29. Cui X, Hetke JF, Wiler JA, Anderson DJ, Martin DC. Electrochemical deposition and characterization of conducting polymer polypyrrole/PSS on multichannel neural probes. *Sensors and Actuators A: Physical* 2001;93:8-18.

30. Wong JY, Langer R, Ingber DE. Electrically conducting polymers can noninvasively control the shape and growth of mammalian cells. *Proc Natl Acad Sci U S A*. 1994;91:3201-4.

31. Rivers TJ, Hudson TW, Schmidt CE. Synthesis of a novel, biodegradable electrically conducting polymer for biomedical applications. *Advanced Functional Materials* 2002;12:33-7.

32. Whaley SR, English DS, Hu EL, Barbara PF, Belcher AM. Selection of peptides with semiconductor binding specificity for directed nanocrystal assembly. *Nature* 2000;405:665-68.

33. Flynn CE, et al. Synthesis and organization of nanoscale II VI semiconductor materials using evolved peptide specificity and viral capsid assembly. *J Mater Chem* 2003;13:2414-21.

34. Mao C, et al. Viral assembly of oriented quantum dot nanowires. *Proc Natl Acad Sci* 2003;12: 6946-51.

35. Sano K, Shiba K. A hexapeptide motif that electrostatically binds to the surface of titanium. J *Am Chem Soc* 2003;125: 14234-35.

36. Adey NB, Mataragnon AH, Rider JE, Carter JM, Kay BK. Characterization of phage that bind plastic from phage-displayed random peptide libraries. *Gene* 1995;156: 27-31.

37. Sarikaya M, Tamerler C, Schwartz DT, Baneyx F. Materials assembly and formation using engineered polypeptides *Annu Rev Mater Res* 2004;34:373–408.

38. Scott JK, Hoess R, Jackson S, Degrado W. Bioactive peptides identification by panning against immobilized purified receptor*s. Proc Natl Acad Sci* 1992;89:5398-5402.

39. Devlin JJ, Panganiban LC, Devlin PE. Random peptide libraries: a source of specific protein binding molecule*s. Scienc*e 1990;249:404-6.

40. Doorbar J, Winter G. Isolation of a peptide antagonist to the thrombin receptor using phage displa*y. J Mol Biol* 1994;244:361-9.

41. Barry MA, Dower WJ, Johnston SA. Toward cell-targeting gene therapy vectors: selection of cell-binding peptides from random peptide-presenting phage librarie*s. Nature Medicin*e 1996;2:299-305.

42. Smith MM, Shi L, Navre M. Rapid identification of highly active and selective substrates for stromelysin and matrilysin using bacteriophage peptide display librarie*s. J Biol Chem* 1995;270:6440-9.

43. Parmley SF, Smith GP. Antibody-selectable filamentous fd phage vectors: affinity purification of target gene*s. Gen*e 1988;73:305-18.

44. Prabhu S, Sullivan JL, Betageri GV. Comparative assessment of in vitro release kinetics of calcitonin polypeptide from biodegradable microspheres. Drug Deliv. 2002;9:195-8.

45. Cutright DE, Beasley JD, Perez B. Histologic comparison of polylactic and polyglycolic acid sutures. Oral Surg. 1971;32:165.

46. Bryant SJ, Bender RJ, Durand KL, Anseth KS. Encapsulating chondrocytes in degrading PEG hydrogels with high modulus: engineering gel structural changes to facilitate cartilaginous tissue production. Biotechnol Bioeng. 2004;30:747-55.

47. Das GS, Rao GH, Wilson RF, Chandy T. Colchicine encapsulation within poly(ethylene glycol)-coated poly(lactic acid)/poly(epsilon-caprolactone) microspheres-controlled release studies. Drug Deliv. 2000;7:129-38.

48. Zhang T, Gu M, Yu X. Degradation and drug delivery properties of poly(1,4-cyclohexanedicarboxylicanhydride). J Biomater Sci Polym Ed. 2001;12:491-501.

49. Fisher JP, Jo S, Mikos AG, Reddi AH. Thermoreversible hydrogel scaffolds for articular cartilage engineering. J Biomed Mater Res A. 2004;71:268-74.

50. Jiao YY, Ubrich N, Marchand-Arvier M, Vigneron C, Hoffman M, Maincent P. Preparation and in vitro evaluation of heparin-loaded polymeric nanoparticles. Drug Deliv. 2001;8:135-41.

51. Pires NM, van der Hoeven BL, de Vries MR, Havekes LM, van Vlijmen BJ, Hennink WE, Quax PH, Jukema JW. Local perivascular delivery of anti-restenotic agents from a drug-eluting poly(epsilon-caprolactone) stent cuff. Biomaterials. 2005;26:5386-94.

52. Mousa WF, Kobayashi M, Shinzato S, Kamimura M, Neo M, Yoshihara S, Nakamura T. Biological and mechanical properties of PMMA-based bioactive bone cements.*Biomaterials* 2000;21:2137-46.

53. Li LH, Kong YM, Kim HW, Kim YW, Kim HE, Heo SJ, Koak JY. Improved biological performance of Ti implants due to surface modification by micro-arc oxidation. Biomaterials. 2004;25:2867-75.

54. Sheu MS, Hoffman AS, Feijen J. A glow discharge process to immobilize PEO/PPO surfactants for wettable and nonfouling biomaterials. J. Adhes. Sci. Technol. 1992;6:995-1101.

55. Mao C, Zhu JJ, Hu YF, Ma QQ, Qiu YZ, Zhu AP, Zhao WB, Shen J. Surface modification using photocrosslinkable chitosan for improving hemocompatibility. Colloids Surf B Biointerfaces. 2004;10:47-53.

56. Wang LF, Wei YH, Chen KY, Lin JC, Kuo JF. Properties of phospholipid monolayer deposited on a fluorinated polyurethane. J Biomater Sci Polym Ed. 2004;15:957-69.

57. Siegers C, Biesalski M, Haag R. Self-assembled monolayers of dendritic polyglycerol derivatives on gold that resist the adsorption of proteins. Chemistry. 2004;10:2831-8.

58. Queiroz AC, Santos JD, Vilar R, Eugenio S, Monteiro FJ. Laser surface modification of hydroxyapatite and glass-reinforced hydroxyapatite. Biomaterials. 2004;25:4607-14.

59. Suh KY, Seong J, Khademhosseini A, Laibinis PE, Langer R. A simple soft lithographic route to fabrication of poly(ethylene glycol) microstructures for protein and cell patterning.Biomaterials. 2004;25:557-63.

Chapter 2: Characterization of conducting polymer – polypyrrole

Polypyrrole (PPy), an electrically conductive polymer, is unique and has tremendous potential as a biomaterial. One of the most interesting aspects of polypyrrole, other than its conductivity, is the ability to tailor its properties by incorporating various molecules via electrochemical synthesis. Researchers have realized the potential of using polypyrrole for numerous applications ranging from sensors to cell manipulation. Additional use of polypyrrole has been in surface coatings as the synthesis conditions, either electrochemical or chemical, can be controlled where thin films can be doposited with various dopants. Polypyrrole has some limitations including the lack of a functional group for surface modification and biomolecule immobilization. Using electrochemical synthesis, various dopants including biologically relevant molecules can be incorporated, but dopant incorporation is limited by size and charge. There has been tremendous interest in developing a more versatile polypyrrole-based material, and for this reason polypyrrole was chosen as a model polymer for phage-displayed peptide selection. In this chapter, the applications of polypyrrole in medicine and its electrochemical synthesis including characterization of PPyCl are presented.

2.1 INTRODUCTION

The diversity of applications and flexibility in processing make conductive polymers attractive in the biomedical field. Polymers of particular interest in this field

are polypyrrole, polythiophene, polyacetylene and derivatives of such polymers. More specifically, conductive polymers such as polypyrrole provide flexibility in tailoring the surface properties for cell interaction (e.g., hydrophobicity/hydrophilicity, surface charge, and roughness) by oxidation or reduction. Conducting polymers characteristically have a π-conjugated backbone system that contains alternating single and double bonds along the polymer chain. This π-conjugation is responsible for unique properties such as electroconductivity, high electron affinity, low ionization potential, and low energy optical transitions. The conduction mechanism is quite complex and varies depending on the polymer-dopant system (e.g., anions incorporated during synthesis). Conductivity is generated by inter-chain hopping of electrons (e.g., bipolarons), which can be influenced by various factors such as polaron length, chain length, charge transfer to adjacent molecules, and conjugation length [1]. This variation of conductivity by changing the dopant anion has generated research in numerous fields. The many applications of conductive polymers include analytical chemistry and biosensing devices, electrocatalysis and chromatography, tissue engineering, neural probes, prosthetics, and drug delivery [2-5].

One specific example of applying the unique properties of polypyrrole in biomedicine has been in the field of biosensors. The basic premise of biosensor development is in producing a digital signal that can be proportionally correlated to the concentration of a specific chemical or molecule. Conducting polymers have been extensively researched for the production of transducers that can generate that specific

signal based on direct binding of the biocatalyst [6]. One specific example is in the development of a glucose biosensor that highlighted the entrapment of glucose oxidase (GOX) on different polymer matrices such as polyprrole, polyaniline, and polyaminobenzoic acid. This method provides a quick and simple means for molecule deposition to selectively defined areas on the electrodes via electropolymerization. The functional activity of the sensor can be measured in many ways including amperometrically, potentiometrically, conductometrically, or optically. Several other bimolecular sensors have also been developed, some of which include biosensors for urea, lactate, cholesterol, and DNA. A specific example of a biosensor developed for DNA detection implements oligonucleotides covalently bound to polypyrrole [7]. Such a technique would have resounding effects on the study of genetic diseases.

Electrically conducting polymers have also been shown to permit finer control over drug delivery. Reynolds *et al.* demonstrated that drugs encapsulated by polypyrrole can be released in a pulsatile fashion upon electrical stimulation [8]. Not only is controlled drug delivery of great interest, but so is route of drug administration. Conducting polymers, such as poly(ethylene oxide), have made it possible to deliver drugs transdermally via iontophoresis, thereby avoiding the need for pills or injection [9].

A breakthrough in research that further increased the possible applications for conductive polymers was the discovery that electrical fields and charges led to the proliferation and differentiation of a number of cell types including nerve, skin, cartilage, and bone. This has allowed tissue engineers to focus on the development of conducting

polymers for cell regeneration [2,3,8,10,11]. This was of particular importance to neuroscientists in their effort to develop methods for regenerating peripheral or central nerves. While there has been little success in the regeneration of nerves of the central nervous system (CNS), current medical treatment exists for bridging the gap of severed peripheral nerves. These clinical procedures, however, have many limitations including incomplete regeneration of neurons at the injury site.

In an effort to develop therapies for PNS regeneration, researchers have applied conductive materials with limited success [12,13]. In developing conduits for nerve therapy, recent work has been focused towards materials modification to mimic and organize molecules for guided neurite growth [14]. For achieving such guided growth, specific molecules (e.g., cell adhesion molecules and growth factors) have been incorporated within the lumen of synthetic nerve conduits [15-18]. Numerous approaches have been researched and implemented to surface functionalize polymers for promoting cellular activity. As discussed in **Chapter 1**, modification of polypyrrole has been performed through adsorption or incorporation of molecules during synthesis. To address the limitations of non specific interactions in adsorption and selective incorporation of molecules during electrochemical polymerization, the goal of this work was to develop a novel and versatile method for surface functionalization of polypyrrole.

PPy electrochemical synthesis has been developed by Diaz *et al.* and has had tremendous potential because of its electrical properties [19] (**Figure 2.1**). In addition to its inherent electrical conductivity, another useful aspect of PPy is that its synthesis

requires the incorporation of a negatively charged dopant molecule. By choosing an appropriate dopant, the properties of PPy can be tailored to a specific application. Commonly used dopants are chloride ions and poly(styrene sulfonate), which give rise to PPyCl and PPyPSS materials, respectively. PPy has also been doped with a wide variety of other materials, including small anions [20], polymeric anions [21], buffer salts [22], and biologically active anions such as ATP [23], collagen [24], hyaluronic acid [25], heparin [26], and enzymes [27]. It was also established that anions have remarkable influence on the formation of the morphology of the polypyrrole film as well as conductivity [20,21]. Although dopant ions can be used to modify the surface character of PPy, this approach has several drawbacks, including being limited to the use of negatively charged molecules and difficulty with the incorporation of large anions [25].

The goal of the work presented in this chapter was to synthesize chlorine-doped polypyrrole (PPyCl) using electrochemical methods for phage-displayed peptide selection. The synthesis conditions used were from previous work in our laboratory and thickness characterization was performed to ensure reproducibility. Surface morphology and chemical analysis were performed to understand the surface architecture and properties related to potential interactions of the phage selected using phage display analysis (described in **Chapter 3**).

2.2 MATERIALS AND METHOD

2.2.1 Electrochemical synthesis of polypyrrole

PPyCl and PPyPSS films were electrochemically deposited onto indium tin oxide (ITO)-conductive borosilicate glass (Product # CG-801N-S115, Delta Technologies, Still Water, MN) [19] (**Figure 2.2**). Both pre-coated ITO and Au glass slides were cleaned before use by sonication in hexane, methanol, and dichloromethane for 5 min each. Immediately prior to film synthesis, the pyrrole monomer solution was purified by passing through an alumina column. A three-electrode setup consisting of a saturated calomel reference electrode, platinum gauze counter electrode, and an ITO slide as the working electrode were used for the electrochemical deposition of the PPy films. PPy films were deposited at a constant potential of 720 mV versus the saturated calomel reference from an aqueous solution of 0.1 M pyrrole monomer (Fisher Scientific, Palatine, IL) containing either 0.1 M NaCl (Fisher Scientific) providing the chloride ion as dopant or 0.1 M sodium salt of poly(styrene sulfonate) (PSS; Product #24,305-1, Avg. MW = 70,000; Aldrich, Milwaukee, WI). A Pine Instruments AFRDE5 bipotentiostat was used as the DC voltage source. The film thickness for the PPyCl and PPyPSS films were varied between (250 – 300 nm), as determined using a well developed current integration over time method [19]. A standard value of the total charge passed, established by Diaz *et al.*, of 50 mC/cm^2 was used to calculate the film thickness [19]. The charge allowed to pass through the working electrode was measured with a current integrator (IT001,

Cypress Systems, Inc.), which was coupled to a multimeter (Sperry, DM-8A). The films were rinsed with Millipore water and stored in a dessicator for two days before use. Film thickness was verified used a profilometer (Alpha-Step 200, Tencor Instruments, Mountain View, CA).

2.2.2 PPyCl surface morphology and chemistry characterization

The PPyCl films were characterized using scanning electron microscopy (SEM) and atomic force microscopy (AFM) for surface morphology and roughness. X-ray photoelectron spectroscopy (XPS) was used to determine the surface elemental composition. The SEM micrographs were taken using a Norian detection system mounted on a Hitachi 4700 field emission scanning electron microscope at 1.00 kV (Texas Materials Institute, The University of Texas at Austin). PPyCl films of thickness 200 nm were mounted dry on a metal stage using double-sided carbon tape and sputter-coated with ~30 nm chromium and then imaged at 55 – 9000x magnification.

To obtain PPyCl surface roughness, an Asylum Research (Santa Barbara, CA) model MFP3D was used in contact mode (Center for Nano and Molecular Institute, The University of Texas at Austin). Approximately 1 mL of sterile 10 mM PBS (pH 7.4) was placed on top of a ~200-250 nm PPyCl film polymerized on Au coated slides (prevented film floating). The surface was scanned using a silicon nitride tips (Veeco, Santa Barbara, CA) mounted on the AFM. PPyCl morphology was analyzed in a scanning area of 1 X 1

μm with scan rates of the order of 1 ± 5 mm/s. The surface roughness was analyzed using IGOR-MFP3D software provided for AFM control and analysis.

To establish PPyCl film surface chemistry XPS was used to determine qualitative atomic concentra analysis using a Physical Electronics Phi ESCA 5700 equipped with dual monochromatic sources: Mg X-ray source (1,254 eV X-rays) and Al X-ray source (1,487 eV X-rays).

2.3 RESULTS

2.3.1 Evaluation of surface morphology using SEM and AFM

Previous research with polypyrrole films has established that anions have a significant influence on surface morphology. This heterogeneity in surface topography can potentially be an important factor in the evaluation of PPyCl-specific phage/peptide binding and surface coverage. **Figure 2.3**, illustrates the SEM of PPyCl thin films that demonstrate anisotropic surface topography. The images of the PPyCl films that are seen in **Figure 2.3** are shown in increasing resolution from left to right. SEM analysis also ensured that our PPyCl film is consistent throughout and has no pinholes or breakages along the polymer surface. Film inconsistencies could present problems during the biopanning process. The wrinkled effect seen in **Figure 2.3** is characteristic of PPy and is consistent with the literature [28].

Surface roughness characteristics results, highlighted in **Figure 2.4**, indicate that the shape of the surface globules changes and the surface of a single globule becomes

rougher as the thickness increases. This is consistent with previously studied results [29,30] and illustrates the potential role of morphology in controlling the surface coverage of phage and peptide, as discussed in **Chapter 4**.

2.3.2 Evaluation of surface chemistry using XPS

Using XPS, we were able to analyze the surface of the polymer and to determine atomic concentrations based on peak intensities at various energies associated with particular elements. This information is essential to understanding the polymer's chemical structure, which in turn provides information on the conductivity of the polymer. **Figure 2.5** is an XPS low resolution "survey" spectrum of PPyCl, which provides atomic concentrations in the polymer. This spectrum is consistent with previous published studies [31]. Polypyrrole can have three types of monomer linkages, which affect conductivity: α–α, α–β, or β–β. PPyCl monomer linkages are usually constrained to the α–α attachment (which increases conductivity) and the α–β attachment (which decreases conductivity) because of the probability of the lowest energy binding. The α–α linkage is a linear attachment and the α–β linkage provides for some degree of branching to occur in the polymer (**Figure 2.6**). Using a higher resolution XPS spectrum (**Figure 2.7**), we are able to resolve the C1s peak area from 292-282 eV, which can determine whether the monomers are linked either by α–α linkages or α–β linkages. The C1s peak area represents the accumulation of photoelectrons, produced by excitation of the sample by X-rays, which correlates in binding energy to the carbon 1s electron shell. In the

spectrum (**Figure 2.7**), the α–α linkage is centered on 284.5 eV and the α–β linkage is centered on 283.6 eV [31,32].

2.4 DISCUSSION

In the work presented here we synthesized and characterized PPyCl prior to phage-displayed peptide selection. PPy has previously been studied for numerous applications in biomedicine [2-5], but lacks the ability to be easily surface modified for promoting biofunctionalization. Electrochemical synthesis of PPyCl was performed [19] on both ITO and Au slides and the thickness was varied by controlling the total charge passed. To obtain films that can be easily removed off of the ITO slides without affecting the integrity, thick films (~ 250-300 nm) were synthesized. As previously described [26,30], the effect of film thickness is directly represented in the surface morphology and therefore, both SEM and AFM methods were used to analyze surface structure. As presented in **Figures 2.3 and 2.4**, the surface morphology of PPyCl films demonstrates a heterogeneous surface topography with many crevices. Previous research with polypyrrole films has established that anions have a significant influence on the surface morphology [20,21]. This heterogeneity in surface topography will be an important factor in evaluating PPyCl-specific phage/peptide binding and surface coverage.

Additionally, the surface chemistry of PPyCl films was characterized to evaluate consistency in film synthesis and the possible role of phage/peptide binding to PPyCl surface (discussed in **Chapter 4**). Using XPS surface spectra of polypyrrole in its

oxidized form, five major peaks are observed, as expected: C1s around 285 eV, N1s around 400 eV, O1s around 525 eV, Na1s around 1100 eV, and Cl2 around 200 eV. The presence of Na and Cl are due to the dopant, NaCl used, and indicates an oxidized form of PPy with entrapped Cl anions (**Figure 2.5**). Furthermore, the C1s spectrum (**Figure 2.7**) illustrates that the C-C linkages are predominantly α-α, indicating that the polymer synthesized gives the spectrum of the C1s area of PPyCl (designated are the binding energies associated with the α–α and α–β linkages). Based on these data, we can conclude that the linkages in PPyCl are mainly α–α linkages, which increase conductivity and are consistent with previous studies [31,32].

In conclusion, we report PPyCl synthesis and characterization results to demonstrate the consistency of film synthesis as previously reported [26,30]. The resulting PPyCl films were characterized for film thickness along with surface morphology and chemistry. PPy presents tremendous opportunities for use as a model synthetic biopolymer for surface functionalization using phage-displayed peptide selection. Additionally, because of the recent applications and advantages of electrically conducting polymers in biomedicine, this work can potentially have broader impact for numerous applications including tissue engineering and drug delivery.

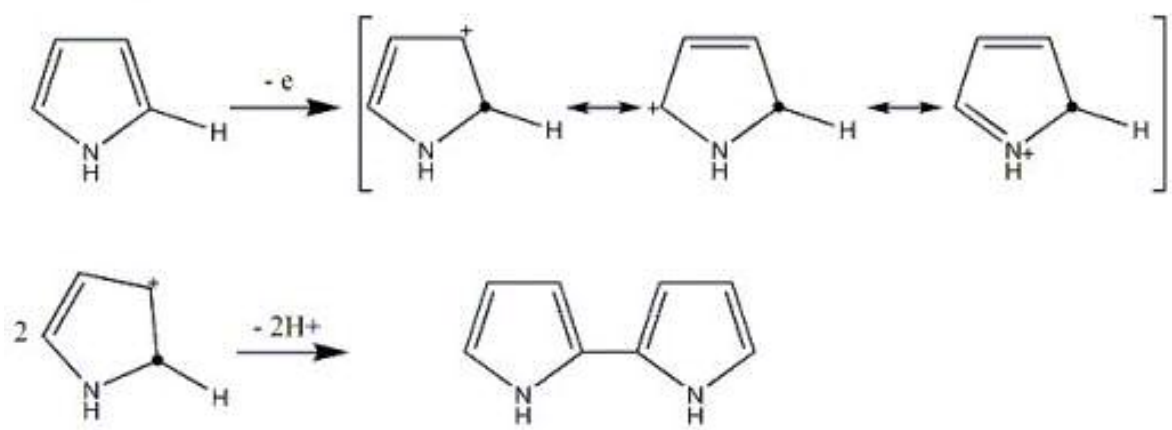

Figure 2.1 Mechanism of polypyrrole polymerization. PPy synthesis occurs by the formation of a radical cation through electrochemical oxidation. When two radical-cations combine and undergo deprotonation to form a dimer. The dimer then undergoes further oxidation, which results in the formation of oligomers and polymers on the positive electrode (ITO) [19].

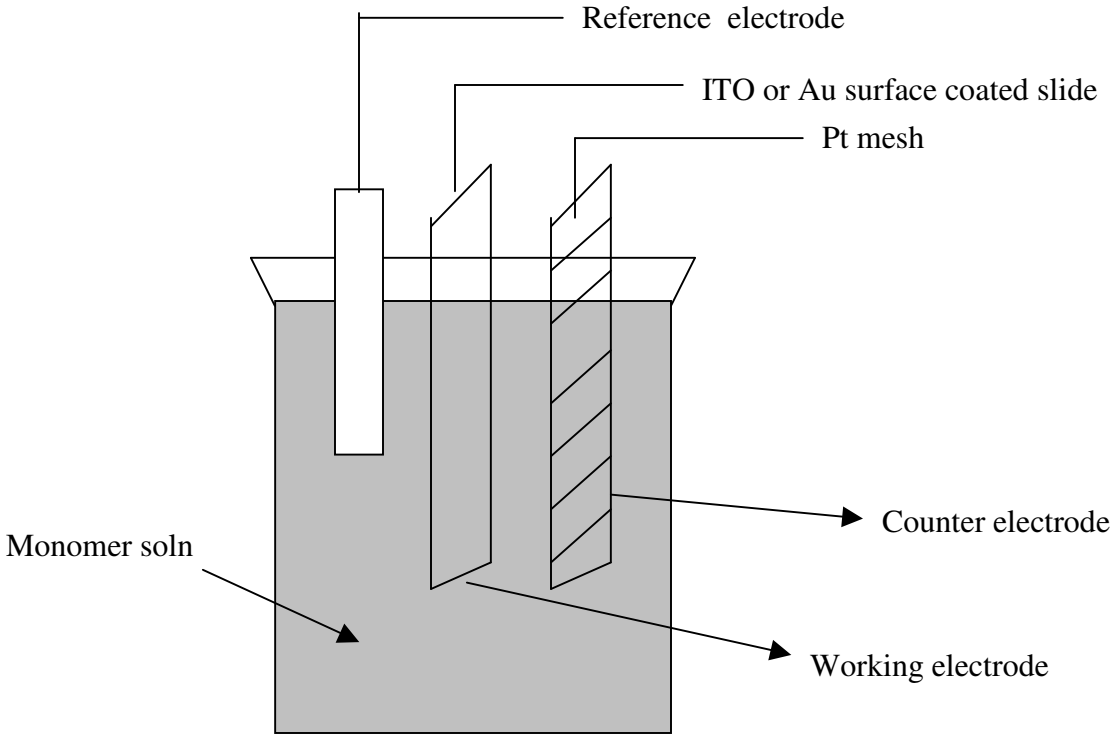

Figure 2.2 PPy electrochemical synthesis apparatus. The three electrodes, reference (KCl calomel electrode), counter (Pt mesh), and working (either ITO or Au) are placed in parallel where the working electrode is in the middle facing the Pt mesh. All of the electrodes are immersed in the monomer and dopant solution for PPy film synthesis on the working electrode.

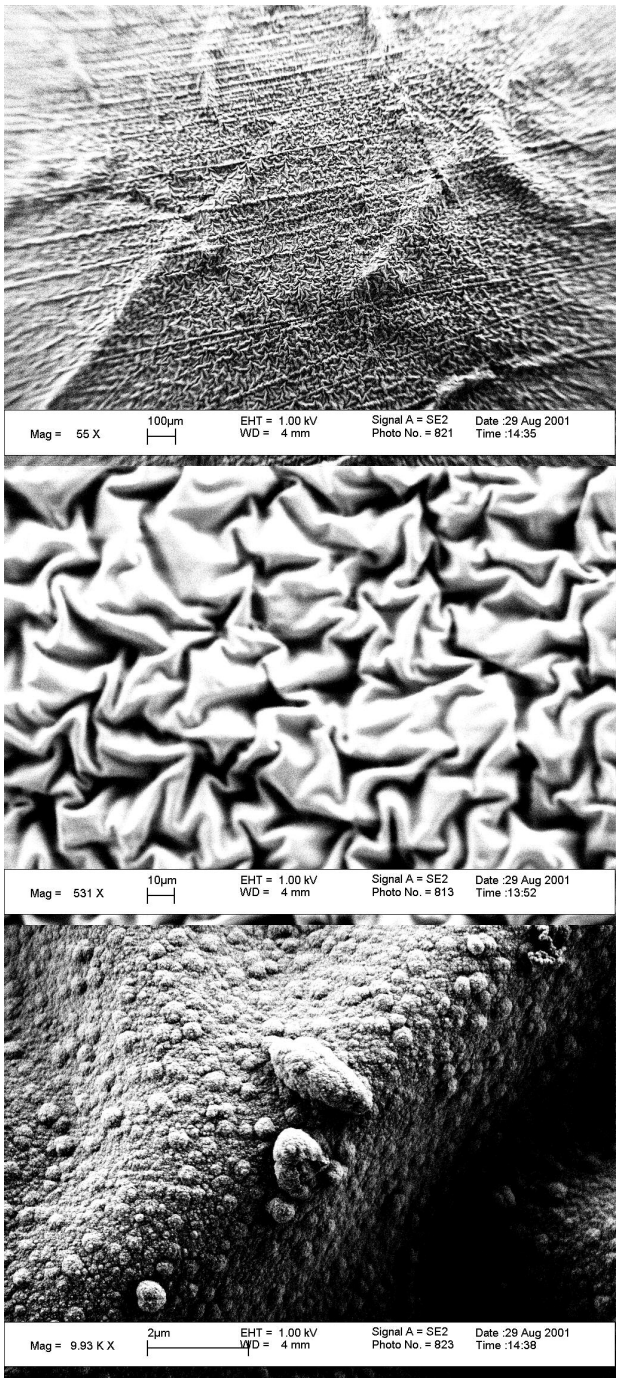

Figure 2.3 SEM micrographs of PPyCl with increasing resolution from top to bottom, showing polymer film consistency.

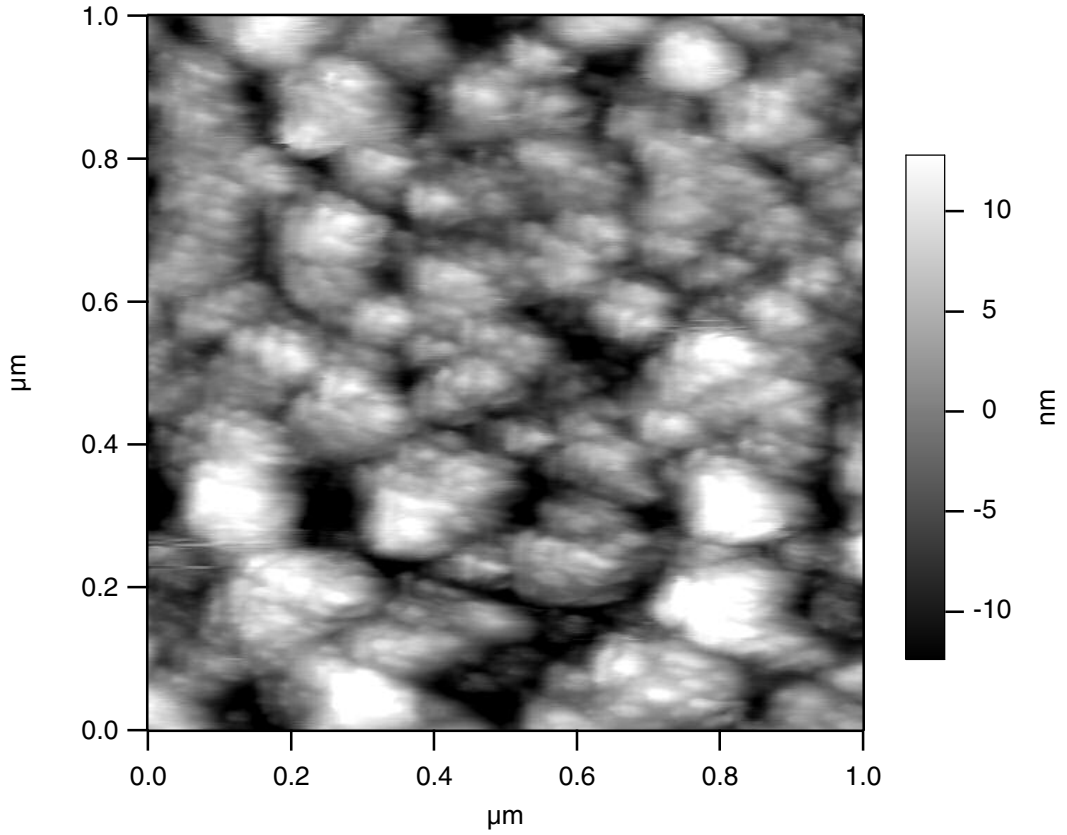

Figure 2.4 Atomic force microscopy image of PPyCl illustrating the heterogeneous and rough surface morphology. Surface roughness of 6 nm (root mean square).

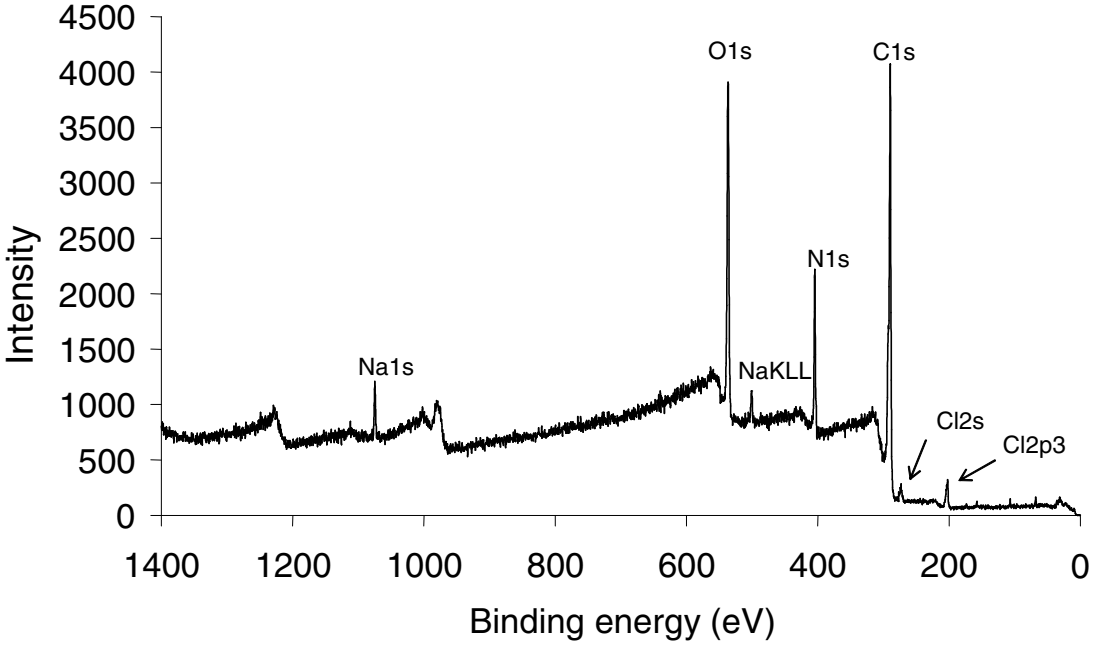

Figure 2.5 XPS survey spectrum of PPyCl. The low resolution survey scan simply confirms published literature atomic concentrations for PPyCl [31,32].

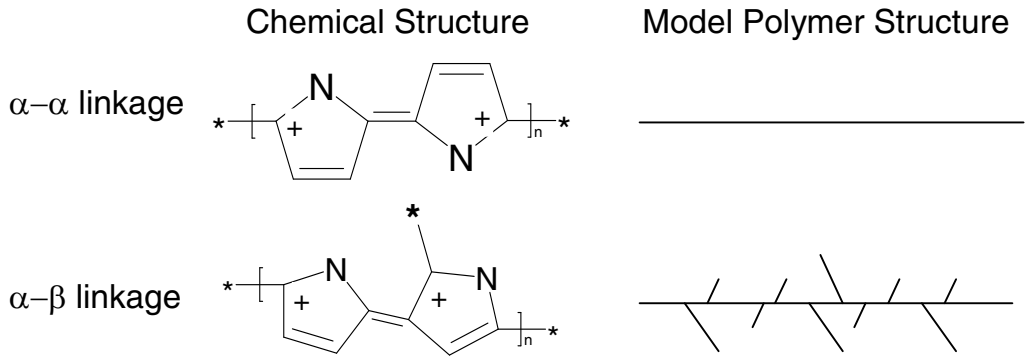

Figure 2.6 Variable carbon linkages in PPy. PPyCl can contain different monomer linkages which affect conductivity.

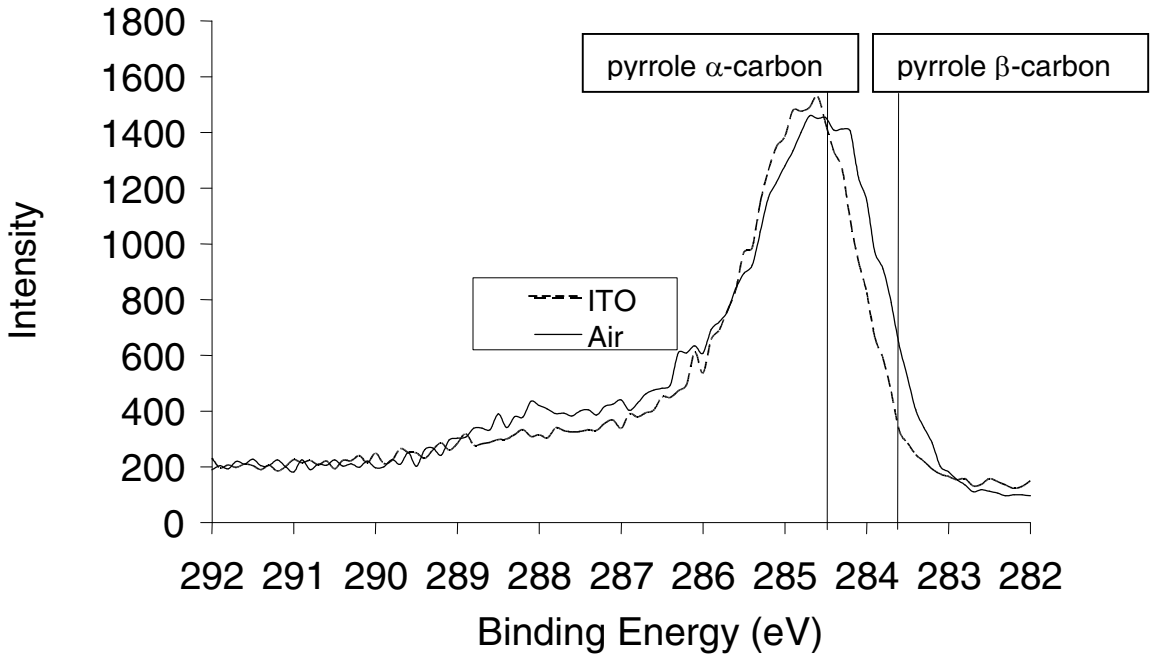

Figure 2.7 XPS C1s Spectrum of PPyCl. The carbon XPS scan demonstrates that the linkages in PPyCl are mainly of the α−α type (peak at 284.5 eV).

2.5 REFERENCES

1. Rakovic D. Structure and properties of conducting polymers. *Mat Sci Forum* 1996;214:139-146.
2. Wong JY, Langer R, Ingber DE. Electrically conducting polymers can noninvasively control the shape and growth of mammalian cells. *Proc. Natl. Acad. Sci. USA* 1994;91:3201-3204.
3. Cui X, Hetke JF, Wiler JA, Anderson DJ, Martin DC. Electrochemical deposition and characterization of conducting polymer polypyrrole/PSS on multichannel neural probes. *Sensors and Actuators A: Physical* 2001;93:8-18.
4. Yang J, Marin DC. *Sensors and Actuators* 2004;113:204-211.
5. Supronowicz PR, Ajayau PM, Ullmann, K. R.; Arulanandam, B. P.; Metzger, D. W.; Bizios, R. *Journal of Biomedical Materials Research* 2002;59:499-506.
6. Gerard, M.; Chaubey, A.; Malhotra, B.D. *Biosensors & Bioelectronics* 2002;17:345-359.
7. Korri-Youssoufi, H.; Barnier, F.: Srivastava, P.; Godillot, P; Yassar, A. *J. Am. Chem. Soc.* 1997;119:7388-89.
8. Pernaut, J.M.; Reynolds, J. R. *Journal of Physical Chemistry B* 2000;104:4080-90.
9. Sahota, T. S.; Latham, R. K.; Linford, R. G.; Taylor, P. M.; *Drug Development and Industrial Pharmacy* 2000;26:1039-44.
10. Kotwal, A.; Schmidt, C. E. *Biomaterials* 2001;22:1055-64.

11. Ikada, Y.; Shikinami, Y.; Hara, Y.; Tagawa, M.; Fukada, E. *Journal of Biomedical Materials Research* 1996;30:553-58.
12. Wang X, Gu X, Yuan C, Chen S, Zhang P, Zhang T, Yao J, Chen F, Chen G. Evaluation of biocompatibility of polypyrrole in vitro and in vivo. *J Biomed Mater Res A.* 2004;68:411-22.
13. Kimura K, Yanagida Y, Haruyama T, Kobatake E, Aizawa M. Electrically induced neurite outgrowth of PC12 cells on the electrode surface. *Med Biol Eng Comput.* 1998;36:493-8
14. Schmidt CE, Shastri VR, Vacanti JP, Langer R. Stimulation of neurite outgrowth using an electrically conducting polymer. *Proc Nat Acad Sci US*A 1997;94:8948-53.
15. Seal, B.L.; Otero, T.C.; Panitch, A. Review: polymeric biomaterials for tissue and organ regeneration. *Materials Science and Engr*. 2001;34:147-230.
16. Evans, G.R.D. Peripheral nerve injury: A review and approach to tissue engineering constructs. *The Anatomical Record.* 2001;263:396-404
17. Barras FM, Pasche P, Bouche N, Aebischer P, Zurn AD. Glial cell line-derived neurotrophic factor released by synthetic guidance channels promotes facial nerve regeneration in the rat. *J Neurosci Res.* 2002;70:746-55.
18. Fine EG, Decosterd I, Papaloizos M, Zurn AD, Aebischer P. GDNF and NGF released by synthetic guidance channels support sciatic nerve regeneration across a long gap. *Eur J Neurosci.* 2002;15:589-601.

19. Diaz AF, Castillo JA, Logan JA, Lee WY. Electrochemistry of conductive polypyrrole films. *J Electroanal Chem* 1981;129:115–132.
20. Vork FTA, Schuermans BCAM, Barendrecht E. Influence of inserted anions on the properties of polypyrrole. *Electrochim. Acta.* 1990;35:567-75.
21. Prezyna LA, Qiu Y-J, Reynolds JR, Wnek GE. Interaction of cationic polypeptides with electroactive polypyrrole/poly(styrenesulfonate) and poly(N-methylpyrrole)/ poly(styrenesulfonate) films. *Macromolecules* 1991;24:5283-87.
22. Genies EM, Marchesiello M, Bidan G. Preparation and properties of polypyrrole made in the presence of biological buffers. *Electrochim Acta* 1992;37:1015-20.
23. Boyle A, Genies E, Fouletier M. Electrochemical behaviour of polypyrrole films doped with ATP anions. *J Electroanal Chem* 1990;279:179-86.
24. Li HC, Khor E. A collagen-polypyrrole hybrid: influence of 3-butanesulfonate substitution. *Macromol. Chem. Phys.* 1995;196;1801-12.
25. Collier JH, Camp, JP, Hudson TW, Schmidt CE. Synthesis and characterization of polypyrrole-hyaluronic acid composite biomaterials for tissue engineering applications. *J. Biomed. Mater. Res,* 2000;50:574-84.
26. Silk T, Tamm J. Voltammetric study of the influence of cations on the redox-switching process of halogenide-doped polypyrrole. *Electrochimica Acta.*1996;41:1883-85.
27. Tamm J, Hallik A, Alumaa A, Sammelselg V. Electrochemical properties of polypyrrole/sulphate films. *Electrochimica Acta.* 1997;42:2929-34.

28. Kassim A, Basar ZB, Mahmud HNME. Effects of preparation temperature on the conductivity of polypyrrole conducting polymer. *Proc. Indian Acad. Sci*., 2002;114:155-62.

29. Chyla AT, Ryley S, Walton DJ, Liu X, Chetwynd, DG. Effect of dopant counter-anion on tribological properties of polypyrrole. *Adv Mat Opt Electron* 1998;8:87-91.

30. Silk T, Hong Q, Tamm J, Compton RG. AFM studies of polypyrrole film surface morphology I. The influence of film thickness and dopant nature. *Syn Metals* 1998;93:59-64.

31. Cairns DB, Armes SP, Chehimi MM, Perruchot C, Delamer M. X-ray photoelectron specstroscopy characterization of submicrometer-sized polypyrrole-polystyrene composites. *Langmuir* 1999;15:8059-66.

32. Pfluger P, Krounbi M, Street GB, Weiser G. The chemical and physical properties of pyrrole-based conducting polymers: the oxidation of neutral polypyrrole. *Journal of Chemical Physics* 1983;78:3212-18.

Chapter 3: PPyCl-Specific Peptide Selection Using Phage Display

As discussed and presented in **Chapter 2**, we synthesized chlorine-doped polypyrrole (PPyCl) and characterized the surface morphology for consistency and surface chemistry. Additionally, PPyCl films were polymerized on ITO with approximate thickness of ~250 nm for phage-displayed peptide selection using a commercially available library. The goal of the study presented in this chapter was to select peptides expressed on M13 filamentous bacteriophage that were genetically engineered to present 12-amino acid peptide inserts on the minor-coat (pIII) protein.

A commercially available library, Ph.D.12^{TM} was purchased from New England Biolabs (NEB) and selection was performed using the biopanning process. An initial library with a total of 10^{12} (of which 10^{9} are unique) phage was incubated with PPyCl film. After washing non-specifically bound phage and eluting the phage that bound to the surface, the eluted phage were amplified using bacterial culture. This process was repeated a total of five times to enrich the pool of phage with the best binding peptide sequence. To ensure that the phage selected were not biased by the amplification process, an amplification comparison study was performed with the PPyCl-selected phage and wild-type (WT) phage. The eventual goal of selection against PPyCl was to use the strong binding peptides for further modification and functionalization to promote bioactivity.

Some of the results from this chapter are presented in, Sanghvi AB, Miller KP-H, Belcher AM, Schmidt CE. ***Nat. Mat.*** *2005, 4(6):496-502.*

3.1 INTRODUCTION – PHAGE DISPLAY TECHNOLOGY

Peptides identified using phage display analysis can have specific binding to many different substrates, ranging from proteins to semiconductors. Once material-specific peptides are identified, any biomolecule or cell, can potentially be immobilized in order to functionalize biomaterials. Previously, phage display has been used in various applications such as identifying cancer-specific ligands [1], receptor-ligand interactions [2], and in selecting unique peptides against inorganic semiconductor materials [3-6]. Recent reviews [7,8] have highlighted the application of phage display in selecting peptides to functionalize biomaterials such as titanium. Other researchers have used phage display to select peptides against synthetic polymers such as polystyrene [9], which was inadvertent, and yohimbine imprinted methacrylate polymer [10] for molecular imprinted receptors. Although the use of phage display has been widely studied, there have been few studies with polymers, and even fewer investigations into using this approach to functionalize polymeric scaffolds for specific biomedical applications (**Table 3.1**). This prompted the research to explore the versatility of phage display in developing a method for surface functionalization of a model biopolymer, chlorine-doped polypyrrole (PPyCl).

Phage display analysis was performed on PPyCl thin films and the peptide sequences capable of binding to the PPyCl were identified via the biopanning process (**Figure 3.1**). A commercially available phage library (Ph.D.-12™ Phage Display Peptide Library Kit, New England Biolabs, Beverly, MA) was used to screen peptides. The 12-

mer peptide library was used because the increased length of the displayed peptide allows folding into small structural elements (short helices, beta-turns, etc.) that may be necessary for target binding [11]. This library provided ~10^9 unique 12 amino acid linear peptide inserts fused to the pIII coat protein of M13 bacteriophage [11]. Thus, one can "pan" for the sequences with the highest binding affinity to a particular surface.

As illustrated in **Figure 3.1**, the process was carried out by incubating a library of phage-displayed peptides with PPyCl, washing away the unbound phage, and eluting the specifically-bound phage using a change in pH. The eluted phage were then amplified and taken through additional cycles of panning and amplification to successively enrich the pool of phage in favor of the tightest binding sequences. Usually five rounds of biopanning are sufficient to determine a consensus peptide sequence. Once this was complete, the phage were isolated and the peptide sequences determined. Nucleotide sequences from the phage DNA were obtained from The Institute for Cellular and Molecular Biology DNA Core Facility (The University of Texas, Austin, TX) and then translated into N-terminus to C-terminus peptide sequences.

3.2 MATERIALS AND METHODS

A commercially available library of phage, specifically the Ph.D.-12™ Phage Display Peptide Library Kit (New England Biolabs, Beverly, MA) was used to screen peptides (Figure 3). An initial volume of 1 µl of phage display library solution, corresponding to a total of $1x10^{12}$ phage/µl, was used to begin biopanning, in 1 ml of

Tris-buffered saline containing 0.1% vol:vol Tween-20 (0.1% Tris-buffered saline-Tween (TBS-T)). The library was incubated with the material for 1 hr at room temperature. The materials were then washed 2-3 times with 1 ml of 0.1% TBS-T to discard non-specifically or weakly bound phage. To disrupt binding of the phage that did bind to the surface of the material, 500 µl of glycine-HCl (pH 2.2) was added to the interaction vial for 9 min at room temperature. The solution is then collected and brought to neutral pH with Tris-HCl (pH 9.13). Half of the volume of the elution was then introduced into a 1:100 dilution of LB (Luria-Bertani) medium and overnight culture of *Escherichia coli* ER2837 bacteria (New England Biolabs, Beverly, MA) and was allowed to re-infect its bacterial host to amplify. The amplification took place over a period of 5 hr in a shaker at 37^{o}C. The bacteria were then removed by centrifugation at 14,000 rpm for 10 min. The phage were then precipitated with poly(ethylene glycol) or PEG for 15 min at 4^{o}C. The PEG-precipitated phage were then centrifuged at 10,000 rpm for 15 min to pellet the phage. The phage were then resuspended in 200 µl of TBS. From the amplification suspension and the elution of the phage from the surface of the material, dilutions were made to determine the concentration of phage. This was done by plating, or allowing a sequential difference in phage concentration to infect a known amount of bacterial host. We used a ten fold serial dilution of the amplification solution and the elution to infect 185 µl of titer culture, LB media and *E. coli* (Optical Density = 0.5). The genetically engineered phage and infected bacteria, which contain the lac*Z* gene, were then plated on LB plates in the presence of isopropyl-β-D-thiogalactopyranoside (IPTG), which induces

the production of β-D-galactosidase in bacteria, and 5-bromo-4-chloro-3-hydroxyindolyl-β-D-galactose (X-gal), which was blue from the X-gal side group of 5-bromo-4-chloro-3-hydroxyindole. β-D-galactosidase hydrolyzes X-gal, forming an indigo-type blue-green precipitate. Thus, bacteria which express the lac*Z* gene produce blue colonies when grown in the presence of X-gal. From these "titer plates" of known dilution, a phage concentration was determined by Equation 1.

Molar Concentration of Phage (mol/L):

$$[phage]\ \frac{mol}{L} = [phage]\ \frac{pfu}{\mu l}\ x\ (\frac{1\mu l}{10^{-16}\ L})\ x\ (\frac{5 copies}{1 pfu})\ x\ (\frac{1 mol}{6.023 x 10^{23}\ molecules}) \qquad [1]$$

Five rounds of biopanning were sufficient to determine a PPyCl-binding peptide sequence. The dilutions of the elution were plated as described previously, but from the 3rd to the 5th round of biopanning the blue plaques were selected with a tooth pick and amplified individually in 1:100 LB media and an overnight culture of *E. coli* with a total volume of 1 ml. Again the phage were allowed to amplify in their bacterial host for 5 hr. The bacteria were then separated by centrifugation for 30 sec. 500 µl of the phage were then PEG precipitated for 10 min at room temperature and pelleted by centrifugation for 10 min. The pellet was suspended in a solution of NaI to rupture the phage protein coat. Ethanol (250 µl) was used to precipitate the DNA from the phage. The precipitated DNA was suspended in 60 µl Millipore water. Nucleotide sequences from the phage DNA were obtained from The Institute for Cellular and Molecular Biology DNA Core Facility (The

University of Texas, Austin, TX) and translated into N-terminus to C-terminus peptide sequences (see binding sequences in **Figure 3.2**). It is also of interest to note that the non-genetically engineered (naturally occurring, or wild type (WT)) phage has no peptide insert on its pIII protein coat, but when plated on LB plates in the presence of IPTG and X-gal it is a clear plaque. After the materials were screened, the peptide sequences were analyzed for a predominant sequence, indicating the preferential binding motif for the material.

3.3 RESULTS

3.3.1 Peptide sequences identified via biopanning

The phage display selection process against PPyCl was performed using the Ph.D.12^{TM} library. The DNA sequences acquired from each phage selected from the five biopan round were analyzed per protocol from New England Biolabs [11]. DNA sequence analysis, highlighted in the Ph.D.12^{TM} manual [11], resulted in the amino acid sequence for the peptide insert (12-mer sequence inserted in that particular phage at the pIII protein coat). The amino acid sequences where then analyzed by determining the percent abundance of a particular sequence of biopan rounds 3, 4, and 5 (**Figure 3.2**). Because of the higher possibility of non-specific binding in the first two rounds, analysis was only performed on the last three rounds from panning. The resultant analysis yielded the consensus sequence (designated as T59 phage or ϕT59) (**Figure 3.3**). A total of 25

peptide sequences were acquired from biopan rounds 3, 4, and 5. Each alpha-numeric symbol represents a distinct phage that bound to PPyCl, and its associated amino acid sequence. For instance, "T36" represents: T=PPyCl, 3=3rd round, 6=6th clone sequenced. Note the high recurrence of the T59 sequence (23 out of the 25 sequences), suggesting that this was the predominant phage with the 12-mer sequence that demonstrated selective binding to PPyCl (**Figure 3.3**).

3.3.2 Phage amplification analysis

Once the consensus sequence was determined, the consensus phage was amplified and compared to wild-type (WT) phage. WT phage is a non-genetically engineered phage that occurs naturally in the library and lacks a peptide insert in its pIII protein coat. The titer count (i.e., amplification as reflected by phage "counts") of T59 phage was compared to the amplification of wild type phage to determine that T59 phage was not preferentially selected because of its ability to amplify better (**Figure 3.4**). This can be a concern because of the multiple rounds of selection/bacteriological infection that the phage undergo in the biopanning process. If the phage multiply better than a naturally occurring WT phage, then there is a possibility that the phage containing the consensus sequence peptide was selected because of its ability to amplify and not because of its specific binding ability to the surface of PPyCl. The data in **Figure 3.4** demonstrate that the WT and T59 phage amplify at indistinguishable rates, confirming that the selection of T59 is the result of binding to PPyCl.

3.4 DISCUSSION

Phage-displayed peptide selection is a unique method utilized traditionally for biological molecules such as antigen-mapping of antibodies and determination of ligand-receptor interactions. In the recent years, other researchers have demonstrated the potential of using phage display screening as a combinatorial approach for iteratively selecting unique peptides against non-biological materials (**Table 3.1**). To design peptides that selectively bind to such substrates, a tremendous amount of time and effort would be necessary. Phage display provides a unique opportunity to "naturally" select a peptide screened from billions of different combinations in one single process. The focus of the research presented in this chapter was to demonstrate the feasibility of using phage-displayed peptide selection to select unique peptides against synthetic biopolymers. The model material used was PPyCl, as it does not contain modifiable functional groups and is stable under the selection process. Furthermore, PPy has demonstrated tremendous potential for biomedical applications [12-14].

Our approach is based on using a commercially available 12-mer peptide-displayed M13 phage library (New England Biolabs Inc., Ph.D.12^{TM}). Biopanning was performed for peptide selection using an established protocol [3,4]. We used this library to select a strong binding peptide (T59) to the model polymer, PPyCl. The 12-mer peptide library was used because the increased length of the displayed peptide allows folding into small structural elements (short helices, beta-turns, etc.) that may be

necessary for target binding. This presented a high-throughput method to screen a total of ~10^{12} (of which 10^9 where unique) different peptide inserts at one time.

The selected phage, ϕT59, was determined to be a binding clone to PPyCl. Prior to performing additional studies to determine the extent of binding and relative specificity of interaction, amplification results were performed to ensure that the ϕT59 was not selected because of its ability to amplify better. As the amplification comparison between wild-type phage (**Figure 3.4**) suggests, ϕT59 was present throughout the biopan rounds because of its ability to bind PPyCl.

The probability of selecting at least one independent clone with the 12-mer peptide sequence (T59, THRTSTLDYFVI) was calculated using the probability equation [11], $P(k>0) = 1\text{-}e^{-np}$, where p represents the absolute probability of obtaining that sequence (calculated by multiplying the observed frequency in **Table 3.2**), and n is the complexity number ($2.7x10^9$). The probability is 4.485×10^{-6}, which indicates that this sequence was rare in the library and the binding to PPyCl must be specific for its selection after five rounds of biopanning. It is interesting to note that the number of hydroxyl amino acid groups in ϕT59 is almost double in comparison to the average number in the entire combinatorial peptide library (New England Biolabs). The polymer backbone of PPyCl has alternating secondary amines on adjacent pyrrole monomers. The increase in hydroxyl groups in the peptide is significant because of the possible amide interaction that could occur between these two functional groups at the surface of the

material. We hypothesize that this type of interaction, which commonly occurs between proteins, may play an integral role in the binding of the ϕT59 to PPyCl.

Table 3.1 Non-biological materials studied for phage-displayed peptide selection

Material	**Reference**
TiO_2	[6]
Au	[15,16]
Ag	[17]
SiO_2	[18]
GaAs	[4]
ZnS	[19]
Zeolites	[20]
$CaCO_3$	[21]
Polystyrene	[9]
Methacrylated polymer	[10]

Table 3.2 Amino acid distribution in native Ph.D.12™ phage library

Amino Acid	Observed Frequency	Amino Acid	Observed Frequency
Thr (T)	11.1 %	Asp (D)	2.8%
His (H)	6.3%	Tyr (Y)	3.6%
Arg (R)	4.7%	Phe (F)	3.3%
Ser (S)	10.0%	Val (V)	3.9%
Leu (L)	9.3%	Ile (I)	3.4%

Adapted from the Ph.D.12™ library manual [11].
As determined by New England Biolabs and presented in the manual [11], a total of 104 clones from the native library were sequenced and the overall amino acid distribution from the 1176 sequenced codons were used to determine the observed frequency of each amino acid.

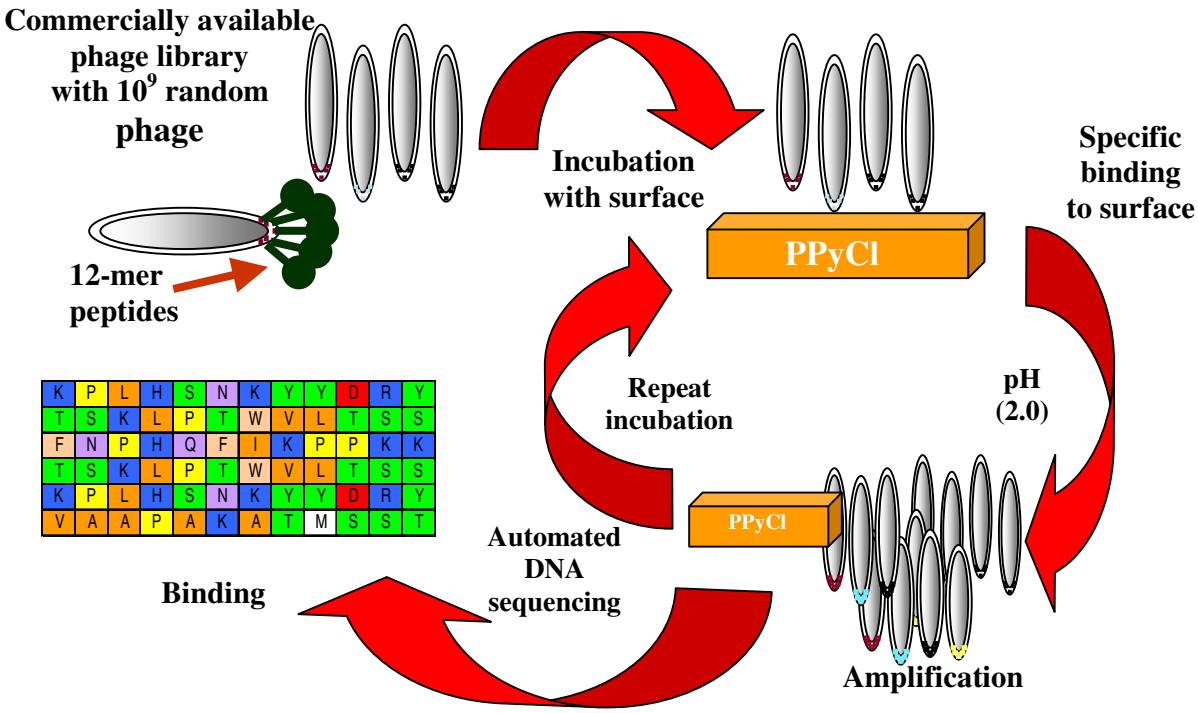

Figure 3.1 Biopanning with Ph.D.-12 peptide library.

Biopanning is performed by incubating a library of phage-displayed peptides with a desired surface (e.g., PPyCl), washing away the unbound phage, and eluting the specifically-bound phage. The eluted phage are then amplified and taken through additional cycles of panning and amplification to successively enrich the pool of phage in favor of the tightest binding sequences. Once this is complete, the phage can be isolated and the peptide sequences determined.

T31	T	H	R	T	S	T	L	D	Y	F	V	I
T32	T	H	R	T	S	T	L	D	Y	F	V	I
T33	T	H	R	T	S	T	L	D	Y	F	V	I
T34	T	H	R	T	S	T	L	D	Y	F	V	I
T36	T	I	K	M	H	T	L	S	Y	T	G	L
T37	T	H	R	T	S	T	L	D	Y	F	V	I
T38	T	H	R	T	S	T	L	D	Y	F	V	I

T41	T	H	R	T	S	T	L	D	Y	F	V	I
T42	T	H	R	T	S	T	L	D	Y	F	V	I
T43	S	H	K	Y	P	K	P	P	Y	F	H	W
T44	T	H	R	T	S	T	L	D	Y	F	V	I
T45	T	H	R	T	S	T	L	D	Y	F	V	I
T46	T	H	R	T	S	T	L	D	Y	F	V	I
T47	T	H	R	T	S	T	L	D	Y	F	V	I
T48	T	H	R	T	S	T	L	D	Y	F	V	I
T49	T	H	R	T	S	T	L	D	Y	F	V	I
T410	T	H	R	T	S	T	L	D	Y	F	V	I

T51	T	H	R	T	S	T	L	D	Y	F	V	I
T52	T	H	R	T	S	T	L	D	Y	F	V	I
T53	T	H	R	T	S	T	L	D	Y	F	V	I
T54	T	H	R	T	S	T	L	D	Y	F	V	I
T55	T	H	R	T	S	T	L	D	Y	F	V	I
T56	T	H	R	T	S	T	L	D	Y	F	V	I
T57	T	H	R	T	S	T	L	D	Y	F	V	I
T58	T	H	R	T	S	T	L	D	Y	F	V	I
T59	T	H	R	T	S	T	L	D	Y	F	V	I

Figure 3.2 Peptide sequences acquired from biopan rounds 3 (T31-T38), 4 (T41-T410) and 5 (T51-T50) on PPyCl thin films. Each unique number represents a phage that bound to PPyCl, and its associated peptide sequence. Note the high similarity in the sequences, suggesting that a single sequence binds to PPyCl.

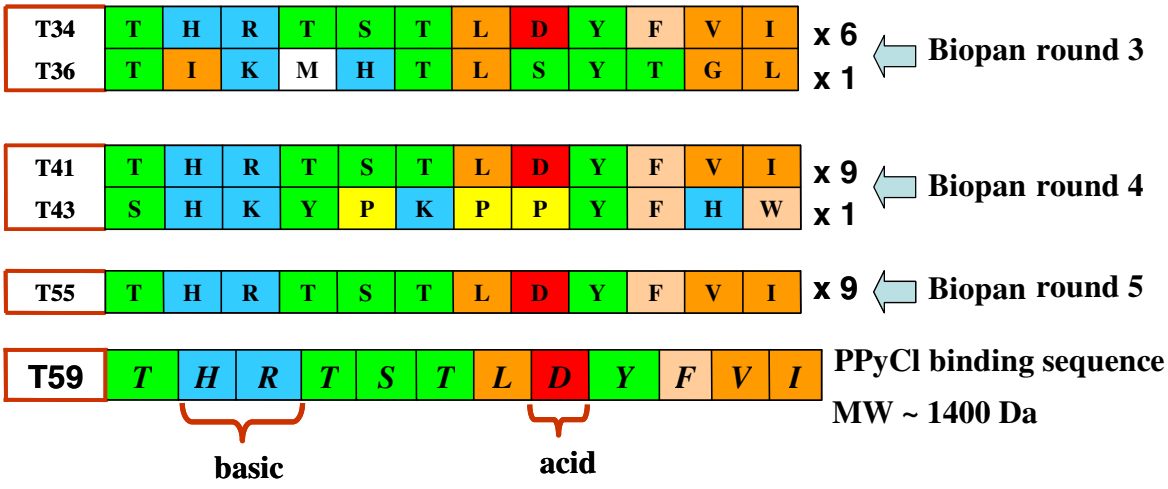

Figure 3.3 A peptide sequence binding to PPyCl is determined from the peptide sequences illustrated above. The 12-amino acid peptide with the sequence THRTSTLDYFVI occurred 23 out of the 25 phage sequence from biopan rounds 3 through 5. This clone, labeled ϕT59, appeared a hundred percent of the time from the 9 sequences cloned in the 5th biopan round, suggesting that this phage bound well to PPyCl.

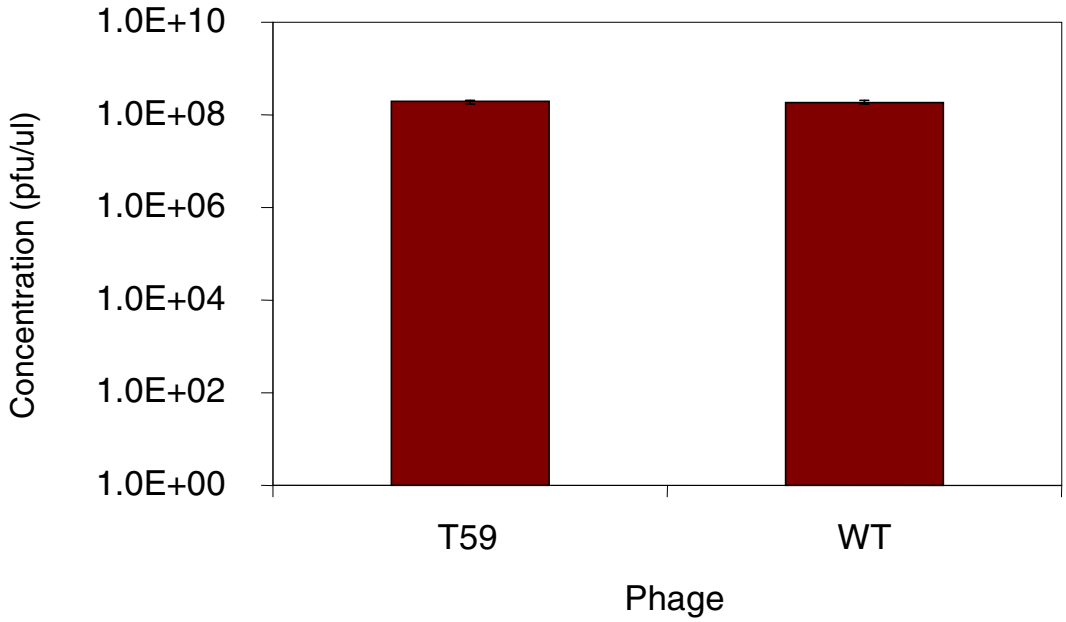

Figure 3.4 Amplification rates of T59 phage compared to WT phage (n=6).
WT and T59 phage amplify at indistinguishable rates, confirming that the selection of T59 reflects the selection for a peptide sequence that binds to PPyCl (and is not simply an artifact of any amplification differences between the two phage).

3.5 REFERENCES

1. Mori T. Cancer-specific ligands identified from screening of peptide-display libraries.

   Curr. Pharm. Des. 2004;19:2335-43.

2. Rowley MJ, O'connor K, Wijeyewickrema L. Phage display for epitope determination: A paradigm for identifying receptor-ligand interactions. *Biotechnol. Annu. Rev*. 2004;10:151-88.

3. Whaley SR, English DS, Hu EL, Barbara PF, Belcher AM. Selection of peptides with semiconductor binding specificity for directed nanocrystal assembly. *Nature* 2000;405:665-668.

4. Flynn CE, *et al*. Synthesis and organization of nanoscale II VI semiconductor materials using evolved peptide specificity and viral capsid assembly. *J. Mater. Chem.* 2003;13:2414-2421.

5. Mao C, *et al*. Viral assembly of oriented quantum dot nanowires. *Proc. Natl. Acad. Sci*. 2003;12:6946-51.

6. Sano K, Shiba K. A hexapeptide motif that electrostatically binds to the surface of titanium. J. *Am. Chem. Soc.* 2003;125:14234-35.

7. Sarikaya M, Tamerler C, Jen AK, Schulten K, Baneyx F. Molecular biomimetics: nanotechnology through biology. *Nat. Mater*. 2003;2:577-85.

8. Sarikaya M, Tamerler C, Schwartz DT, Baneyx F. Materials assembly and formation using engineered polypeptides, *Annu. Rev. Mater. Res.* 2004;34:373–408.

9. Adey NB, Mataragnon AH, Rider JE, Carter JM, Kay BK. Characterization of phage that bind plastic from phage-displayed random peptide libraries. *Gene* 1995;156:27-31.

10. Berglund J, Lindbladh C, Nicholls IA, Mosbach K. Selection of phage display combinatorial library peptides with affinity for a yohimbine imprinted methacrylate polymer. *Analytical Communications* 1998;35:3-7.

11. Ph.D.™ Phage Display Peptide Library Kits; Technical Bulletin E8100, E8110, E8120; New England Biolabs: Cambridge MA, 2004; 1-4.

12. Collier JH, Camp, JP, Hudson TW, Schmidt CE. Synthesis and characterization of polypyrrole-hyaluronic acid composite biomaterials for tissue engineering applications. *J. Biomed. Mater. Res,* 2000;50:574-84.

13. Schmidt CE, Shastri VR, Vacanti JP, Langer R. Stimulation of neurite outgrowth using an electrically conducting polymer. *Proc Nat Acad Sci US*A 1997;94:8948-53.

14. Wong, J. Y.; Langer, R.; Ingber, D. E. Electrically conducting polymers can noninvasively control the shape and growth of mammalian cells. *Proc. Natl. Acad. Sci. USA* 1994;91:3201-04.

15. Brown, S. Metal recognition by repeating polypeptides. *Nature Biotechnol.* 1997;15:269–72.

16. Brown S, Sarikaya M, Johnson E. Genetic analysis of crystal growth. *J. Mol.Bio*l. 2000;299:725–32.

17. Naik, R. R., Stringer, S. J, Agarwal, G., Jones, S. E. & Stone, M. O. Biomimetic synthesis and patterning of silver nanoparticles. *Nature Mater.* 2002;1:169–72.

18. Naik RR, Brott L, Carlson SJ, Stone MO. Silica precipitating peptides isolated from a combinatorial phage display libraries. *J. Nanosci. Nanotechno*l. 2002;2:1–6.

19. Lee WS, Mao C, Flynn CE, Belcher AM. Ordering quantum dots using genetically engineered viruses. *Science* 2002;296:892–95.

20. Scembri MA, Kjaergaard K, Klemm P. Bioaccumulation of heavy metals by fimbrial designer adhesions. *FEMS Microbial. Lett.* 1999;170:363–71.

21. Gaskin DJH, Starck K, Vulfson EN. Identification of inorganic crystal-specific seqeunces using phage display combinatorial library of short peptides:A feasibility study. *Biotech. Lett.* 2000;22:1211–16.

Chapter 4: PPyCl-Specific Phage and Peptide Binding Analysis

As discussed in **Chapter 3**, we selected a phage-displayed peptide ("T59") against PPyCl. The process of biopanning enabled the pool to be enriched with a peptide that had selective binding to PPyCl. The goal of the studies presented in this chapter was to characterize the binding of ϕT59 and T59 peptides to PPyCl when compared to other substrates. Furthermore, T59 peptide variants were synthesized to identify essential amino acids in recognizing PPyCl. Additionally, the relative strength of interaction of T59 peptide to PPyCl was analyzed using AFM.

Competitive binding analysis between ϕT59 and other phage was performed, in addition to binding to other substrates including polystyrene sulfonate (PSS) doped PPy (PPyPSS) and polystyrene (PS). The results indicated that ϕT59 binds significantly better to PPyCl when compared to other substrates and phage clones. Synthesized T59 peptides, independent of the phage, demonstrated binding to PPyCl and an initial mechanism of interaction was determined by identifying a key amino acid (Asp, position 8) in recognizing PPyCl. Binding strength analysis of T59 peptides to PPyCl was compared to non-specific adsorption (GRGDS binding to PPyCl) and to a strong non-covalent bond (streptavidin-biotin) using atomic force microscopy. The results suggest that T59 peptides bind to PPyCl with strength on the order of possibly a weak antigen-antibody interaction. These studies suggest that T59 peptide, selected from the biopanning process, has unique binding to PPyCl and can potentially be used for surface modification.

Some of the results from this chapter are presented in, Sanghvi AB, Miller KP-H, Belcher AM, Schmidt CE. ***Nat. Mat.*** *2005, 4(6):496-502.*

4.1 INTRODUCTION

As discussed in **Chapter 3**, a phage that recognizes PPyCl was identified. This was one of possibly many phage that have binding affinity to PPyCl. As highlighted in **Chapter 3**, phage-displayed peptide selection has been applied to numerous non-biological materials [1-5]. This was one of the first known examples for using phage display to select peptides against synthetic biopolymers for surface functionalization applications. Therefore, prior to studying the potential functional applications of these peptides, it is important to compare the relative binding among other phage and the actual binding of the 12-mer peptide to PPyCl. Additionally, further characterization including a potential mechanism and strength of interaction are necessary for future applications in surface modification.

4.1.1 Characterization of ϕT59 and T59 peptide binding to PPyCl

Numerous researchers that have selected peptides against non-biological materials using phage display have demonstrated the selective binding of selected-phage and their potential mechanism of interaction [1,3]. One such example is TiO_2, where a unique 12-mer peptide was selected that demonstrated binding via the N-terminal end (hexapeptide) [1]. Binding was a result of strong electrostatic interactions (negative and positive charges) to the oxide layer of TiO_2 when in biological fluid. Overall, phage-displayed peptide selection has proved to be a useful method for producing unique biological entities that can interact with non-biological materials.

The goal of the work presented in this chapter was to assess the binding specificity of ϕT59 and T59 peptides to PPyCl and characterize the interaction by determining an initial binding mechanism and strength of interaction. We studied the binding of ϕT59 in comparison to other phage: ϕS36 (semi-conductor binding phage isolated in A.M. Belcher's laboratory), ϕC511 and ϕT125-4 (other selected phage from previous incomplete screens against PPyCl), and wild-type (WT, non-engineered) phage using titer count analysis. The use of titer count analysis is semiquantitative and provided a relative binding comparison of phage counts for ϕT59. Binding comparison of ϕT59, ϕC511, and ϕWT to other substrates, including PPyPSS and PS, was studied using titer count analysis as well. Furthermore, T59 peptides were synthesized and their binding to PPyCl was qualitatively determined using immunofluorescence and a fluorescamine assay (for relative binding comparison). Additional studies included pH 2 elution of T59 peptides from PPyCl surface and XPS analysis of PPyCl and PPyCl-T59 samples to quantitatively determine the extent of T59 binding.

4.1.2 Determining essential amino acids in T59 peptide in binding PPyCl

T59 peptide variants (**Table 4.1**) were synthesized to determine a possible role of specific amino acids in recognizing and binding to PPyCl. Based on physicochemical properties of three of the twelve amino acids in T59 peptide, His, Arg, and Asp, [6,7] we anticipate that either acidic (carboxylic acid of D) or basic (imidazol of H and guanidine of R) or both functionalities will be involved in the binding process (**Table 4.2**). The

overall surface charge of PPyCl is positive, as the ratio of chlorine ions to pyrrole monomer is 3:1 [8], in phosphate-buffered saline solution. Thus, it can be speculated that the Asp residue with a carboxylic acid R-group may contribute to the recognition of PPyCl. Furthermore, enantiomeric characteristics of T59 were also studied by reversing the sequence (IVFYDLTSTRHT, T59 reverse) order to determine the importance of position of the amino acids in binding to PPyCl.

4.1.3 Binding strength of T59 peptides to PPyCl using AFM

The recent development of AFM and advancements in molecular force spectroscopy has resulted in enormous possibilities for detailed analysis of molecular interactions. The development and introduction of AFM by Binnig, Quate, and Gerber in 1986 allowed analysis of materials at the molecular level [9]. Recently, AFM's versatility has been explored in the field of biomedical science with the advent of single molecule force spectroscopy to analyze the biophysical nature of molecular interactions. Numerous applications for biophysical studies of molecular forces that govern receptor-ligand interactions have been studied for various biological and non-biological entities [10-18] (**Table 4.3**). One particular receptor-ligand pair, streptavidin-biotin, has been extensively studied under static and dynamic externally applied forces [10,11]. Recently, additional studies have utilized AFM for measuring picoNewton molecular binding forces for antigen-antibody and peptide-porphyrin molecules [18,25].

Using these principles and methods for studying molecular binding strengths, the strength of binding between T59 peptides and PPyCl was studied. Specifically, a unique AFM tip modification technique [12] was used to attach biotinylated-T59 peptides to the AFM tips and their strength of interaction to PPyCl films deposited on Au was studied (**Figure 4.1**). Comparisons were made with non-specific adsorption peptides (binding of GRGDS peptides to PPyCl) and specific interaction of the strongest non-covalent bond between streptavidin-biotin. Furthermore, modified T59 peptides, T59 synthesized with GRGDS at the C-terminus, was evaluated in comparison to T59-PPyCl strength of interaction in order to determine the effect of peptide modification in binding PPyCl.

Additionally, recent theory developed by Evans and Ritchie for biomolecular interactions that are largely noncovalent has resulted in dynamic force spectroscopy, where the force/rate of pulling (f = rt) results in an unbinding force depended on the pulling rate (r). This theory was based on the Bell model that described the effect of force on the lifetime of a bond. By varying loading rates versus the unbinding force, a plot of (force spectrum) of F vs. log (r) can be generated. As postulated by Evans and Ritchie, this plot can be used to derive an energy landscape along a one-dimensional path needed to traverse the energy barrier [11,26,27]. When an external force is applied, the activation energy barrier between the two interacting species decreases until complete separation is achieved. Using these principles and an incremental change in external force, the energetics of bond strength have been studied and modeled [28]. In the studies performed with T59 peptides and PPyCl, the resultant force based on varying loading rate ($r_f = k_f v_t$)

was used to determine the off rate (k_{off}) based on the power law at low forces applied for bond rupture [28,29].

4.2 MATERIALS AND METHODS

4.2.1 Titer count analysis to study binding of ϕT59

The binding specificity of the selected phage (ϕT59) was studied using titer count analysis. Binding specificity studies were conducted using other random peptide-expressing phage and various substrates (e.g., polystyrene, polypropylene, and poly (styrene sulfonate)-doped PPy). Specifically, ϕS36 (semi-conductor binding phage isolated in A.M. Belcher's laboratory), ϕC511 and ϕT125-4 (other selected phage from previous incomplete screens against PPyCl), and wild-type (WT, non-engineered) phage were used to compare their binding to PPyCl with respect to ϕT59. Interaction of particular phage was carried out as described in the peptide selection section (**Chapter 3,** *Section 3.2*). Binding was assessed by counting the plaque forming units (pfu), also known as one phage clone, after bacterial infection (see Ph.D. 12^{TM} manual from NEB, Inc. [30]). The various phage were initially allowed to interact with the particular substrates, as described in *Section 3.2* of **Chapter 3**. Briefly, the phage were individually amplified and 10^8 pfu/ul concentration was incubated with either PPyCl or PP or PS substrates for 1 hr in 0.5 μM Tris-buffered saline with 0.1% vol:vol Tween-20 detergent

pH = 7.5 (0.1% TBS-T) with medium rocking (25 RPM) at room temperature. After initial phage/substrate interaction, the film was removed from solution and washed three times with 0.3% TBS-T pH = 7.5. The substrates were then incubated with 0.1 M Glycine-HCl pH = 2.2 for 9 min with medium rocking (25 RPM) at room temperature to obtain the phage bound. The eluted phage from each substrate interaction where then combined with a solution of *E. Coli* bacteria (Optical Density = 0.5) (as highlighted in **Chapter 3**, *Section 3.2*) and plated. The bacteria which express the lacZ gene produce blue colonies when grown in the presence of X-gal. These plaques that stain blue (pfu) were then used to quantify binding of phage to the substrates for relative comparison analysis.

4.2.2 Immunofluorescence study of ϕT59/T59 peptide binding PPyCl

To qualitatively analyze the binding of both ϕT59 and T59 peptide on PPyCl, we used immunofluorescence labeling. ϕT59 was incubated (10^8 pfu/ul) with PPyCl (sample size ~ 0.5 cm^2) and with PPyPSS in 0.1% TBS-T for 1 hr at room temperature with medium rocking (25 RPM). PPyCl films were removed and washed three times with 0.3% TBS-T (pH = 7.5). The samples were incubated with 4% bovine serum albumin (Jackson ImmunoResearch Lab Inc., Westgrove, PA) in TBS for blocking for 30 min with medium rocking (25 RPM) at room temperature. Binding of the phage was qualitatively analyzed using an anti-fd bacteriophage-biotin conjugate (Sigma, St. Louis, MO), an antibody to the pIII protein of M13 phage (1:500 in tris buffered saline (TBS))

for 30 min and then rinsed in TBS. Streptavidin-labeled fluorescein isothiocyanate (FITC) (1:500 in PBS, Sigma) was attached to the biotin conjugated phage through a biotin-streptavidin interaction; the surfaces were exposed to the label for 30 min in the dark and at room temperature and then rinsed several times with PBS. The samples were placed immediately in the dark at 4°C for fluorescence analysis. All of the samples from the experiments were imaged immediately using a confocal laser scanning microscope (Institute of Cellular and Molecular Biology, University of Texas at Austin, Leica TCS 4D, 488 nm FITC excitation).

T59 peptide corresponding to the phage was synthesized (Institute of Cellular and Molecular Biology Core Facilities, University of Texas at Austin) with a Gly-Gly-Gly-Ser (GGGS) linker for stability at the C-terminus, making the peptide sequence THRTSTLDYFVI-GGGS-K-biotin. The biotin group (K-biotin) was attached at the C-terminus for streptavidin-FITC labeling. The reason for attaching a linker at the C-terminal end was to mimic how the T59 peptide is presented on the phage. In the native bacteriophage expressing the peptide, the WT pIII protein is at the C-terminus of the inserted peptide, which has a free N-terminus. 15 μM peptide in 10 mM PBS (pH = 7.4) was incubated with 0.5 cm^2 sample size of PPyCl, PS, and PPyPSS. The samples were washed a minimum of three times with PBS. 4% bovine serum albumin (Jackson ImmunoResearch Lab, Inc., West Grove, PA) in PBS was used as a blocking buffer for 30 min with gentle rocking (25 RPM) at room temperature. The samples were then rinsed with PBS three times. After optimization of streptavidin-FITC concentration (1:500

dilution), samples were labeled in the dark for 1 hr with gentle rocking (25 RPM) at room temperature and then analyzed using a confocal microscope.

4.2.3 Fluorescamine assay and XPS to study T59 peptide binding PPyCl

To determine the role of specific amino acids (H, R and D) in T59 peptide binding to PPyCl, T59 peptide variants were synthesized (Biopolymers Lab, MIT, Cambridge, MA), as highlighted in **Table 4.2**. A fluorescence assay using fluorescamine (4-phenylspirol[furan-2(3H),1'-phthalan]-3,3'dione) reagent (Molecular Probes, Eugene, OR) was used to evaluate peptide binding to PPyCl. Fluorescamine is a nonfluorescent compound that reacts with primary amines (RNH_2) at room temperature to form pyrrolinones, which upon excitation at 390 nm emits strong fluorescence at 475 to 490 nm [31].

A standard curve was prepared using T59 (or variant) peptides in solution with concentrations ranging from 0 - 20 μM. The fluorescence intensity values for each known peptide concentration in solution (ranging from 0 - 20 μM) was measured and a linear plot of known concentration versus intensity was generated. This plot was used to determine the actual bound peptide on PPyCl using a mass balance method, described below. The same procedure for standard curve preparation was followed for each variant. The fluorescamine reagent was prepared in HPLC grade acetone. After incubation of various concentrations of T59 peptide (or variants), ranging from 0 - 20 μM in 10 mM PBS, with PPyCl (0.5 cm^2 sample size, n = 6), the PPyCl samples were removed and the

unbound peptide solution was used for fluorescamine evaluation. The unbound peptide solution, excluding the PPyCl films, was transferred to a 96 well plate (Becton Dickinson, Franklin Lakes, NJ) and then analyzed using a fluorescence plate reader (Synergy HT, Biotek, Winooski, VT) after adding 50 μL of fluorescamine reagent and incubating for 25 sec at room temperature. For measuring the bound peptide on PPyCl, baseline fluorescence intensity was established by using a PPyCl sample without the presence of the peptides and then measuring the intensity of that solution using fluorescamine reagent. Baseline fluorescence intensity was subtracted from each sample. To calculate the actual bound concentration of peptide to T59 a mass balance method was used in which the unbound peptide concentration (measured using fluorescamine reagent) was subtracted from the known input peptide concentration (input = bound + unbound). This provided a relative binding comparison of T59 peptide variants for determining potential key amino acids of T59 peptide in binding PPyCl.

Furthermore, the conditions at which ϕT59 was selected (**Chapter 3**) from the biopanning process, where low pH (2) elution was used to elute (or unbind) phage bound to PPyCl, was used to elute T59 peptides off of the PPyCl surface after incubating T59 peptides with PPyCl sample. The input concentrations of T59 peptides was varied from 0 – 20 μM and PPyCl samples (0.5 cm^2 sample size, n = 6) were incubated at 25^oC for 1 hour while rotating. The PPyCl samples were washed with 10 mM PBS three times followed by incubation with 1 mL of pH 2 10 mM PBS for 30 minutes. This solution was then removed from the PPyCl samples and combined with 200 μL of 0.1 M NaOH to

bring final solution to a neutral pH (7-9). The solution from each different input concentration condition was aliquoted into 150 μL and combined with 50 μL of fluorescamine reagent in a 96-well plate for fluorescence analysis as described previously. A standard curve, as described previously, was prepared ranging from 0 – 20 μM and used to determine the extent of T59 peptides eluted.

XPS elemental surface scan analysis (described in **Chapter 2**) was used to determine the binding of T59 peptide to PPyCl. 30 μM T59 peptide input concentration was incubated with PPyCl sample (0.5 cm^2) at 25^oC for one hour. After washing the sample with 10 mM PBS three times, PPyCl-T59 sample was analyzed for presence of key surface elements including oxygen (O1s, where O represents oxygen and 1s represents the orbital electron detected using XPS), nitrogen (N1s), carbon (C1s), and chloride (Cl2p). To determine the presence of T59 peptide, a total of four samples were prepared: (1) PPyCl incubated with T59 (30 μM), (2) PPyCl incubated with 10% serum-containing cell culture medium, (3) PPyCl incubated with T59 peptides (30 μM) followed by incubation with 10% serum-containing cell culture medium for 1 hour, and (4) PPyCl without any incubation as a control baseline substrate for elemental analysis. The purpose of this experiment was to determine relative binding of T59 peptide to PPyCl by analyzing the various PPyCl samples through the comparison of the relative percentage of the presence of the four elements that occur in PPyCl, serum-proteins (as in the case with serum-containing medium incubation), and T59 peptides.

4.2.4 Atomic force microscopy analysis of T59 peptide and PPyCl

We investigated the strength of T59 peptides in binding PPyCl using AFM [11,26,28]. Initially AFM-tips (Si_3Ni_4-microlever) coated with Au (Model # MSCT-AUNM, Veeco, Santa Barbara, CA) were functionalized with biotinylated bovine serum albumin (biotin-BSA) [32]. Each cantilever contains six tips (**Figure 4.1a**), each of varying dimensions and thus of varying spring constants ranging from 0.01 N/m to 0.5 N/m. During the functionalization procedure, all six tips on the cantilever were functionalized simultaneously, but only one tip was used for adhesion force analysis based on the spring constant (~ 0.01 – 0.15 N/m) necessary for optimal results.

The first step in AFM tip functionalization was immersion in acetone for 5 min and then irradiation with ultraviolet light for 30 min. The irradiated tips were then incubated with 50 μL of biotin-BSA (Sigma, St. Louis, MO; 0.5 mg/mL) overnight at 37^{o}C and then rinsed by immersing in 10 mM PBS (pH 7.4). For streptavidin-biotin surface force analysis (a well studied binding pair), a streptavidin coated surface (Xenopore, Hawthorne, NJ) was used with biotin-BSA functionalized AFM tips. Negative controls were performed, where BSA was interacted with a streptavidin-coated surface. For AFM tip functionalization with GRGDS, T59 and T59-GRGDS peptides, the same procedure was followed where the resultant tips (biotin-BSA-coated tips) were then incubated with 50 μL of streptavidin (Sigma, St. Louis, MO; 0.5 mg/mL in PBS) for 5 min at room temperature. The streptavidin-functionalized tips were then washed in 10 mM PBS, followed by incubation with the peptide solution (15 μM in 10 mM PBS). All

of the peptides used for AFM analysis were synthesized (Biopolymers Lab, MIT, Cambridge, MA) with a biotin group at the C-terminus (T59, THRTSTLDYFVI-K-biotin, T59-GRGDS, THRTSTLDYFVI-GRGDS-K-biotin, and GRGDS-biotin) for linking to the streptavidin-functionalized tips (**Figure 4.1b**).

Binding strength experiments were conducted using AFM at the Center for Nano and Molecular Science and Technology as developed by Asylum Research (Asylum Research 3D MFP, Santa Barbara, CA). The experiments were performed in sterile PBS (10 mM, pH 7.4) and at 25 ^{o}C, where the functionalized tip was brought into close contact to the PPyCl or streptavidin surface. PPyCl samples were synthesized on Au-coated surface to ensure that the films did not detach, as described in **Chapter 2**. A piezo translator with a strain gauge position sensor built into the AFM head was used to rotate a lever, which in turn set the position of the AFM tip relative to the substrate. As the tip approached the surface with the specified approach and retraction velocity (using the MFP3D software equipped with the AFM), the interaction between the AFM tip and the substrate was determined from the deflection of the AFM cantilever. This deflection was monitored using a focused laser spot reflected off the reverse side of the cantilever. The force apparatus was equipped with an inverted optical microscope for visualization of the tip over the substrate. The unbinding force for each curve was determined by taking the difference between the approach line and the maximum point of retraction (**Figure 4.9**). Force measurements were taken at constant loading rates ($r_f = k_f v_t$, where k_f is the spring constant and, v_t is the vertical piezo velocity of 500 nm/s) where the spring constant (12 ±

5 pN/nm) of the tip was calibrated in PBS by the thermal fluctuation method [33]. The most probable unbinding force was determined by fitting a Gaussian to the histogram generated by the force distribution (n = 300, 10 spots per sample and 30 curves per spot) [11,28]. The error was estimated by $SD/(N)^{1/2}$, where SD is the width of the distribution and N is the number of unbinding events in the histogram.

As proposed and developed by Evans and Ritchie, for better understanding of interaction between two molecules it is necessary to examine the dynamic response of the complexes to external mechanical forces by varying loading rates, the rate at which the two interacting species are pulled apart [28]. For this study, loading rates were varied from 900 to 54,000 pNs^{-1} by varying the pulling velocity (piezo velocity) from 50 to 3000 nms^{-1} with a spring constant of 18 ± 3 pN/nm determined using thermal analysis function in the MFP3D software equipped with the AFM. For each loading rate, 150 different plots were acquired and 10 sample curves at 15 different spots were used to generate a histogram, as previously described. Based on these results, a plot of the dependence of the unbinding force (F) on the loading rate (r) (plot of F vs. ln r) was generated to evaluate binding regimes based on the energy landscape involved in T59 peptides binding to PPyCl. Additionally, as developed by Bell and Evans [28,33], this plot was also used to characterize a dissociation rate (k_{off}) in the absence of applied force or load. As developed by Bell, the theory suggests that an applied force F decreases the activation energy for dissociation from $\Delta E^{\ddagger}$ to $\Delta E^{\ddagger}(F)$ with the relation $\Delta E^{\ddagger} - \Delta E^{\ddagger}(F) = -\chi_{\beta} \bullet F$, leading to an exponential increase in k_{off} with increasing force [$k_{off}(F) = k_{off} \bullet e\text{^}(F \bullet \chi_{\beta}/k_B T)$] ($k_B T$

= *thermal energy per molecule*). The proportionality factor (χ_β) is described as the dimension of length that characterizes the relationship between force and dissociation rate. Using these conditions the most probable unbinding force F can be calculated:

$$F = (k_B T/ \chi_\beta) \bullet \ln (r \chi_\beta / k_{off} k_B T)$$

[2]

From the experimental plot generated, k_{off} was determined, where the slope, $k_B T/\chi_\beta$, was calculated from the plot and the k_{off} value was calculated from F = 0 ($k_{off} = rx_B/k_B T$).

4.3 RESULTS

4.3.1 Titer count analysis to evaluate specificity of ϕT59 to PPyCl

Titer count analysis was used as a relative binding comparison of phage counts between T59 phage, randomly selected phage from other substrates, and WT (non-engineered) phage. Results from the first binding study demonstrate that T59 phage binds significantly better to PPyCl, by an order of magnitude, when compared to randomly selected phage and WT phage (**Figure 4.2**). Substrate binding specificity of the T59 phage to PPyCl was evaluated by comparing the extent of binding with other polymers (i.e., polypropylene and polystyrene). Polystyrene and polypropylene were selected because they are common polymers used in the lab and are part of the plasticware used in the biopanning experiments. The results show that the T59 phage binds to PPyCl, but exhibits negligible binding to the other selected substrates (**Figure 4.3**). The results

illustrate the dominant binding of ϕT59 to PPyCl by two orders of magnitude with equal input concentrations (10^8 pfu/ul) of each phage. This further confirmed the results of selection in which the occurrence ϕT59 was greater than ninety percent in the last biopan round (**Chapter 3**), suggesting selective binding to PPyCl.

4.3.2 Immunfluorescence evaluation of ϕT59 and T59 peptide binding

To visualize the extent of surface coverage of ϕT59 on PPyCl, immunofluorescence was used by labeling the phage with a biotinylated anti-pIII protein antibody (2^oAb, streptavidin-FITC) (**Figure 4.4**). The results demonstrate that ϕT59 binds to PPyCl with near uniform surface coverage, whereas a negative control phage, ϕC511 (selected from a previous incomplete screen of PPyCl), demonstrates no binding. This comparative study suggests that ϕT59 surface coverage was not selective for specific regions of the surface, rather throughout the surface, indicating that the overall PPyCl properties such as overall surface charge may potentially be involved in controlling ϕT59 binding.

The eventual goal of using phage-displayed peptide selection is for surface functionalization using the 12-mer peptide as a bi-functional linker, where one end of it is free to interact with PPyCl and the other end for modification with a biomolecule, for example a cell adhesion promoting peptide (e.g., RGD) [35]. To study the potential applications of T59 peptide as a bifunctional linker, the peptide (independent of the phage) was synthesized and qualitatively studied for binding to PPyCl. During the

synthesis a biotin group was added at the C-terminus (T59-GGGS-K-biotin), and qualitative binding was demonstrated using streptavidin-FITC labeling (**Figure 4.5**). The lack of T59 peptide binding to both polystyrene and PPyPSS shows that the peptide is not only specific to PPyCl, but that it is inert to other surfaces, thereby excluding binding through nonspecific adsorption. When comparing T59 peptide binding to PPyCl versus binding to PPyPSS, we can speculate that the binding is dopant specific, but additional studies using dopant and polymer analogs are necessary to elucidate the precise mechanism of binding and the effects of structural topography. Additionally, T59 peptide did not completely and uniformly cover PPyCl's surface, as illustrated by the fractured pattern (**Figure 4.5b**). The reasons for this are not completely understood, although the heterogeneous surface topography (as illustrated in **Figure 2.3** in **Chapter 2**) and as previously demonstrated by Silk et al. [36], may be an important factor for the actual binding of T59 peptide to PPyCl.

4.3.3 The role of key amino acids in T59 peptide binding to PPyCl

To study the role of specific amino acids of T59 in binding PPyCl, an initial set of peptide variants (**Table 4.1**) was synthesized. Using a fluorescamine assay, relative binding concentration of each variant was evaluated with varying input concentrations (0 - 20 μM). The results in **Figure 4.6** demonstrate that variant T59D (Asp replaced with Gly) and FT59 (front six amino acids of T59 alone) did not bind to PPyCl, whereas BT59 (back six amino acids of T59 alone), BRT59 (back six amino acids reversed), and RT59

(T59 sequence reversed) demonstrated comparable binding to native T59 at varying input concentrations. The binding of T59, RT59, BT59, and BRT59 was statistically insignificant at each different input concentration. From these results it was difficult to assess the precise bound concentration by the presence of large standard deviation, rather a trend can be visualized. For this reason, **Figure 4.7** was generated to illustrate percent binding with respect to T59 at 15 μM input concentration. These results suggest that aspartic acid is a critical amino acid for T59 peptide binding to PPyCl. Studies with varying pH (**Figure 4.8**) further confirmed the significance of aspartic acid in modulating the binding of T59 peptides to PPyCl. The binding at pH below 4 was below 25% of T59, whereas above pH 6, the binding was significantly greater and comparable to T59 binding ($p<0.05$). As the pH became more acidic (Asp R-group $pK_a \sim 4.0$) and dropped below the pK_a of the Asp R-group, the binding diminished significantly.

T59 peptide binding to PPyCl was studied using pH 2 elution, as the conditions used in ϕT59 elution (**Chapter 3**, *section 3.2*) was a low pH elution to remove the bound phage where ϕT59 was one of the phage that demonstrated significant binding through various biopanning rounds. The pH 2 elution of T59 peptide results, as illustrated in **Figure 4.9**, demonstrate that as the input concentration T59 peptide is increased the amount of bound T59 peptide eluted was negligible and unchanged. Standard controls were used where T59 peptide was diluted in 10 mM PBS with increasing concentration (0 - 20 μM) to demonstrate the ability to use fluorescamine reagent to detect changes in T59 peptide concentration for comparison with the T59 peptide elution results. This suggests

that T59 peptides was not able to be eluted from PPyCl surface after binding as was hypothesized by the low pH elution of ϕT59 during the biopanning process. The detection of T59 peptide on PPyCl studied using XPS elemental analysis (**Figure 4.10**) was inconclusive as the change in relative percent occurrence of the key elements (O1s, N1s, C1s, and Cl2p) was unchanged with respect to the PPyCl sample control. Additionally, when serum proteins from serum-containing medium incubation with PPyCl was performed (**Figure 4.10**), the ability to detect proteins on the PPyCl surface was inconclusive, suggesting that XPS elemental analysis was insufficient in obtaining significant results. The binding of T59 peptides to PPyCl at an extremely low concentration with serum protein was evaluated in combination, which also resulted in inconclusive results.

4.3.4 Atomic force microscopy to evaluate strength of interaction

The strength of interaction between T59 peptides and PPyCl was assessed using AFM to measure discrete intermolecular forces. As illustrated (**Figure 4.11**), the binding strength of T59 peptide to PPyCl was compared to other relevant biomolecular interactions such as the biotin-streptavidin bond. The retract trace exhibits an unbinding force before it reaches the set point (**Figure 4.12**). The rupture force (adhesion force) was determined for each binding partner using a constant loading rate ($f = \kappa_s \times \nu_c$) 6000 ± 1500 pN/s , where κ_s is the spring constant and ν_c is the retraction velocity [11]. The binding strengths of T59 and T59-GRGDS peptides to PPyCl were evaluated and compared to a well known streptavidin-biotin interaction [10] (**Figure 4.13**). GRGDS, a

cell adhesion promoting peptide derived from extracellular matrix proteins such as fibronectin [37,38], was used for PPyCl functionalization via T59 peptide, as described below. The results demonstrate that the strength of interaction between the T59 peptides and PPyCl is greater than nonspecific adsorption, but significantly lower than that of the streptavidin-biotin bond (consistent with previously published data) [10], the strongest non-covalent bond known. Appropriate controls (biotin and streptavidin interaction to PPyCl) were performed to ensure that the measurements correspond to the specific T59-PPyCl interactions and not to other nonspecific sources (**Figure 4.14 and 4.117**).

Figure 4.18, panels A through D show force histograms obtained at loading rates of 900 to 54,000 pNs^{-1}. The corresponding mean rupture forces were 36 ± 14 pN, 50 ± 21 pN, 74 ± 28 pN, and 132 ± 58 pN (n = 150 for each different loading rate). This increase in resultant force (F) based on an increasing pulling force, indicates the dependence of force application in the resultant rupture strengths, as suggested by the Bell model and Evans' theory. Using the equation presented by Bell on the dynamic force response (*Equation 2*) and based on the results presented in **Figure 4.19** (F vs. log r), a dissociation rate k_{off} of the bonds between T59 peptides and PPyCl was calculated in the absence of an applied force. From the plot we can obtain the slope $k_B T/x_\beta$ and by extrapolating to F = 0, *Eq. 2* reduces to $k_{off} = r \bullet x_\beta / k_B \bullet T$. For T59 peptides-PPyCl, k_{off} = 0.252 s^{-1}. This type of dissociation rate constant approximation has been attempted for other molecules including ligand-receptor interactions where a k_{off} was determined for different single-chain F_v fragments [18].

4.4 DISCUSSION

The specific goals of the work presented in this chapter were to characterize the binding of both ϕT59 and T59 peptides in an effort to better understand the specificity and strength of interactions with PPyCl. To determine the specificity of ϕT59 phage binding to PPyCl, we investigated two methods: titer count analysis for comparing ϕT59 and various phage binding to PPyCl and other selected substrates and immunofluorescence for qualitative binding analysis. The outcome of these studies (**Figure 4.2-4.4**) indicate that the ϕT59 bound significantly better than the other selected phage compared, as demonstrated by the lack of ϕT59 binding to both PPyPSS and PS. Although these results do not demonstrate binding affinity and direct specificity, they did demonstrate selective binding in comparison to the applied conditions.

In an effort to study the binding of T59 peptides, independent of the phage, T59 peptides synthesized with a GGGSK-biotin linker were qualitatively imaged using streptavidin-FITC labeling. The results demonstrated non-uniform binding to PPyCl (**Figure 4.5**). The actual binding of the T59 peptides to PPyCl seemed to indicate that the peptides may potentially be modifiable and applicable as a bifunctional linker for surface functionalization of PPyCl. Therefore, to better understand the actual binding mechanism and involvement of key amino acids in recognizing PPyCl, an initial set of T59 peptide variants were synthesized based on an inspection of the physicochemical properties of the individual amino acid R-groups and a limited combinatorial approach based on the charged amino acids present (His, Arg, and Asp) (**Table 4.1**).

We examined these variants using a fluorescamine assay to detect the actual presence of the peptides on PPyCl using an indirect mass-balance approach (input = unbound + bound). The outcome of this study (**Figure 4.6**) suggested that an apparent trend was not present in binding as input concentration was increased based on the large standard deviations for all of the variants studied. Although conclusive results were not acquired, possibly due to the lack of sensitivity in the assay, the results do suggest a statistically significant difference between the T59D and FT59 variants when compared to T59, BT59, and BRT59 (**Figure 4.7**). From this comparison it can be concluded that Asp is an important amino acid in the recognition and binding of T59 peptides to PPyCl. Additionally, as suggested by the pH studies presented in **Figure 4.8**, as the pH of the interaction condition between T59 peptides and PPyCl was dropped below the pK_a of Asp ($pK_a \sim 4$), the binding diminished significantly, further confirming the importance of Asp.

The binding of RT59 (reverse T59) to PPyCl was comparable to T59 (**Figure 4.7**), indicating the importance of the presence of amino acids rather than the sequence order in which they occur. From the T59 variant results, a hypothesis can be derived stating that the binding is not sequence specific, but rather is composition specific. When observing the overall T59 peptide sequence, the N-terminal end has a hydrophilic character, suggesting its potential importance in solubility. The C-terminal end of the peptide contains the negatively charged aspartic acid residue (at pH 7.4). This negative charge on the R-group (-COOH) of aspartic acid provides an acidic ion that controls binding to the

overall positively charged PPyCl. Lastly, the aspartic acid residue is surrounded by a hydrophobic region, which could provide its own affinity for modulating the folding of the peptide. This initial study was performed using a limited number of combinatorial peptides. To elucidate the precise mechanism of interaction, a combinatorial approach with computational modeling will be required.

Moreover, in the Ph.D.12^{TM} M13 library used to select the ϕT59, 2.8% occurrence of aspartic acid was reported [30] (highlighted in **Table 4.4**), indicating that other peptide inserts in the library did contain aspartic acid residues. Additionally, Asp is present at positions 1 and 10 in clone ϕT125-4 (**Figure 4.2**). Based on this we speculate that although the presence of aspartic acid in T59 peptide is critical for PPyCl recognition, it is not the only essential amino acid (as ϕT125-4 did not bind to PPyCl). Based on TiO_2-binding peptide studies [1], we may also speculate the formation of a salt bridge between the Arg and Asp residues that may lead to the folding of the T59 peptide to recognize PPyCl. If this salt bridge is crucial in T59 binding to PPyCl, then a peptide variant that contains only the back six amino acids (**Table 4.1**, BT59 peptide variant), would lose the ability to bind to PPyCl. Future studies using both a combinatorial approach and computational modeling will be used to elucidate the exact mechanism of interaction.

The pH 2 elution studies reflected the inability to unbind T59 peptides from PPyCl surface as was hypothesized based on the low pH ϕT59 elution during the biopanning process. This suggests that the binding of T59 peptide is potentially governed by more than electrostatic interactions between Asp and the PPyCl backbone.

Additionally, a possible variation of sequence confirmation and folding of T59 peptide when compared to the sequence on the ϕT59 may have led to the inability to elute using low pH. In the future this could be tested by studying peptide models and empirical analysis of both the phage-containing peptide and the peptide alone. If charge interaction was the sole method of T59 peptide and PPyCl surface binding; pH 2 elution would have resulted in unbinding of T59 peptides, which was not observed (**Figure 4.9**). Additionally, the unbinding of T59 peptides may have occurred at extremely low concentrations near the nanomolar range, and because of the detection limits of the fluorescamine assay the unbinding of T59 peptides in this range would not be detected [31]. To address these issues, in future studies it would be beneficial to use radiolabeled T59 peptides for radioactive determination of binding as it would provide greater sensitivity. The attempt to detect the binding of T59 peptides using XPS elemental analysis was unsuccessful as presented in **Figure 4.10**. The relative comparison of the presence of the key elements in PPyCl, T59 peptides, and serum proteins demonstrated insignificant results. The binding of T59 peptides to PPyCl is noncovalent and potentially based on electrostatic and van der Waals interactions (suggested by the AFM and T59 peptide variant studies); therefore the change in the state of elemental interactions cannot be detected using XPS elemental analysis. For detection using XPS it would be necessary to have change in electron spin states, as would occur with covalent bonds [41]; this is not the case in T59 and serum proteins interacting with PPyCl.

We also explored the strength of interaction between T59 peptides and PPyCl using atomic force microscopy based on the theory of dynamic fore spectroscopy. As suggested by the Bell model [34] an increased rate of bond dissociation under external force can be used to extrapolate the off rate (k_{off}) between two species. Initial studies were performed using a single loading rate (6000 pNs^{-1}) for studying the strength of interactions between T59 peptides and PPyCl. This binding strength was compared to a well known streptavidin-biotin interaction [10] and non-specific adsorption of GRGDS peptides to PPyCl (**Figure 4.11**). When compared to streptavidin-biotin interactions, T59 peptide-PPyCl binding was significantly lower. However, a direct correlation cannot drawn from these results as the amount T59 peptide present when interacting with PPyCl was not deduced. In comparing the strength of T59 and T59-GRGDS to nonspecifically adsorbed GRGDS to PPyCl, roughly two times greater strength was achieved. Additionally, when compared to published data for van der Waals interactions (12 pN) and hydrogen bonding (17 pN) [10,40], the binding of T59 and T59-GRGDS to PPyCl is an order of magnitude greater.

A preliminary study using loading rate variations to derive an energy landscape and dissociation constant was performed using dynamic force spectroscopy. By developing a plot of strength versus loading rate (expressed on a log scale) a map of the most prominent barriers traversed in the energy landscape guided along the force-driven pathway (externally applied as a function of loading rate) can be deduced, as described by Evan Evans [28]. The kinetics of escape is demonstrated as a stationary flux of

probability density along a preferential path from the energy minima past the barrier and transition into the energy surface. Evans schematically demonstrated the effect of external force leading to a mechanical potential that tilts the energy landscape resulting in a diminishing energy barrier at the transition state to a free state [28]. A particular study of streptavidin-biotin demonstrated a presence of multiple barriers on a plot of loading rate versus strength where at a lower loading rate a distinct linear regime was present and as the loading rate increased an abrupt change in slope was occurred, suggesting a sharp barrier. The analysis, as concluded by Evans, was based on the presence of sharp changes in slope that suggestsmultiple barriers were traversed. This lead to the conclusion that the binding between streptavidin-biotin was composed of three binding regimes. A dynamic force spectroscopy study of T59 functionalized tip binding to PPyCl resulted in a similar analysis as Evan Evans [28,29]. As the results presented in **Figure 4.17** and **4.18** suggest, a binding constant (k_{off} = 0.252 s^{-1}) in the range of weak antigen-antibody forces [18] was detected. Furthermore, by analyzing the F vs. ln(r) in **Figure 4.18**, it can be hypothesized that a potential single binding regime is present where the unbinding of peptide with a single binding domain, which interacts with PPyCl either via electrostatic interaction or simple hydrophobic interactions. Based on the results, a single slope is present, which results in a potential conclusion that binding between T59 peptides and PPyCl is based on a single interaction, where a single binding domain on T59 peptides recognizes the PPyCl surface. A thorough analysis is necessary in the future where the concentration of T59 peptides on the AFM tip is controlled and quantifiable. Additionally,

the ability to assess binding strength at lower loading rates can significantly enhance the accuracy of the results.

In conclusion, we report a series of studies indicating binding of both ϕT59 and T59 peptide to PPyCl using various methods. As the initial studies suggest, the Asp residue plays an important role in the binding of the peptide to PPyCl. Furthermore, the specificity of interactions was not clearly identified, although the AFM studies suggest that the binding is not strong and in the order of weak antigen-antibody interactions. We believe that other well defined and absolute quantitative methods are necessary to better characterize the peptide binding to PPyCl, possibly by using thermal techniques and other combinatorial peptides.

Table 4.1 T59 peptide variants

Variant	Sequence	Rationale for selection
T59	THRTSTLDYFVI	Control: original T59 sequence selected from biopanning
RT59	IVFYDLTSTRHT	T59 reversed sequence (to study the role of sequence order)
FT59	THRTSTGGGGGG	T59 with only the front six amino acids preserved (to study the role of the basic amino acids (HR) found in the front half of the T59 sequence); back six amino acids replaced with Gly (G)
BT59	GGGGGGLDYFVI	T59 with only the back six amino acids preserved (to study the role of acidic amino acid (D) found in the back half of the T59 sequence); front six amino acids replaced with Gly (G)
T59D	THRTSTLGYFVI	T59 with aspartic acid (D) replaced by Gly (G) (to study the importance of Asp)
BRT59	GGGGGGIVFYDL	T59 with the order of the back six amino acids reversed (to study the role of sequence order)

Table 4.2 Properties of the charged amino acids in T59 peptide

T59 peptide amino acid	**Position ($^{1}N \rightarrow {}^{12}C$)**	**pK_a (R)**	**Charge (R) at pH 7.4**	**Classification**
His (H)	2	6.0	Neutral (96%)	Active aromatic & basic
Arg (R)	3	12.5	Positive	Basic
Asp (D)	8	3.9	Negative	Acidic

Table 4.3 AFM measurements on biomolecular forces with varying binding partners

Binding pairs (partners)	**Reference**
Biotin-(strept)avidin	[10-12]
Covalent bonds	[13]
Polysaccharides	[14,15]
Antibody-antigen	[16-18]
Intramolecular Titin	[19-21]
DNA	[22-24]

Table 4.4 Amino acid distribution in native Ph.D. 12 phage library

Amino Acid	Observed Frequency	Amino Acid	Observed Frequency
Thr (T)	11.1 %	Asp (D)	2.8%
His (H)	6.3%	Tyr (Y)	3.6%
Arg (R)	4.7%	Phe (F)	3.3%
Ser (S)	10.0%	Val (V)	3.9%
Leu (L)	9.3%	Ile (I)	3.4%

Adapted from the Ph.D.12-library manual [30]
Reduced genetic code NNK (32 codons) was used in constructing this library. A total of 104 clones from the native library were sequenced and the overall amino acid distribution from the 1176 sequenced codons were used to determine the observed frequency of each amino acid.

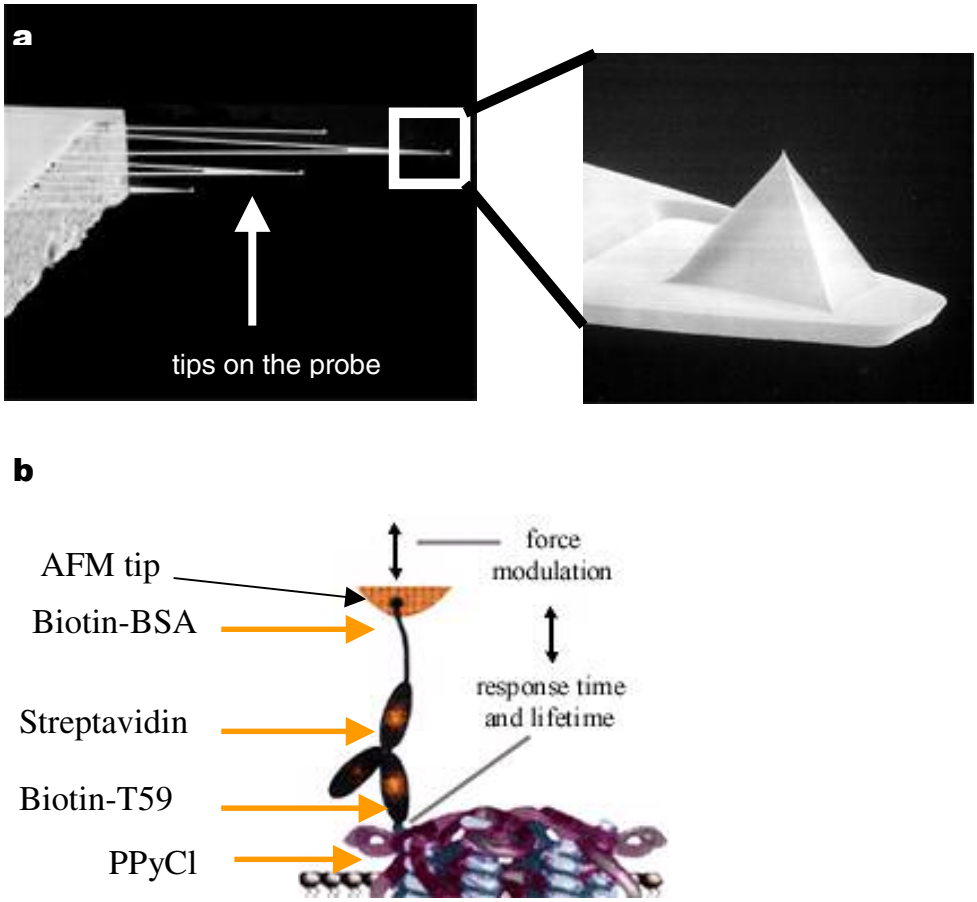

Figure 4.1 Illustration of the Au-coated Si_3N_4 cantilever and functionalized tips.

(a) Each probe contains six tips that vary in dimension, which imparts different spring constants (0.01 N/m to 0.5 N/m). (left) Enlarged image of one of the tips. By probing with different tips on the cantilever, the loading rate (spring constant X velocity) can be varied. *(figure from http://www.veeco.com)*

(b) Functionalized AFM tip used to determine the unbinding force of T59 peptides and PPyCl. Image is a schematic of the molecules immobilized and does not reflect the actual ratio of numbers of molecules present (nor is the image to scale). *(figure adapted from http://www.veeco.com)*

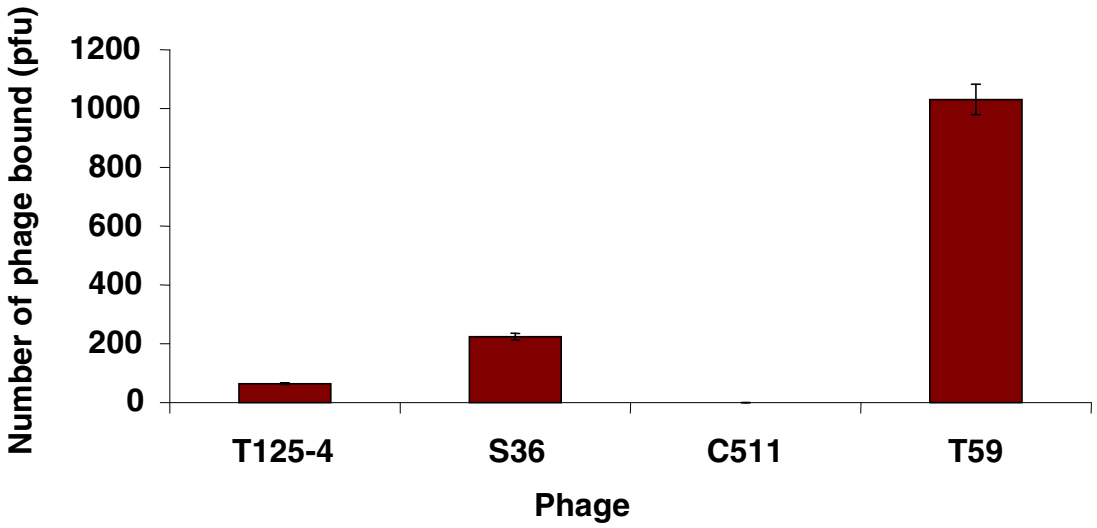

T125-4	D	I	I	S	S	W	Y	M	P	D	H	P
S36	W	T	V	Q	T	P	T	M	L	P	M	M
C511	M	P	A	V	M	S	S	A	Q	V	P	R
T59	**T**	**H**	**R**	**T**	**S**	**T**	**L**	**D**	**Y**	**F**	**V**	**I**

Figure 4.2 ϕT59 binding to PPyCl compared to the binding of random phage selected from various panning rounds. The T59 phage binds significantly better to PPyCl compared to the other phage. Thus, the binding of T59 to PPyCl is unique because of the peptide sequence that is expressed on the pIII coat protein of the M13 phage (n=3). Note: the binding for C511 is so low that it is not visible on the plot above.

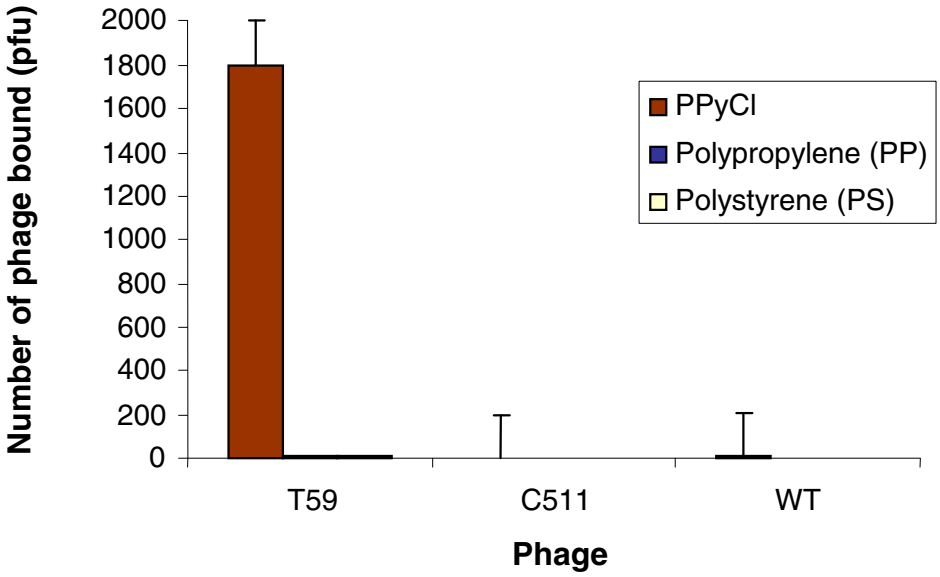

Figure 4.3 ϕT59 binding is relatively specific to PPyCl. The T59 phage exhibits insignificant binding to the other polymers, further confirming that T59 is specific to PPyCl (n = 3). Note: the binding of the different phage to the PP and PS surfaces are too low to be distinguished on the plot above.

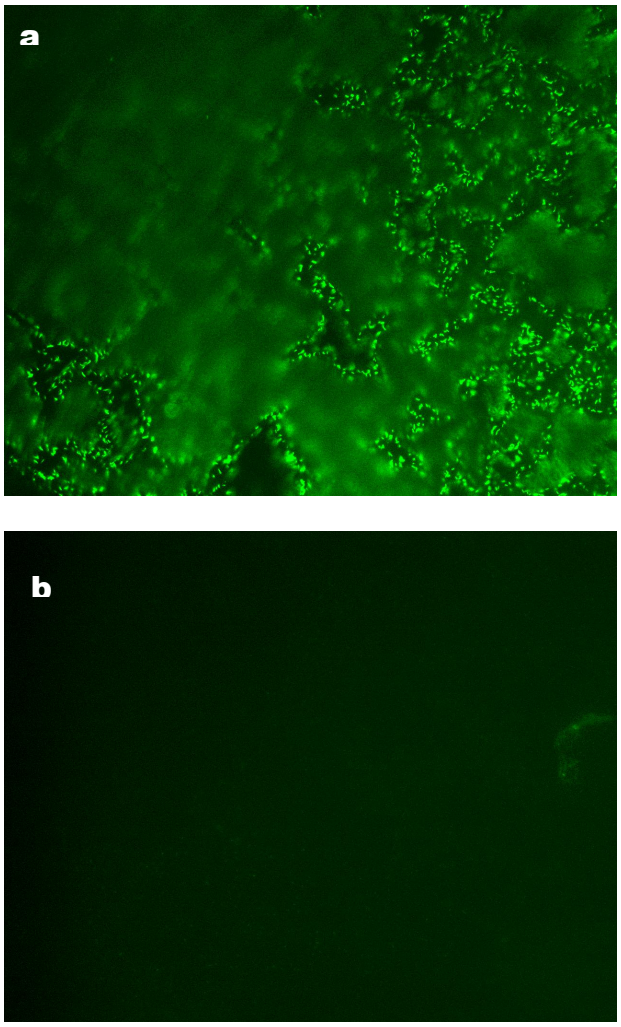

Figure 4.4 T59 phage, compared to a random phage, uniquely binds to PPyCl.
(a) T59 phage bound to PPyCl was visualized using an antibody-biotin-streptavidin-FITC label and fluorescence microscopy. (b) Random phage (ϕC511) bound to PPyCl. No binding to PPyCl was observed in this case. Bar, 100 μm.

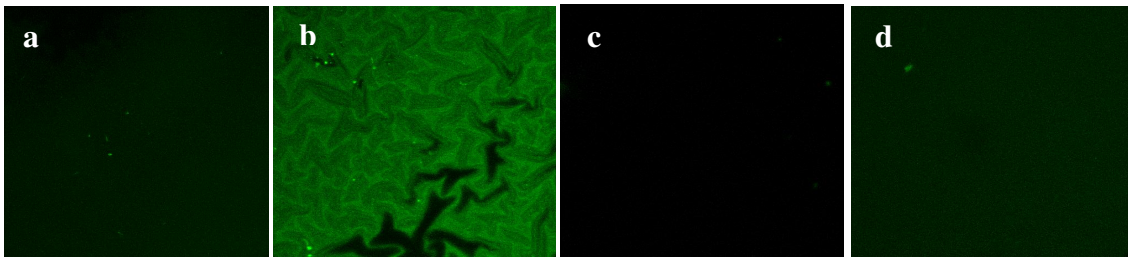

Figure 4.5 T59 peptide (synthesized from the sequence from the T59 phage) binds to PPyCl and not to PPyPSS or to polystyrene (PS). Binding was studied using biotinylated T59 peptide and streptavidin-FITC labeling. (a) control substrate in which no T59 peptide was added. (b) 15 μM peptide bound to a 0.5 cm^2 PPyCl substrate. (c) 15 μM peptide bound to a 0.5 cm^2 PPyPSS substrate. (d) 15 μM peptide bound to 0.5 x 0.5 cm^2 polystyrene (PS) substrate. All samples were incubated with equal concentrations of streptavidin-FITC. Bar, 100 μm.

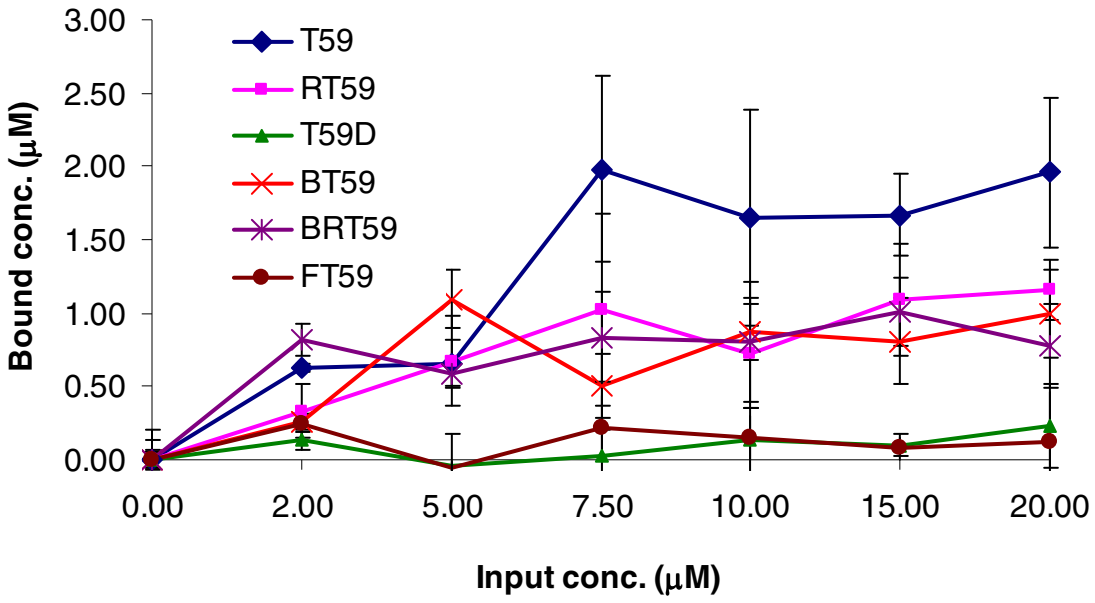

Figure 4.6 Relative binding of T59 and variants was compared using fluorescamine assay. The relative binding of T59 peptides variants, highlighted in Table 4.1, to PPyCl (0.5 cm^2) was compared by incubating PPyCl samples with varying concentrations. An indirect method using a mass balance method (input = bound + unbound) was used to determine the bound concentration of peptides to PPyCl. The large standard deviations present throughout all of the concentrations did not permit actual bound peptide analysis, rather a relative comparison suggests that when aspartic acid residue is not present (T59D and FT59), the binding of the peptide significantly diminishes ($p < 0.05$). The errors are standard deviation, where n = 6.

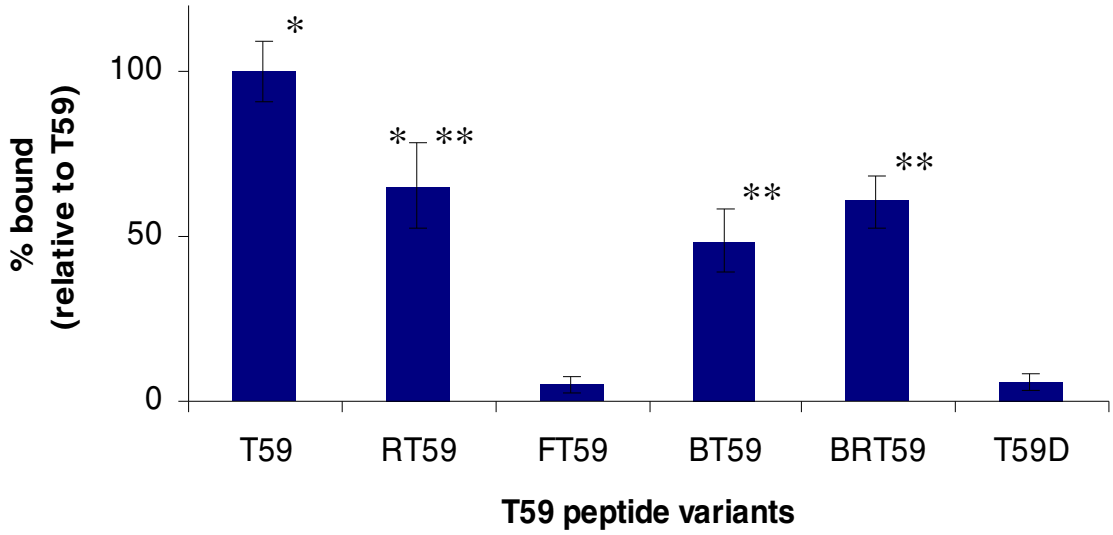

Figure 4.7 Illustration of relative binding of T59 variants to PPyCl with respect to T59 peptides. When aspartic acid is present (T59, RT59, BT59, BRT59) binding is maintained, but diminishes with its absence (FT59 and T59D). (*):T59 and RT59 binding is statistically significant. (**): RT59, BT59, and BRT59 binding is not statistically significant ($^{**}p<0.05$). The errors are standard deviation. For all samples n = 6.

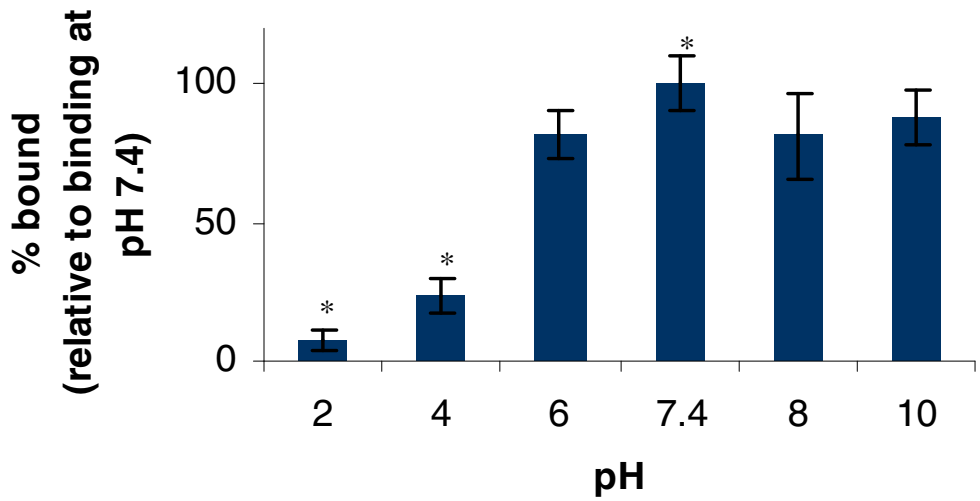

Figure 4.8 The role of Asp was further confirmed by varying the pH of the input concentration of T59 peptide (15 μM). The results show that below the pK_a of the oup of Asp (~4.0), the binding is significantly reduced as the R-group (-COOH) is in its protonated state (neutral) and no longer reactive. The symbol (*) indicates that T59 peptide binding above pH 7.4 is statistically significant ($n = 4$, $p < 0.05$).

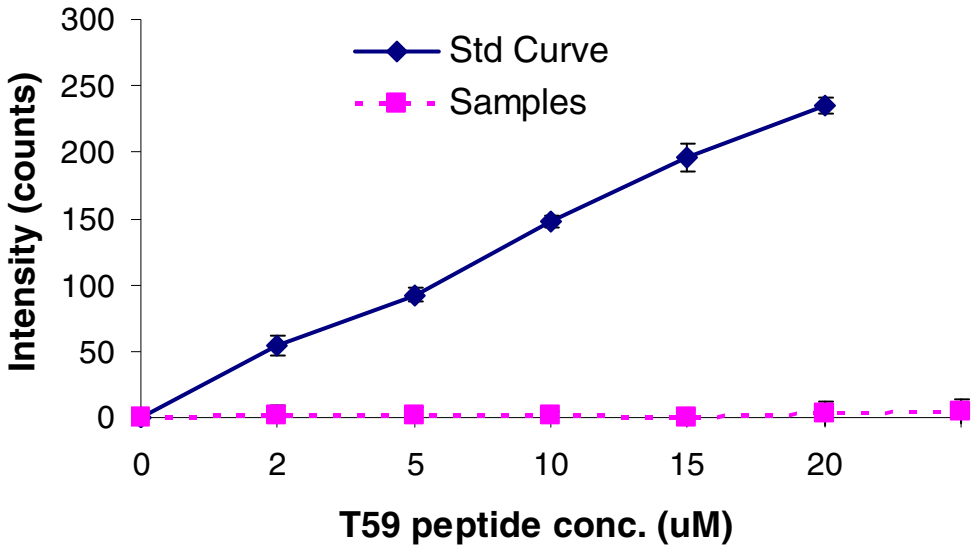

Figure 4.9 T59 peptide elution using pH 2 conditions post-T59 peptide incubation with PPyCl. Fluorescamine assay was used to determine the intensity because of T59 peptide presence after elution by comparing to standard curve (solid line, n = 6). As the input concentration was increased the fluorescence intensity increased almost linearly in the standard condition where T59 peptide was present in solution at known concentrations. This was not observed in the pH 2 elution condition (dotted line, n = 6), as this indicates that low pH elution did not remove the bound T59 peptides from PPyCl at varying input concentrations.

Sample	Element	Concentration (%)
PPyCl	O1s	31.68
	N1s	10.41
	C1s	69.94
	Cl2p	5.98
PPyCl-T59	O1s	18.12
	N1s	9.67
	C1s	71.15
	Cl2p	1.05
PPyCl-serum proteins	O1s	17.25
	N1s	11.30
	C1s	69.21
	Cl2p	2.25
PPyCl-T59-serum proteins	O1s	20.57
	N1s	12.98
	C1s	65.53
	Cl2p	0.92

Figure 4.10 XPS elemental survey scan of the four elements present in PPyCl and potential variation in their occurrence as indicated by binding of T59 peptides and serum-proteins resulted in the lack of significant variation amongst samples. For example, when comparing N1s element in the four samples there appears to be an insignificant variation in the percent occurrence suggesting that T59 peptide and serum-proteins could not detected on PPyCl. If binding of T59 peptides or serum proteins on PPyCl could be detected, there would be a change in the relative concentration percentage for both N1s and O1s elements. Each sample was analyzed with equal areas to ensure accuracy for comparison.

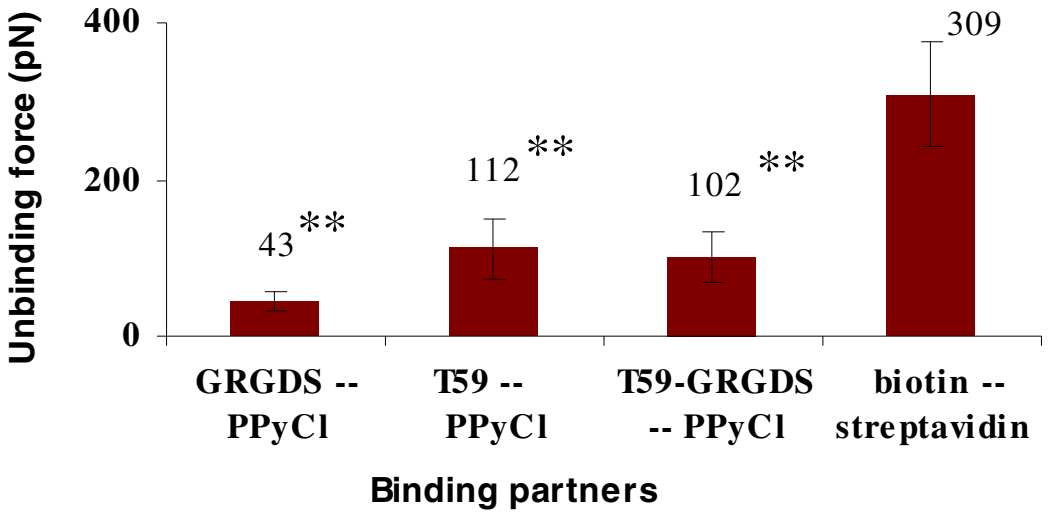

Figure 4.11 Relative binding strength evaluation of T59 peptides to PPyCl. Mean unbinding force for T59-PPyCl is compared to that of biotin-streptavidin. Modification of T59 with GRGDS does not alter its binding to PPyCl. The strength of T59 and T59-RGD binding to PPyCl is statistically higher than that of nonspecifically adsorbed RGD to PPyCl (n = 300, where 10 spots where selected with 30 curves per spot, $^{**}p<0.05$). The error bars are standard deviation.

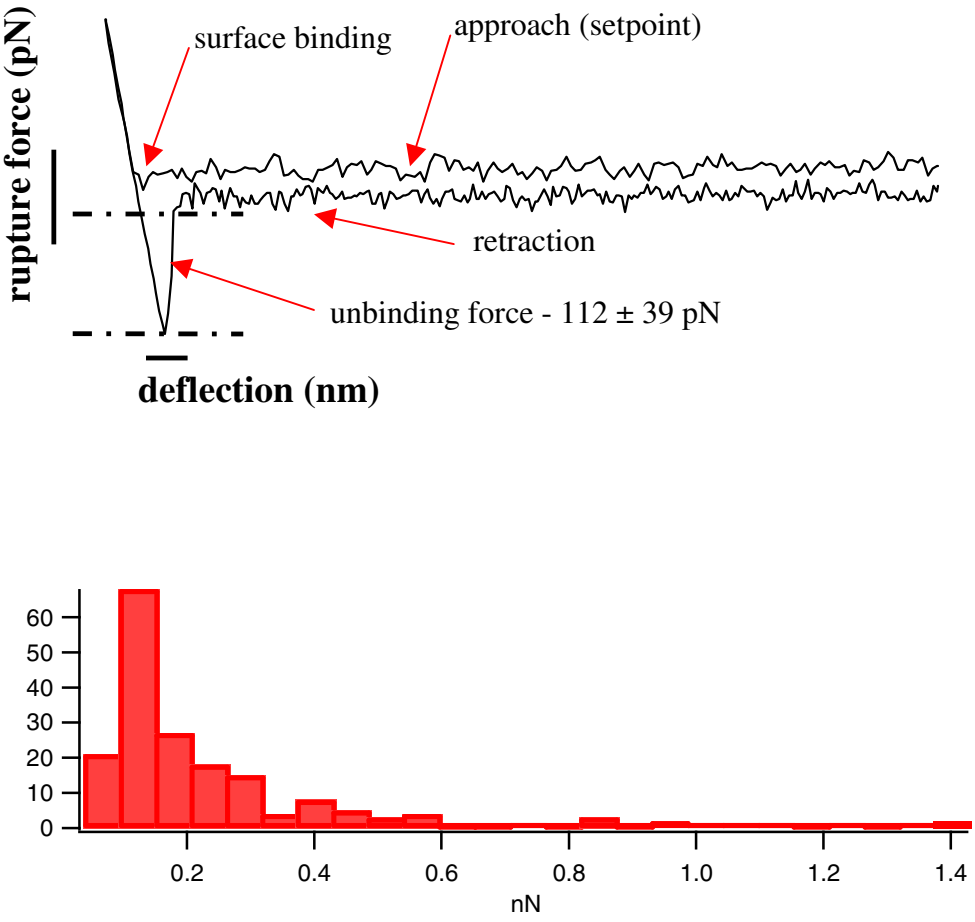

Figure 4.12 Illustration of a typical force plot of T59-PPyCl interactions using biotin-BSA and streptavidin functionalized tip. Biotinylated T59 peptides (T59-K-biotin) were used where a constant loading rate ($f = \kappa_s \times \nu_c$) 6000 ± 1500 pN/s was applied for each force curve. Typical force plot: as the tip approaches the surface, binding between T59 peptides and PPyCl results in a force of adhesion; as the tip is retracted from the surface, force is required to rupture the bonds. The histogram generated was used to determine an average (SD) rupture force where the x-axis is rupture force and y-axis is frequency of that particular force.

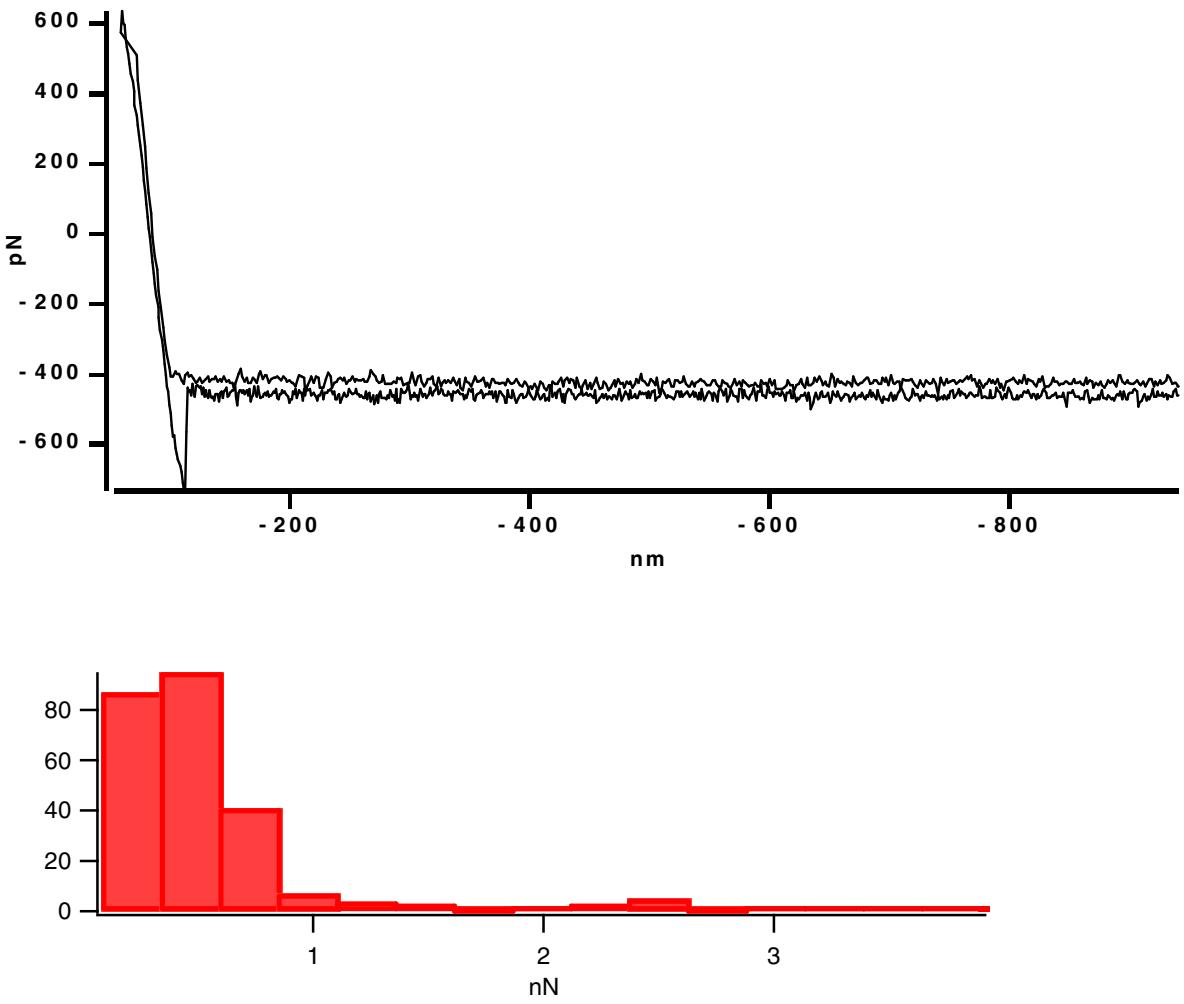

Figure 4.13 Illustration of a typical force plot of streptavidin-biotin interactions. Au coated Si_3N_4 tip was functionalized with biotin-BSA and interacted with streptavidin-coated surface with a constant loading rate ($f = \kappa_s \times \nu_c$) 6000 ± 1500 pN/s was. Typical force plot: as the tip approaches the surface, binding between biotin and streptavidin results in a force of adhesion; as the tip is retracted from the surface, force is required to rupture the bonds (average adhesion force of 309 ± 67 pN). The y and x-axis scales are not absolute. The histogram generated was used to determine an average (SD) rupture force where the x-axis is rupture force and y-axis is frequency of that particular force.

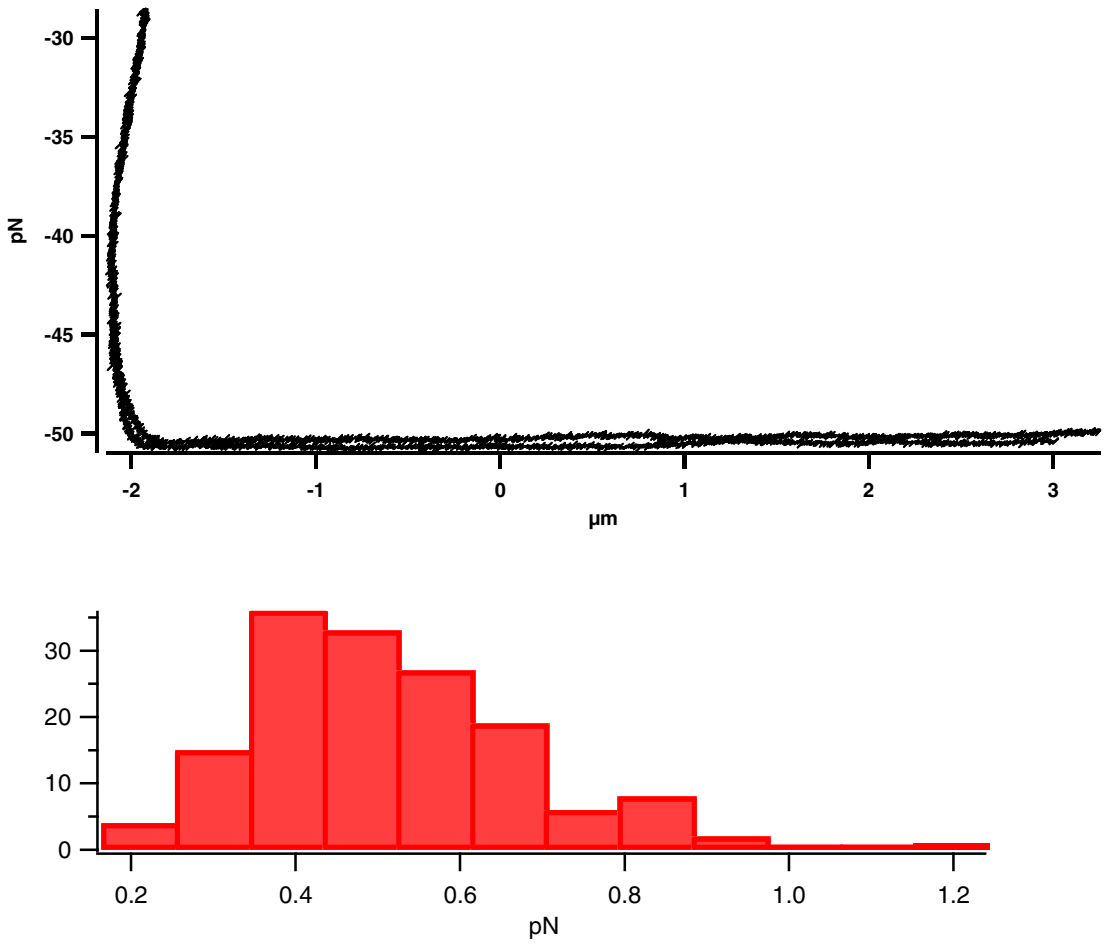

Figure 4.14 Illustration of a typical force plot of a blank tip and PPyCl surface. An unfunctionalized Au coated Si_3N_4 tip was interacted with PPyCl surface (~ 250 nm thickness) with a constant loading rate ($f = \kappa_s \times \nu_c$) 6000 ± 2500 pN/s was. Typical force plot: as the tip approaches the surface, binding between biotin and streptavidin results in a force of adhesion; as the tip is retracted from the surface, force is required to rupture the bonds (average adhesion force of 0.5 ± .12 pN). The y and x-axis scales are not absolute. The histogram generated was used to determine an average (SD) rupture force where the x-axis is rupture force and y-axis is frequency of that particular force.

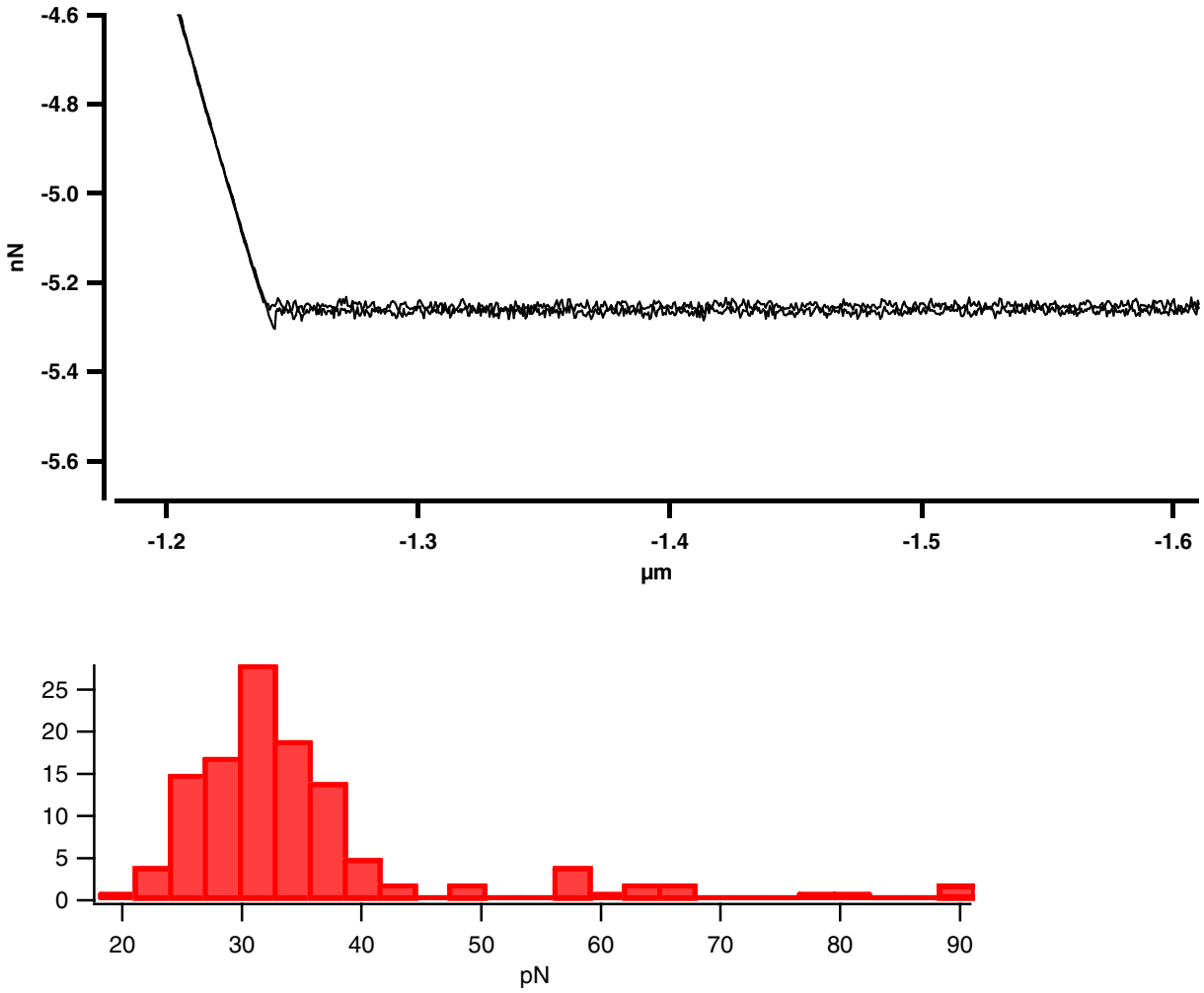

Figure 4.15 Illustration of a typical force plot of a streptavidin-coated tip and PPyCl surface. Au coated Si_3N_4 tip functionalized with streptavidin using biotin-BSA was interacted with PPyCl surface (~ 250 nm thickness) with a constant loading rate ($f = \kappa_s$ x v_c) 6000 ± 2500 pN/s was. Typical force plot: as the tip approaches the surface, binding between biotin and streptavidin results in a force of adhesion; as the tip is retracted from the surface, force is required to rupture the bonds (average adhesion force of 35 ± 13 pN). The y and x-axis scales are not absolute. The histogram generated was used to determine an average (SD) rupture force where the x-axis is rupture force and y-axis is frequency of that particular force.

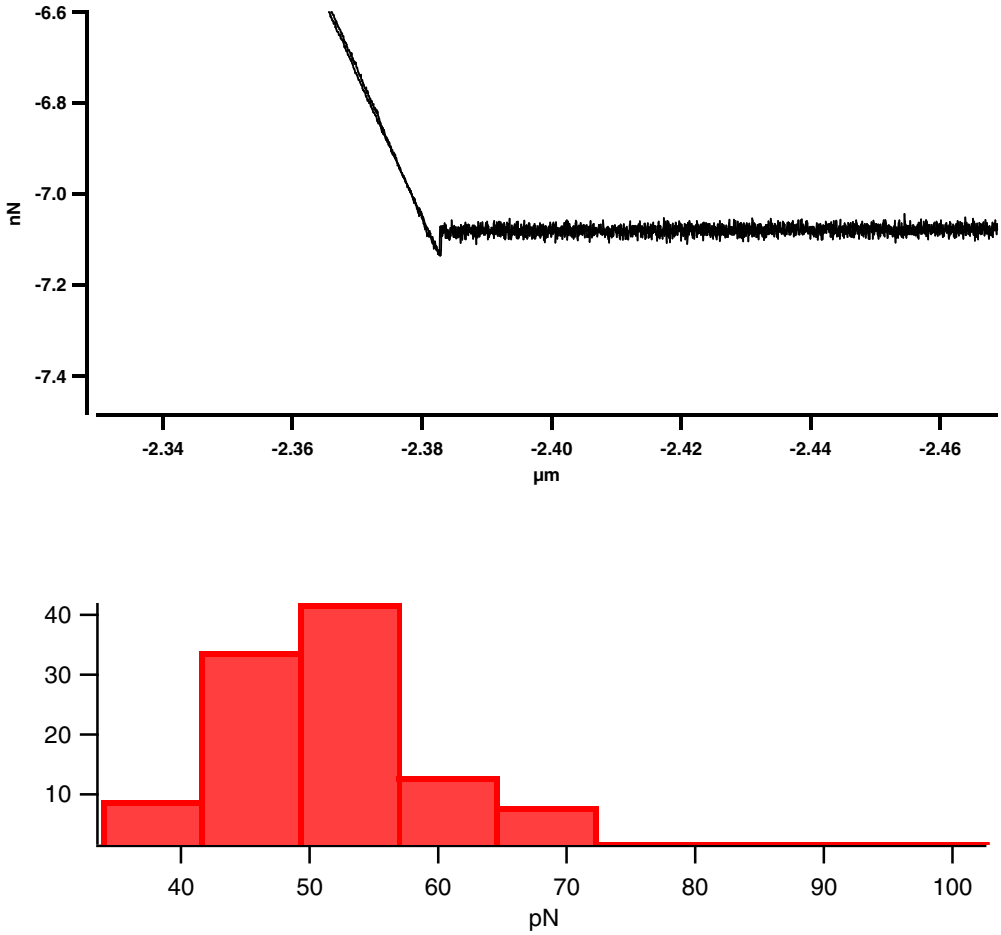

Figure 4.16 Illustration of a typical force plot of GRGDS peptide-coated tip and PPyCl surface. Au coated Si_3N_4 tip functionalized with biotin-GRGDS using biotin-BSA and streptavidin and was interacted with PPyCl surface (~ 250 nm thickness) with a constant loading rate ($f = \kappa_s \times \nu_c$) 6000 ± 1500 pN/s was. Typical force plot: as the tip approaches the surface, binding between biotin and streptavidin results in a force of adhesion; as the tip is retracted from the surface, force is required to rupture the bonds (average adhesion force of 43 ± 12 pN). The y and x-axis scales are not absolute. The histogram generated was used to determine an average (SD) rupture force where the x-axis is rupture force and y-axis is frequency of that particular force.

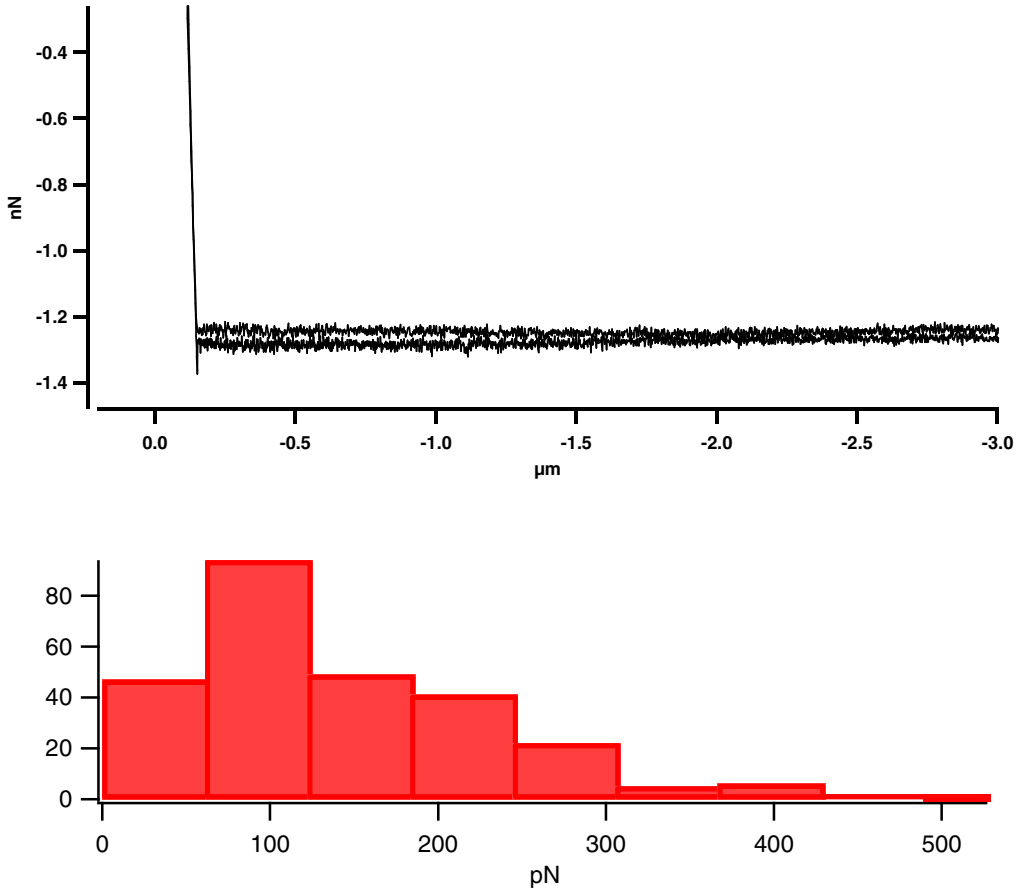

Figure 4.17 Illustration of a typical force plot of T59-GRGDS peptide-coated tip and PPyCl surface. Au coated Si_3N_4 tip functionalized with T59-GRGDS-biotin using biotin-BSA and streptavidin (coated on the tips) and was interacted with PPyCl surface (~ 250 nm thickness) with a constant loading rate ($f = \kappa_s \times \nu_c$) 6000 ± 1500 pN/s was. Typical force plot: as the tip approaches the surface, binding between biotin and streptavidin results in a force of adhesion; as the tip is retracted from the surface, force is required to rupture the bonds (average adhesion force of 102 ± 32 pN). The y and x-axis scales are not absolute. The histogram generated was used to determine an average (SD) rupture force where the x-axis is rupture force and y-axis is frequency of that particular force.

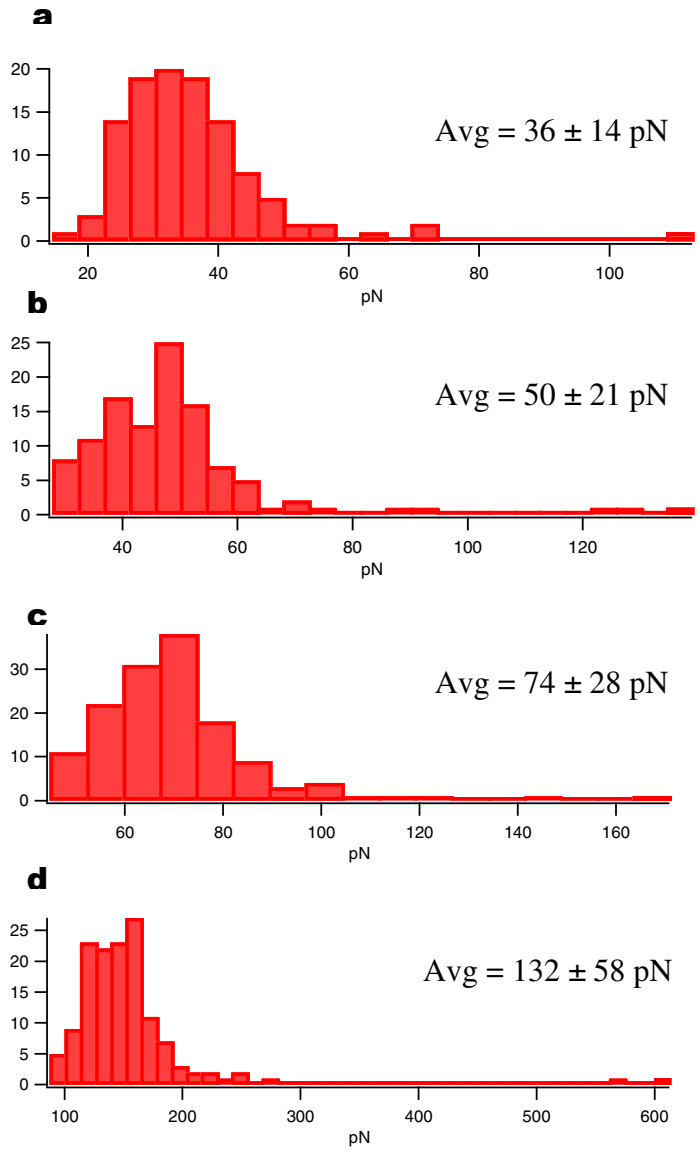

Figure 4.18 Dynamic force spectroscopy with varying loading rates of PPyCl-T59 interactions. Rupture force evaluation was assessed using four varying loading rates ($f = \kappa_s \times \nu_c$) ranging from 900 to 54,000 pNs^{-1} (from A through D). The histograms at each loading rate were generated using n = 150. The y-axis represents the frequency of a particular rupture force (x-axis). As loading rate increases, the rupture force due to the interaction between T59 peptides and PPyCl increases. 36 ± 14 pN, 50 ± 21 pN, 74 ± 28 pN, and 132 ± 58 pN.

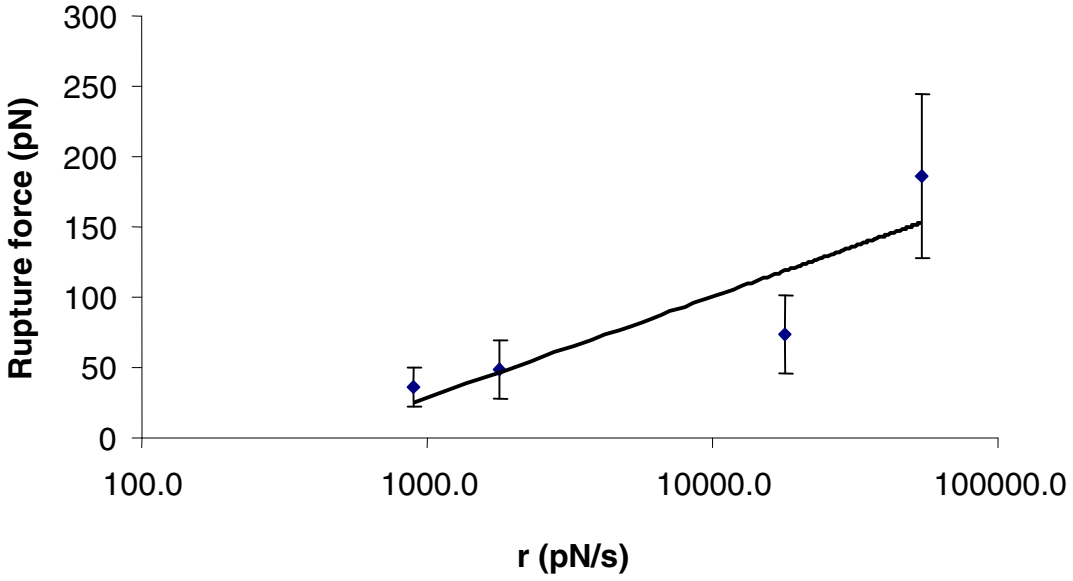

Figure 4.19 Dynamic force spectroscopy evaluation of varying loading rate dependence on T59 peptide interaction with PPyCl surface. A graph of rupture force plotted versus each loading rate suggests a linear dependence on the logrithmic scale, as previously established [11,28]. Based on equation 2, the result suggests a dissociation constant (k_{off}) of approximately 0.252 s^{-1} by extrapolating F = 0, where an external force is absent. Due to the large standard deviations (rupture force) for each loading rate, the presence of a specific binding regime could not be distinguished.

4.5 REFERENCES

1. Sano K, Shiba K. A hexapeptide motif that electrostatically binds to the surface of titanium. J. *Am. Chem. Soc.* 2003;125;14234-235.
2. Berglund J, Lindbladh C, Nicholls IA, Mosbach K. Selection of phage display combinatorial library peptides with affinity for a yohimbine imprinted methacrylate polymer. *Analytical Communications* 1998;35:3-7.
3. Brown S. Metal recognition by repeating polypeptides. *Nature Biotechnol.* 1997;15:269–72.
4. Lee WS, Mao C, Flynn CE, Belcher AM. Ordering quantum dots using genetically engineered viruses. *Science* 2002;296;892–95.
5. Gaskin DJH, Starck K, Vulfson EN. Identification of inorganic crystal-specific seqeunces using phage display combinatorial library of short peptides:A feasibility study. *Biotech. Lett.* 2000;22;1211–16.
6. Baker BM, Murphy KP. Dissecting the energetics of a protein-protein interaction: the binding of ovomucoid third domain to elastase. *J. Mol. Biol.* 1997;268(2);557-69.
7. Makowski M, Chmurzynski L. Ab initio study of the energetics of molecular heteroconjugation reactions in systems modeling side chains of biomolecules. *Theochem* 2004;672:183-190.
8. Skotheim TA. Editor, The Handbook of Conducting Polymers, vol 1. Marcel Dekker, New York (1986).

9. Binning G, Quate CF, Gerber C. Atomic force microscope *Phys. Rev. Lett.* 1986;56:930-933.

10. Lee GU, Kidwell DA, Colton RJ. Sensing discrete streptavidin-biotin interactions with atomic force microscopy. *Lanmuir* 1994;10:354-57.

11. Merkel R, Nassoy P, Leung A, Ritchie K, Evans E. Energy landscapes of receptor-ligand bonds explored with dynamic force spectroscopy. *Nature* 1999;397:50-53.

12. Moy VT, Florin EL, Gaub HE. Intermolecular forces and energies between ligands and receptors. *Science* 1994;266:257-59.

13. Grandbois M, Beyer M, Rief M, Clausen-Schaumann H, Gaub HE. How strong is a covalent bond? *Science* 1999;283:1727-30.

14. Rief J, Fernandez JM, Gaub HE. Elastically coupled two-level systems as a model for biopolymer extensibility. *Phys. Rev. Lett.* 1998;81:4764-67.

15. Li H, Rief M, Oesterhelt F, Gaub HE. Single-molecule force spectroscopy on xanthan by AFM. *Adv. Materials* 1998;10:316-19.

16. Willemsen OH, Snel MME, van der Werf KO, de Grooth BG, Greve J, Hinterdorfer P, et al. Simultaneous height and adhesion imaging of antibody-antigen interactions by atomic force microscopy. *Biophys. J.* 1998;75:2220-228.

17. Hinterdorfer P, Gruber HJ, Schilcher K, Baumgartner W, Haselgruebler T, Schinler H. Antibody-antigen unbinding forces measured by force microscopy using antibodies bound to AFM tips via a specifically designed flexible crosslinker. *Biophys. J.* 1995;68:139a.

18. Dammer U, Hegner M, Anselmetti D, Wagner P, Dreier M, Huber W, Guntherodt HJ. Specific antigen/antibody interactions measured by force microscopy. *Biophys. J.* 1996;70:2437-41.

19. Rief M, Gautel M, Schemmel A, Gaub HE. The mechanical stability of immunoglobulin and fibronectin III domains in the muscle protein titin measured by atomic force microscopy. *Biophys. J.* 1998;75:3008-14.

20. Carrion-Vazquez M, Marszalek PE, Oberhauser AF, Fernandez JM. Atomic force microscopy captures length phenotypes in single proteins. *Proc. Natl. Acad. Sci. USA* 1999;96:11288-292.

21. Yang G, Cecconi C, Baase WA, Vetter IR, Breyer WA, Haack JA, et al. Solid-state synthesis and mechanical unfolding of polymers of T4 lysozyme. *Proc. Natl. Acad. Sci. USA* 2000;97:139-44.

22. Lee GU, Chris LA, Colton RJ. Direct measurement of the forces between complementary strands of DNA. *Science* 1994;266:771-73.

23. Strunz T, Oroszlan K, Schafer R, Guntherodt HJ. Dynamic force spectroscopy of single DNA molecules. *Proc. Natl. Acad. Sci. USA* 1999;96:11277-282.

24. Clausen-Schaumann H, Rief M, Tolksdorf C, Gaub HE. Mechanical stability of single DNA molecules. *Biophys. J.* 2000;78:1997-2007.

25. Nakamura, C. et al. Mechanical force analysis of peptide interactions using atomic force microscopy. *Biopoly. (Peptide Sci.)* 2004;76:48-54.

26. Evans E, Ritchie K. Dynamic strength of molecular adhesion bonds. *Biophys. J.* 1997;72:1541-55.

27. Grubmuller H, Heymann B, Tavan P. Ligand binding: molecular mechanics calculation of the streptavidin-biotin rupture force. *Science* 1996;271:997-99.

28. Evans, E. Introductory Lecture: Energy landscapes of biomolecular adhesion and receptor anchoring at interfaces explored with dynamic force spectroscopy. *Faraday Discuss* 1998;111:1-16.

29. Evan E. Probing the relation between foce-liftime-and chemistry in single molecular bonds. *Annu. Rev. Biophys. Biomol. Struct*. 2001;30:105-28.

30. Ph.D.™ Phage Display Peptide Library Kits; Technical Bulletin E8100, E8110, E8120; New England Biolabs: Cambridge MA, 2004; 1-4.

31. Undenfriend, S., Stein, S., Bohlen, P., Dairman, W. Fluorescamine: A reagent for assay of amino acids, peptides, proteins, and primary amines in the picomole range. *Science* 1972;172:871-72.

32. Yuan C, Chen A, Kolb P, Moy VT. Energy landscape of streptavidin-biotin complexes measured by atomic force microscopy. *Biochemistry* 2000;39:10219-23.

33. Lévy, R., and M. Maaloum. Measuring the spring constant of atomic force microscope cantilevers: thermal fluctuations and other methods. *Nanotechnology* 2002;13:33-37.

34. Bell GI. Models for the specific adhesion of cells to cells. *Science* 1978;200:618-27.

35. Hersel, U., Dahmen, C., Kessler, H. RGD modified polymers: biomaterials for stimulated cell adhesion and beyond. *Biomaterials* 2003;24:4385-4415.

36. Silk, T., Hong, Q., Tamm, J. & Compton, R.G. AFM studies of polypyrrole film surface morphology II. Roughness characterization by the fractal dimension analysis. *Syn. Met.* 1998;93:65-71.

37. Xiao, S.J., Textor, M. & Spencer, N. Covalent attachment of cell-adhesive, (Arg-Gly-Asp)- containing peptides to titanium surface*s. Langmui*r 2000;14:5507-516.

38. Shakesheff, K., Cannizzaro, S. & Langer, R. Creating biomimetic micro-environments with synthetic polymer-peptide hybrid molecules. *J. Biomater. Sci. Polym. Ed.* 1998;9:507-18.

39. Schwesinger F, Ros R, Strunz T, Anselmetti D, Guntherodt HJ, et al. Unbinding forces of single antibody-antigen complexes correlate with their thermal dissociation rates. *PNAS* 2000;97:9972-77.

40. Allison, D.P., Hinterdorfer, P. Han, W. Biomolecular force measurements and the atomic force microscope. *Curr. Opin. Biotech.* 2002;13:47-51.

41. Ratner, B.D., Castner, D.G. Electron spectroscopy for chemical analysis. In: Vickerman, J.C., editor. *Surface analysis: the principle techniques*: New York; 1997.

Chapter 5: Surface functionalization of PPyCl using T59 peptide

As previously described in **Chapter 4**, T59 phage and peptide binding to PPyCl was characterized. ϕT59 binding to PPyCl was assessed using titer count analysis and qualitative imaging to determine the relative specificity of interaction with other selected phage and substrates. Furthermore, the relative binding of T59 peptides was studied using various methods for determining a potential method of interaction and strength of binding to PPyCl. The results of these studies suggest that by modifying the C-terminus of T59 peptides, a biomolecule can be attached to T59 for surface fictionalizations of PPyCl. As presented in **Chapter 3**, PPyCl was selected as a model polymer as it lacked a functional group for surface modification. Thus, in this chapter a cell adhesion promoting peptide (RGD, a fibronectin derived integrin-binding domain) was conjugated at the C-terminus of T59 peptides during synthesis. A nerve-like cell line, rat pheochromocytoma (PC12), which has been previously studied with polypyrrole, was used to evaluate the effect of presenting RGD peptides via T59 as a linker for cell attachment and subsequent viability. This was a model study to evaluate the use of phage-displayed selected peptides for surface functionalization of synthetic polymers. Furthermore, the stability of T59 peptide binding to PPyCl was evaluated in the presence of serum proteins.

Some of the results from this chapter are presented in, Sanghvi AB, Miller KP-H, Belcher AM, Schmidt CE. ***Nat. Mat.*** *2005, 4(6):496-502.*

5.1 INTRODUCTION

Surface fictionalizations for promoting bioactivity has become an increasingly active area of research in the biomaterials field [1]. As highlighted by Hoekstra, et al., the "third generation" biomaterials are being researched and developed to precisely control reactions with proteins and cells at the molecular level [1]. As discussed in **Chapter 1**, one of the key components of tissue engineering is the ability to selectively modify surfaces for controlling cellular activity in a specific environment [2-5]. To develop such surfaces, numerous methods have been researched and implemented including non-specific protein adsorption and self-assembly [5], synthesis of novel graft-copolymers with desired functional groups [6,7], and direct covalent surface modifications [8-10] using methods such as plasma deposition, self-assembled monolayer, and silanization, just to name a few [ref]. However, these approaches have limitations associated with them. Covalent surface modification and the synthesis of new materials both require extensive chemical reactions and processing. Protein adsorption, on the other hand, does not require chemical processing, but unfortunately is largely dependent upon nonspecific interactions between the protein and the surface, and therefore, is difficult to control [5]. To study the possibility of using phage-display selected peptide for surface functionalization, T59 peptides were modified with a cell adhesion promoting peptide to assess the effectiveness of cell attachment using this method.

A model peptide (GRGDS) that promotes cell adhesion [11-13] was used to examine the ability of the T59 peptide to promote cell attachment and thus, to serve as a bifunctional linker. It has been noted that to promote strong cell adhesion, stable linking of biomolecules (e.g., RGD) are necessary [14]. T59 peptide was modified at the C-terminus to maintain consistency with the previous biotin modification used for the qualitative peptide binding studies (**Chapter 4,** *Section 4.2.2*). The activity of T59-GRGDS in promoting cell adhesion on PPyCl was evaluated using PC12 cells [15]. The results were analyzed using both qualitative analysis (live/dead stain) and relative quantitative assessement to evaluate the extent of cell attachment with T59-GRGDS modified PPyCl.

Additionally, the stability of T59 peptides in the presence of serum proteins was evaluated. It is inherent in the design of biomaterials that the ultimate application will be in the human body, and for that reason, it is important to evaluate the stability of the T59 peptide under physiological conditions where proteins (e.g., albumin) can nonspecifically adsorb to the polymer surfaces [16]. These preliminary results suggest that T59 peptides can be modified for surface functionalization and are stable in the presence of proteins that can nonspecifically adsorb to PPyCl.

5.2 MATERIALS AND METHOD

5.2.1 T59 modification and PPyCl surface functionalization

The modified T59 peptide was synthesized with a cell adhesion promoting sequence (GRGDS) at the C-terminus, THRTSTLDYFVI-GRGDS (T59-RGDS) (Institute of Cellular and Molecular Biology Core Facilities, University of Texas at Austin). The peptide (T59-GRGDS) was demonstrated to be >95% pure per HPLC by the manufacturer. PPyCl and TCPS (tissue-culture polystyrene) samples were prepared by sealing Plexiglass wells (1.5 cm x 1.0 cm x 1.0 cm) using silicone rubber sealant (DAP, Inc., Baltimore, MD) onto PPyCl thin films prepared on ITO-coated glass slides. The samples were then placed in sterile tissue-culture polystyrene dishes and UV sterilized for 20 min. Each sample was rinsed three times with 10 mM PBS (pH 7.4) prior to peptide incubation. Incubation of 15 μM T59, T59-GRGDS, and T59-GRDGS peptides (T59-GRDGS peptides were studied only with MTS assay for cell binding quantification, described below) on PPyCl (samples size ~ 0.5625 cm^2) for 1 hr in PBS (total volume of 1 mL in an enclosed plexi glass chamber) at room temperature was followed by thorough rinsing (three times with PBS) to remove any residue and unbound peptide.

PC12 cells, a rat pheochromocytoma cell line was purchased from the American Type Culture Collection. PC12 cells were cultured in F12K media supplemented with 1.5 g/L sodium bicarbonate, 15% horse serum, and 2.5% fetal bovine serum. Cells were maintained at 37 ^{o}C in a humidified 5% CO_2 incubator. Medium was replaced every 2-3

days, and cells were passaged with 1 mM ethyl-enediaminetetraacetic acid (EDAC). PC12 cells (passage #20) were seeded onto each substrate with either serum-containing (positive controls) or serum-free medium at a density of 10^4 cells/cm^2 and were allowed to attach at 37°C in 5% CO_2. The medium for each sample was replaced after 24 hr with serum-containing medium to ensure cell viability. Both positive and negative controls were performed for evaluation. Positive controls consisted of PC12 cells incubated with serum-containing medium on PPyCl and tissue culture polystyrene. Negative controls consisted of PC12 cells incubated on PPyCl in serum-free medium and T59 peptides without the presence of RGD-cell adhesion sequence.

Additionally, one experimental sample (T59-GRGDS peptide incubated with PPyCl in serum-free medium) was incubated with 100 ng/ml βNGF (Invitrogen Corp.) in serum-free media for seven days. After initial cell seeding (24 hr) in serum-free medium, the sample was replaced every other day with serum-containing medium supplemented with βNGF to ensure cell viability. After the cells were seeded for seven days the sample was imaged using an inverted phase contrast microscope to assess the impact of βNGF for PC12 cell differentiation.

24 hr post cell seeding, the medium was removed and washed using sterile 10 mM PBS and then followed with the addition of serum-containing medium (F12K supplemented with supplemented with 1.5 g/L sodium bicarbonate, 15% horse serum, and 2.5% fetal bovine serum) to ensure cell survival. After 48 hr, a fluorescent live/dead stain (Molecular Probes) was used to image the adhesion/viability of cells influenced by

either T59-GRGDS and T59 (negative control) peptides in serum-free conditions. An epifluorescence microscope (IX-70, 20X objective, Olympus, Melville, NY) and a high resolution CCD video camera (Magnafire, Optronics, Goleta, CA) were used to visualize cell adhesion.

Another study was performed to measure relative cell viability using MTS (Promega) assay for quantifying percentage PC12 cell adhesion. This study consisted of comparing relative cell attachment with T59, T59-GRGDS, and T59-GRDGS peptides along with both positive controls. Percent cell adhesion was quantified after 48 hr using the colorimetric MTS assay (Promega, Madison, WI) with tetrazolium compound and an electron coupling reagent (phenazine, according to the manufacturer's protocol). The medium was removed from each sample and each well was rinsed with 10 mM sterile PBS, followed by addition of fresh 0.5 mL medium and 0.1 ml of MTS/phenazine methosulfate mixture. The samples were allowed to incubate for 2 hr at 37°C and 5% CO_2 before absorbance at 490 nm was measured. Background absorbance from medium only was subtracted from each experimental condition.

5.2.2 T59 peptide stability in the presence of serum proteins

Physiological stability of T59 peptides when bound to PPyCl was evaluated *in vitro* by incubating PPyCl-T59 samples in serum-containing medium for time points up to 21 days and compared to PBS incubation. *In vitro* physiological stability of PPyCl-bound T59 peptide was assessed in 10% serum-containing phenol-red free Dulbecco's

Modified Eagle's Medium (DMEM). PPyCl samples (0.5 cm^2, n = 6) were interacted with 15 μM of T59 peptides in 10 mM PBS (previously described). PPyCl-T59 samples were placed in DMEM and 10 mM PBS for up to 18 days at 37°C. The supernatant was collected every other day and replaced with fresh solution of either DMEM or PBS. The presence of T59 peptides in the collected solution was measured using fluorescamine reagent (a variation of this protocol is also described in **Chapter 4,** *Section 4.2.3*). Background fluorescence intensity was measured using PPyCl samples incubated in either DMEM or 10 mM PBS without T59 peptides. The intensity as a result of unbound T59 peptides in the solution was calculated by subtracting the background intensity from the measured intensity for each sample. Experiments were performed for each condition (DMEM and PBS incubation) with n = 6 and then plotted as a percentage of bound T59 peptides with respect to the initial bound T59 peptides (calculated for each sample using the previously described mass balance method).

5.3 RESULTS

An initial study to evaluate the use of T59 peptides to modify PPyCl was performed using GRGDS attached to the C-terminus (T59-GRGDS) during synthesis. The first study was performed to assess the attachment of PC12 cells using phase contrast imaging. The results (**Figure 5.1**) indicate that PC12 cells do not adhere to PPyCl in serum-free medium, but when modified with T59-GRGDS peptides, PPyCl promoted cell adhesion. The negative control used was PPyCl without any peptide and in serum-free

conditions (**Figure 5.1a**). The surface heterogeneity is illustrated in **Figure 5.1a** and because of the change in focus to image the adhered cells, **Figure 5.1b** does not present the same extent of heterogeneity. In the study presented below, other controls (i.e., unmodified T59 peptides) were also used. Additionally, when PC12 cells were placed in a nerve growth factor (βNGF) containing environment to induce differentiation and stimulate neurite outgrowth, the PPyCl surface modified with T59-GRGDS peptide not only permitted cell adhesion, but also allowed the extension of neuronal processes (**Figure 5.1c**). This was a rare image as most of the cells were in an undifferentiated phenotype.

Another study was performed to evaluate not only cell attachment, but also cell viability using live/dead stain and quantification using an MTS assay. The results of this study contained other negative and positive controls for comparison to the experimental samples. The results, illustrated in **Figure 5.2a,** demonstrate adhesion and viability of PC12 cells in the presence of T59-GRGDS. The condition with unmodified T59 peptide, cells did not attach as illustrated by the lack of fluorescence (**Figure 5.2b**).

Cell quantification using the MTS cell proliferation assay [17] was also performed to determine the extent of adhesion when compared to positive controls, cells with serum-containing medium on both tissue culture polystyrene and PPyCl (**Figure 5.2c**). The results show that cells adhered to PPyCl modified with T59-GRGDS to the same extent as positive controls, but did not adhere to PPyCl when modified with the

scrambled peptide (GRDGS) that is known to inhibit cell adhesion [14] (P-T59GRDGS, negative control).

T59 peptide binding stability in serum-containing medium was also evaluated using qualitative immunofluorescence. The results, presented in **Figure 5.3**, illustrate that the T59 peptide remains bound to PPyCl even after 3 weeks of incubation in serum-containing medium, suggesting a stable interaction between the T59 peptide and the PPyCl surface. The binding affinity and kinetics of this interaction will be necessary to explore quantitatively in future studies.

Additionally, psuedoquantitative assessement of T59 peptide binding stability to PPyCl was evaluated using a fluorescamine assay (an indirect mass balance method). Results from fluorescamine studies, presented in **Figure 5.4**, illustrate that the T59 peptide remains bound to PPyCl even after 21 days of incubation in serum-containing medium at 37^{o}C, suggesting a relatively stable interaction between the T59 peptide and the PPyCl surface. The T59 peptide unbinding in serum-containing medium stabilized after 10 days with an approximate loss of 15 ± 7%. When compared to control PBS conditions, where stabilization was achieved after 3 days with a loss of 7 ± 2%, the serum condition had twice the loss.

5.4 DISCUSSION

The specific goals of the work presented in this chapter were to determine the potential use of T59 peptides for surface functionalization of PPyCl and also to evaluate

the stability of T59 peptides when bound to PPyCl in serum protein-containing environment. To assess the bifunctional capabilities of T59 peptides, T59 peptides were synthesized with a cell adhesion promoting peptide (GRGDS) at its C-terminus. An initial evaluation consisted of surface coating PPyCl with T59-GRGDS peptides followed by PC12 cell seeding in serum-free conditions. In the presence of serum proteins (serum-containing medium) PPyCl promotes cell attachment, thus the serum-free condition to evaluate the effects of RGD peptides presented via T59 was selected. The phase contrast images (**Figure 5.1**) indicate that in the presence T59-GRGDS peptides and in serum-free conditions (**Figure 5.1b**), PC12 cells adhered, whereas in the absence of any proteins or peptides PC12 cells did not adhere (**Figure 5.1a**). These results suggested that RGD peptide sequence, presented via T59, was exposed for cell attachment.

In the next set of experiments cell viability was studied, as cell attachment is the first step in functionalizing PPyCl surface using T59-GRGDS peptides followed by evaluation of cell survival. The live/dead fluorescent images (**Figure 5.2b**) suggest that PC12 cells were also viable after 48 hr, where serum-containing medium was added 24 hr after initial cell attachment to ensure cell survival. Cell quantification results (**Figure 5.2c**) to determine the extent of adhesion when compared to positive controls (i.e., cells adhered in the presence of serum to tissue culture polystyrene and PPyCl) demonstrate that cells adhered to PPyCl modified with T59-GRGDS. The results indicate that cell attachment was nearly to the same extent as for positive controls. PC12 cells did not adhere to PPyCl when modified with RGD non-specifically adsorbed (P-GRGDS) and

with a scrambled peptide (GRDGS) that is known to inhibit cell adhesion [14] (P-T59GRDGS, negative control). This supported our hypothesis that the peptide selected using phage display against a synthetic biopolymer (PPyCl) can potentially be used as a surface modification tool for biomolecule immobilization and to subsequently control biological and cellular activity.

Qualitative evaluation of T59 peptide binding to PPyCl in the presence of serum proteins was evaluated for varying time points. The results of this initial study suggest that the peptides are present even after 3 weeks (**Figure 5.3**), suggesting a stable interaction over this time course These results are not a direct correlation to the strength of interaction as the amount of peptide present after each time point was not determined. Additionally, the presence of numerous other proteins in the environment may lead to nonspecific adsorption of the fluorophore (streptavidin-FITC) used, which can then be present over time on the PPyCl surface. Although nonspecific binding of streptavidin-FITC to other serum proteins in the environment was not observed directly, the possibility can lead to nonspecific adorption over time. For this reason T59 peptide binding in the presence of serum proteins was evaluated using fluorescamine assay to determine the relative amount of peptide present over the 21 day time point. The results in **Figure 5.4** indicate that serum proteins can impact the unbinding of T59 peptides from PPyCl, but the unbinding was nonspecific and insignificant as stabilization was reached with 85 ± 10% of the original peptides still remaining. As previously discussed in **Chapter 4**, a fluorescamine assay permitted an indirect method for determine the bound

peptide amount; however, this particular method does have significant error associated, as indicated by the large standard deviations. Although the absolute quantitative measurement was not possible, a relative comparison does suggest the presence of bound peptides over time. Additional experimental work is needed to quantify the binding of T59 peptide to PPyCl and to determine the binding affinity.

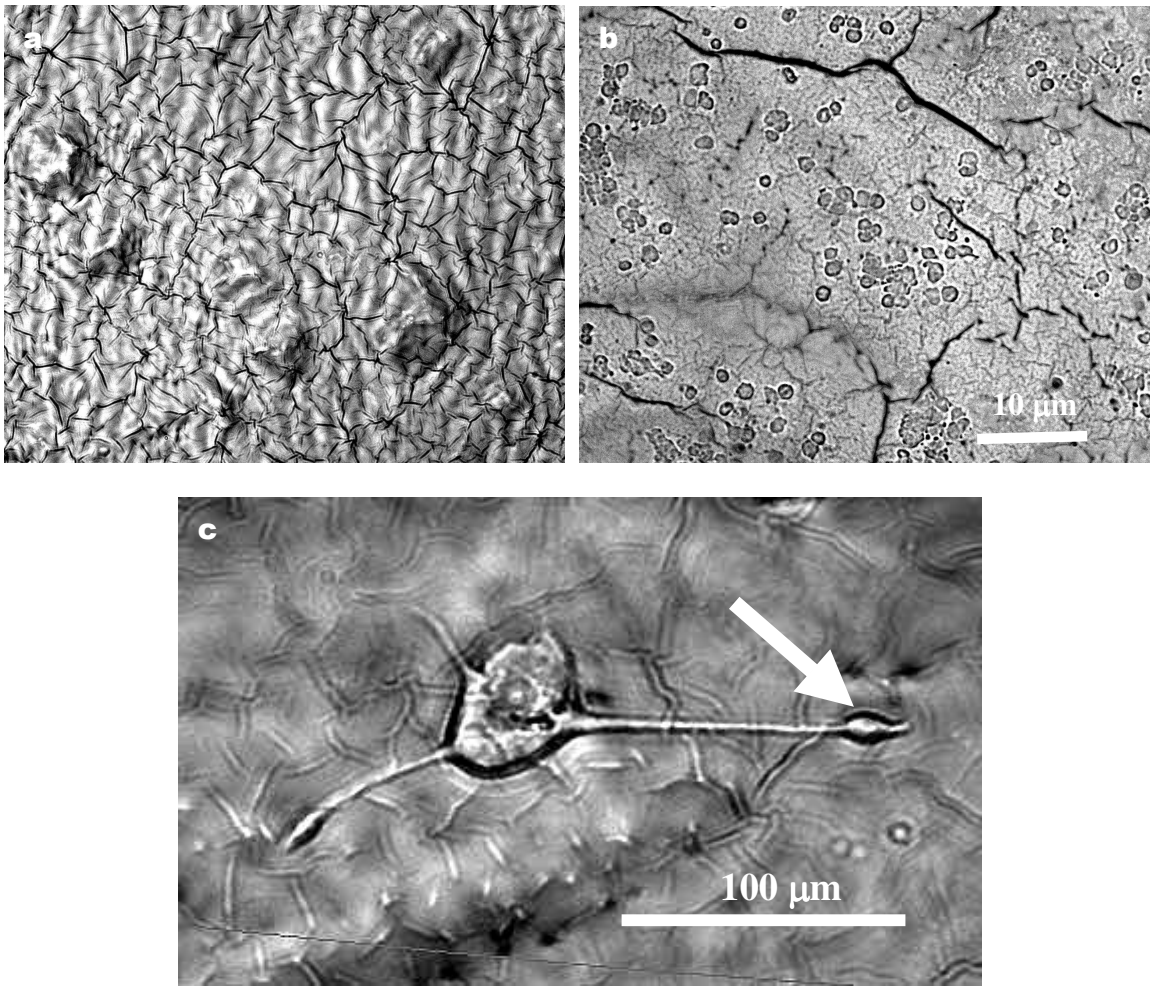

Figure 5.1 T59 peptide modified with GRGDS promotes PC12 cell adhesion in serum-free environment. PC12 cells were plated (10^4 cells/sample) in serum-free media. PPyCl without T59-GRGDS did not permit cell adhesion (a), whereas the PPyCl sample with T59-GRGDS (b) did support cell attachment. The heterogeneity in the PPyCl surface is demonstrated by the topography in image (a), which is not as apparent in the image (b) because this image was taken at a different focal plane to demonstrate cell binding. Extension of neuronal processes was induced with 100 ng/ml βNGF for 7 days in serum-free media (c). In addition to cell attachment, PPyCl-T59-GRGDS modified surface also supported neurite outgrowth.

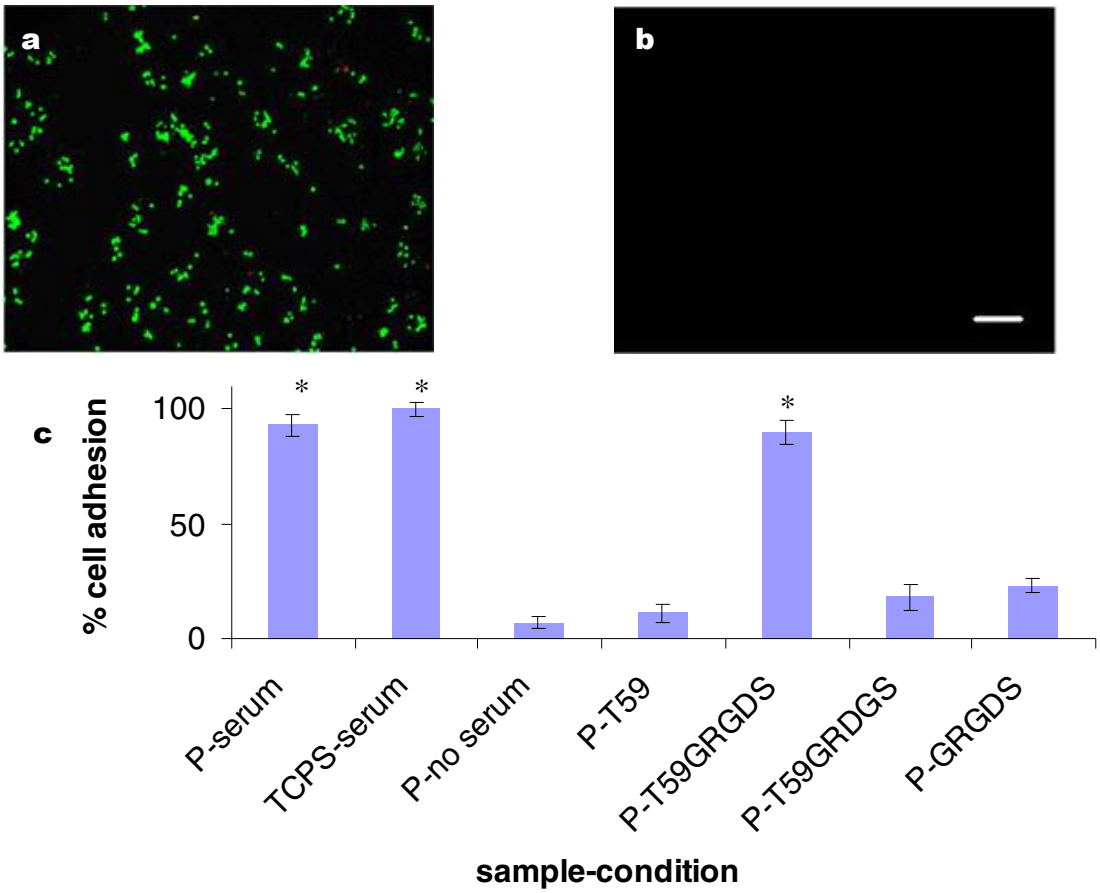

Figure 5.2 Functionalization study of PPyCl surface using T59 peptide complexed with GRGDS and the stability of T59 peptide binding to PPyCl. Cell viability study using both qualitative imaging using live/dead stain (a,b) and MTS assay (c). PC12 cells adhered (serum-free medium) and are viable (after 48 hr) when RGD is presented via T59 on PPyCl (a) and cells did not survive when T59 was present alone (b). Bar, 100 µm. (c) T59-GRGDS promotes PC12 cell attachment on PPyCl (P refers to PPyCl) under serum-free medium conditions comparable to positive controls (tissue culture polystyrene and PPyCl in serum-containing medium). In the absence of GRGDS presented via T59 peptide, cells did not attach as indicated by minimal cell adhesion (P-no serum, P-T59, P-T59GRDGS, and P-GRGDS). Cell seeding was at 10^4 cells/sample and samples were analyzed after 48 hr (n = 4). (*): the difference in percent cell adhesion between the experimental (P-T59GRGDS) and positive controls is not statistically significant.

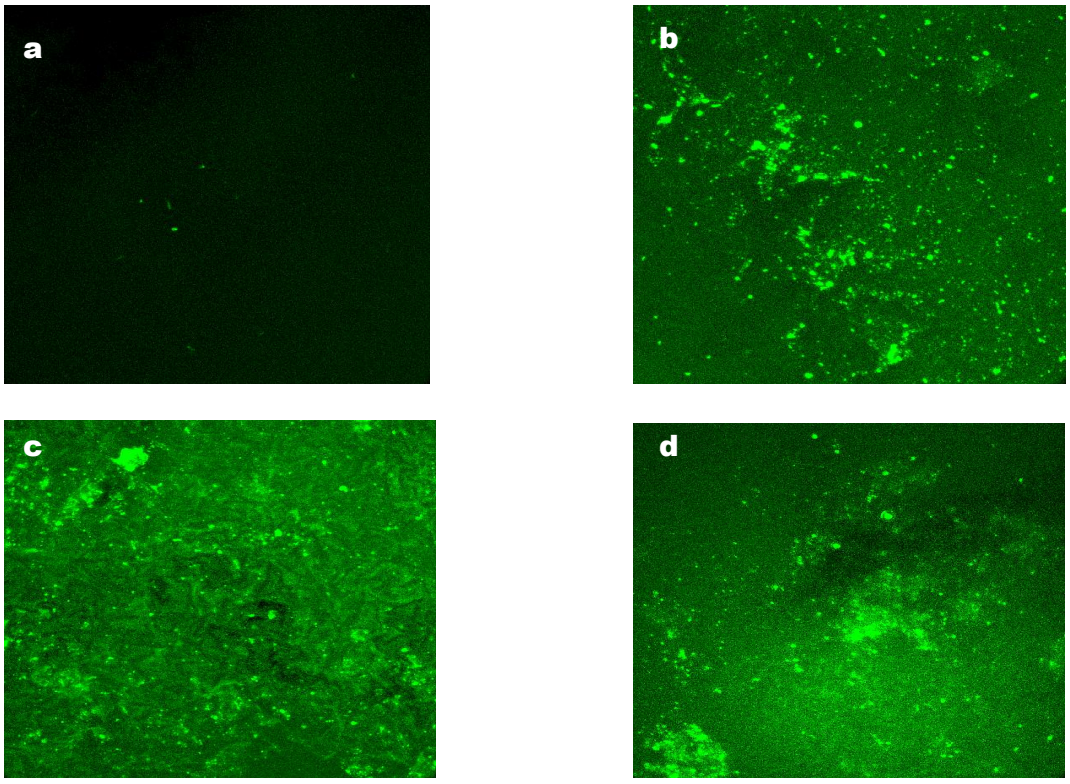

Figure 5.3 Qualitative images of PPyCl-bound T59 peptides after serum incubation for various time points, suggesting stability in binding. Binding was studied using biotinylated T59 peptides and streptavidin-FITC labeling. (a) control substrate in which no T59 peptide was added, 0.5 cm^2 PPyCl substrates (b), (c), and (d) were incubated with 15 μM peptide, the samples were then placed in serum-containing media (pH 7.4 and 15% serum) for 3 hr (b), 7 days (c), and 3 weeks (d). Bar, 100 μm.

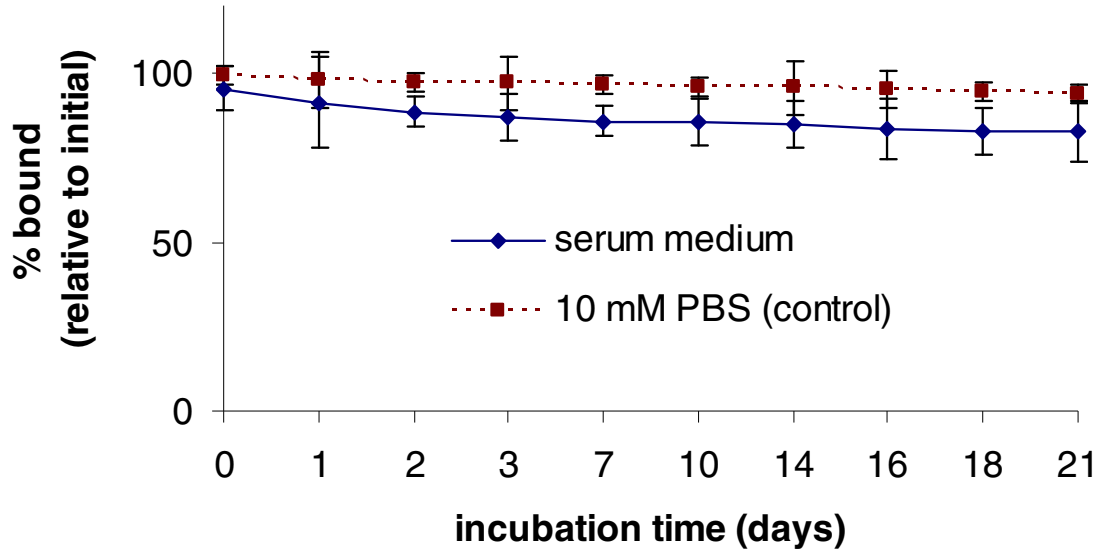

Figure 5.4 T59 peptide binding to PPyCl is stable in the presence of serum proteins with an approximate lost of 15% after 21 days. PPyCl-bound T59 peptides are stable in the presence of serum proteins for up to 21 days. Peptide binding stabilizes to 85% after 10 days of incubation in serum-containing medium, indicating a strong and stable interaction. The stability of T59 peptides in the presence of PBS is significantly greater at day 21 with approximately 95% still remaining when compared to the serum incubation, suggesting that T59 peptides are desorbed off of the surface over time (n = 6).

5.5 REFERENCES

1. Hoerstrup, SP, Lu L, Lysaght, MJ, Mikos AG, Rein D, Schoen FJ. Et al. Tissue engineering, In: Ratner BD, Hoffman AS, Schoen FJ, Lemons JE, editors. *Biomaterials science: an introduction to materials science in medicine*. 2004, Academic Press: Boston.
2. Chen CS, Mrksich M, Suang S, Whitesides GM, Ingber, DE. Geometric control of cell life and death. Science 1997;276:1425-1528.
3. Huang S, Ingber DE. Shape-dependent control of cell growth, differentiation, and apoptosis: switching between atractors in cell regulatory network. Exp Cell Res 2000;261:91-103.
4. Zhang S, Altman M. Peptide self-assembly in functional polymer science and engineering. *Reac & Func Polym* 1999;41:91-102.
5. Shakesheff K, Cannizzaro S, Langer R. Creating biomimetic micro-environments with synthetic polymer-peptide hybrid molecules. *J Biomater Sci Polym Ed* 1998;9:507-18.
6. Tong YW, Shoichet MS. Peptide surface modification of poly(tetrafluoroethylene-co-hexafluoropropylene) enhances its interaction with central nervous system neuron*s. J Biomed Mat Res* 1998;42:85-95.
7. Quirk R, Chan W, Davies M, Tendler S, Shakesheff K. Poly(L-lysine)- GRGDS as a biomimetic surface modifier for poly(lactic acid). *Biomaterials* 2001;22:865-72.
8. Hrkach J, Ou J, Lotan N, Langer R. Poly (L-lactic acid-co-amino acid) graft copolymer*s. J Mater Sci Res* 1999;78:92-102.

9. Cook AD, Pajvani UB, Hrkach JS, Cannizzaro SM, Langer R. Colorimetric analysis of surface reactive amino groups on poly(lactic acid-co-lysine):poly(lactic acid) blends. *Biomaterials* 1997;18:1417-24.
10. Kubies D, Rypacek F, Kovarova J, Lednicky F. Microdomain structure in polylactide-block-poly(ethylene oxide) copolymer films. *Biomaterials* 2000;21:529-36.
11. Xiao, S.J., Textor, M. & Spencer, N. Covalent attachment of cell-adhesive, (Arg-Gly Asp)- containing peptides to titanium surfaces. *Langmuir* 2000;14:5507-16.
12. Massia, S.P., Hubbel, J.A. Covalently attached GRGD on polymer surfaces promotes biospecific adhesion of mammalian cells. *Ann. N.Y. Acad. Sci.* 1988;589:261-70.
13. Pierschbacher, M.D., Ruoslahti, E. Cell attachment activity of fibronectin can be duplicated by small synthetic fragments of the molecule. *Nature* 1984;309:30-33.
14. Hersel, U., Dahmen, C., Kessler, H. RGD modified polymers: biomaterials for stimulated cell adhesion and beyond. *Biomaterials* 2003;24:4385-4415.
15. Schmidt, C.E., Shastri, V.R., Vacanti, J.P. & Langer, R. Stimulation of neurite outgrowth using an electrically conducting polymer. *Proc. Nat. Acad. Sci. USA* 1997;94:8948-53.
16. Jozefonvicz, J., Jozefowicz, M. Review: Interactions of biospecific functional polymers with blood proteins and cells. *J. Biomater. Sci.: Polymer Ed.* 1990;1:147-65.
17. Barltrop, J..A. et al. 5-(3-carboxymethoxyphenyl)-2-(4,5-dimethylthiazoly)-3-(4 sulfophenyl)tetrazolium, inner salt (MTS) and related analogs of 3-(4,5-

dimethylthiazolyl)-2,5-diphenyltetrazolium bromide (MTT) reducing to purple water-soluble formazans as cell-viability indicators. *Bioorg. & Med. Chem. Lett.* 1991;1:611.

Chapter 6: Conclusions and Recommendations

6.1 SUMMARY

The surface properties of polymeric biomaterials applied in biomedicine are equally important to consider along with bulk properties. Specifically, the ability to tailor the surface properties in controlling and guiding cellular activity is at the forefront of tissue engineering. With this goal in mind, we researched the ability to use phage display technology as a tool to select peptides that can potentially be used as vehicle to functionalize surfaces by immobilizing biomolecules. Chlorine-doped polypyrrole (PPyCl) was used a model biomaterial to study the potential use of this method for surface modification. Our work has demonstrated the ability to select a phage that binds to PPyCl and where the binding of both phage and the corresponding peptide (T59) was characterized.

Traditionally, phage display technology has been applied to two categories of materials including biological and non-biological such as semiconductors. The dissertation is organized into three main areas: (1) phage display peptide selection against PPyCl, (2) the characterization of both ϕT59 and T59 peptide binding to PPyCl, and (3) an initial study to apply the selected peptide in functionalizing PPyCl using a cell adhesion promoting peptide, RGD. This dissertation describes a proof-of-principle in applying this method for surface functionalization of a synthetic biomaterial, PPyCl.

Future work, as outlined below, is recommended to better understand and develop a precise binding mechanism of the selected peptide to PPyCl, in addition to studying the in vivo compatibility of PPyCl-T59 material and stability of T59 peptides bound to PPyCl, and to study the potential use of phage display method in selecting peptides against other polymeric biomaterials.

6.2 LIMITATIONS

The work presented in this dissertation included use of numerous techniques for understanding the binding of ϕT59 and T59 peptides to PPyCl. Limitations of the techniques used presented several challenges. Initially, during the biopanning selection against PPyCl (**Chapter 3**), 25 phage were randomly selected from rounds 3-5 to determine the 12-mer amino acid sequence corresponding to that particular phage. For future work for selection against PPyCl and other materials using another library, it would be beneficial to sequence more than 25 phage from the last three biopan rounds to determine a consensus sequence based on statistical analysis. Although the subsequent results demonstrated ϕT59 binding to PPyCl, other phage that perhaps had better binding to PPyCl may have been overlooked.

Although titer count analysis was used to determine relative binding of ϕT59 when compared to other phage and substrates (**Chapter 4**), it would have been beneficial to perform this study to determine binding kinetics by varying input phage concentrations and PPyCl sample size.

Characterization of T59 peptide binding was determined using an indirect fluorescamine assay method, where a mass balance was used to quantify the relative percentage of interaction peptides. This technique has numerous limitations because of the error presented by the sensitivity of the assay along with the inability to control PPyCl sample size and large standard deviations. Although a relative comparison was presented, the actual binding of the peptide was not determined. Fluorescamine assay studies were not sufficient for understanding the binding mechanism of T59 peptide to PPyCl and other techniques are necessary to directly measure binding of peptides to solid surfaces. Additional methods such as radiolabeling can be used to identify the actual binding concentration of T59 peptide to PPyCl as it present better sensitivity and accuracy.

Qualitative studies demonstrating T59 phage and peptide binding to PPyCl were performed using streptavidin-biotin labeling where a blocking buffer (bovine serum albumin) was used to prevent nonspecific binding of streptavidin-FITC (**Chapter 4**). Although appropriate controls were used (PPyCl with bovine serum albumin blocking buffer without T59 peptide), the extent of surface coverage T59 phage and peptide on PPyCl was difficult to distinguish. When comparing to control conditions, both T59 phage and peptide did bind to PPyCl, but quantitative binding assessment was difficult to determine. Additionally, a linker (GGGSK) was attached to the C-terminus of T59 peptide for biotin-streptavidin labeling, where the presence of the linker may have potentially impacted the binding of T59 peptide to PPyCl. Additional studies, perhaps

without the presence of the linker and quantitative labeling using other techniques such as radiolabeling may provide beneficial information for studying the role of linker sequences in effecting binding of T59 peptide to PPyCl.

Atomic force microscopy studies were used determine a relative strength of interaction of T59 peptide modified AFM tips and compared to streptavidin-biotin interactions (**Chapter 4**). Although a relative binding strength was determined by comparing to non-specific adsorption (GRGDS functionalized tip binding to PPyCl) and biotin-streptavidin, the absolute binding strength was not determined. The inability to control the number of T59 peptides interacting with the PPyCl surface presented large standard deviations in the rupture force analysis histograms. Additionally, a linker AFM tip conjugation system that included attachment of bovine serum albumin conjugated to biotin, followed by streptavidin and then biotinylated T59 peptide, may have presented additional nonspecific forces that could have influenced the rupture forces and consequently the strength of interaction in the histogram analysis. Future work that utilizes a more direct method in T59 peptide conjugation to the AFM tip, perhaps by using cysteine residue on T59 peptide and the Au coated tip surface for covalent interaction, may help in acquiring more accurate results without inherent errors. Furthermore, a study comparing variation in T59 peptide concentration during AFM tip conjugation and the resulting strength of interaction can potentially provide the ability to study minimal peptide interactions and therefore, a more quantitative study of T59 peptide binding to PPyCl.

6.3 RECOMMENDATIONS FOR FUTURE RESEARCH

6.3.1 Developing a method to determine the mechanism of peptide interaction

In **Chapter 4**, initial work is presented to determine the role of key amino acids of T59 peptide in binding PPyCl. However, the inability to develop a precise and quantitative method to determine the extent of T59 peptide binding to PPyCl prevented us from successfully elucidating an exact mechanism of interaction and quantifying the amount of peptide bound at a known PPyCl surface. Fluorescamine assay was utilized as an indirect method to qualitatively compare the binding interactions of various T59 variants with some uncertainty where the potential role of aspartic acid was identified. The challenges posed by this issue have resulted in several potential areas of research for assessing other tools and techniques in determining the mechanism of interaction.

As determined by the titer count analysis results of ϕT59 binding to PPyCl relative to other phage and substrates, ϕT59 binds significantly better. Although this analysis resulted in the identification of selective binding of ϕT59 to PPyCl, other rounds of selection did not result in selecting a phage with binding to this extent. In the future it would beneficial to perform phage display selection process with another library, for example a seven amino acid peptide insert library (Ph.D. 7^{TM}), to assess a potential trend in the occurrence of specific amino acids. To determine the binding mechanism, comparison of other peptide inserts isolated with another selection process or other peptide variants will be necessary.

Furthermore, a precise and direct method for quantifying the binding and kinetics of interaction between T59 peptide and PPyCl is necessary. Other methods that were studied without success included surface plasmon resonance and isothermal titration calorimetry. It is extremely important to develop methods that can enable the quantification of binding and assessing the strength of interaction. For potential applications it would also be necessary to determine the equilibrium or saturation binding to selectively and specifically control cellular interactions with a modified peptide. Thus, with the success of developing a quantification method other peptide variants can be studied to determine the mechanism and strength of interaction between T59 peptides and PPyCl.

6.3.2 Evaluate the *in vivo* stability and functionality of PPyCl-T59 peptide

As discussed in **Chapter 2**, polypyrrole has been researched for various applications in biomedicine. Specifically, for tissue engineering applications it will be necessary to evaluate the binding stability of PPyCl with bound and modified T59 peptides. Although various forms of polypyrrole have been shown to biocompatible, it will be necessary to evaluate the biocompatibility of peptide-modified PPyCl. Furthermore, the stability of T59 peptide interaction in an in vivo environment, which contains a complex milieu of components, should be evaluated with various controls. For instance, when the peptides are in such an environment the binding may become unstable

and also the peptides that are release could become toxic and could lead the failure of the material. For potential *in vivo* applications as in tissue engineering, there will need to be a sufficient amount of T59 peptides for controlling and guiding specific cell interactions. Therefore, it will be necessary to use the quantification method developed to assess the extent of bound peptide after interaction in vivo for a specific time.

6.3.3 Use of phage display against other polymeric biomaterials

As mentioned previously, the goal of this dissertation was to evaluate the potential use phage display technology to surface functionalize a model biomaterial, PPyCl. The preliminary results suggest that a peptide that binds to a polymeric biomaterial can be selected using the biopanning process. To demonstrate the versatility of this method as a surface modification tool, it will be important to study other synthetic biomaterials such as poly(l-lactide) and poly(ethylene glycol), which could benefit from the point of developing cell-adhesion promoting surfaces. It is likely that the peptides selected may not permit the attachment of biomolecules for surface functionalization and other techniques such as plasma treatment or silanization may be more stable and robust. By evaluating more synthetic biomaterials and possibly other biological materials such as extra-cellular matrix components such as collagen, it may lead to a definite conclusion on the applicability of phage display technology for surface functionalization.

Bibliography

Adey NB, Mataragnon AH, Rider JE, Carter JM, Kay BK. Characterization of phage that bind plastic from phage-displayed random peptide libraries. *Gene* 1995;156:27-31.

Allison, D.P., Hinterdorfer, P. Han, W. Biomolecular force measurements and the atomic force microscope. *Curr. Opin. Biotech.* 2002;13:47-51.

Baker BM, Murphy KP. Dissecting the energetics of a protein-protein interaction: the binding of ovomucoid third domain to elastase. *J. Mol. Biol.* 1997;268(2);557-69.

Barltrop, J..A. et al. 5-(3-carboxymethoxyphenyl)-2-(4,5-dimethylthiazoly)-3-(4 sulfophenyl)tetrazolium, inner salt (MTS) and related analogs of 3-(4,5-dimethylthiazolyl)-2,5-diphenyltetrazolium bromide (MTT) reducing to purple water-soluble formazans as cell-viability indicators. *Bioorg. & Med. Chem. Lett.* 1991;1:611.

Barras FM, Pasche P, Bouche N, Aebischer P, Zurn AD. Glial cell line-derived neurotrophic factor released by synthetic guidance channels promotes facial nerve regeneration in the rat. *J Neurosci Res.* 2002;70:746-55.

Barry MA, Dower WJ, Johnston SA. Toward cell-targeting gene therapy vectors: selection of cell-binding peptides from random peptide-presenting phage librarie*s. Nature Medicin*e 1996;2:299-305.

Bell GI. Models for the specific adhesion of cells to cells. *Science* 1978;200:618-27.

Berglund J, Lindbladh C, Nicholls IA, Mosbach K. Selection of phage display combinatorial library peptides with affinity for a yohimbine imprinted methacrylate polymer. *Analytical Communications* 1998;35:3-7.

Binning G, Quate CF, Gerber C. Atomic force microscope *Phys. Rev. Lett.* 1986;56:930-933.

Boyle A, Genies E, Fouletier M. Electrochemical behaviour of polypyrrole films doped with ATP anions. *J Electroanal Chem* 1990;279:179-86.

Brown S, Sarikaya M, Johnson E. Genetic analysis of crystal growth. *J. Mol.Bio*l. 2000;299:725–32.

Brown S. Metal recognition by repeating polypeptides. *Nature Biotechnol.* 1997;15:269–72.

Bryant SJ, Bender RJ, Durand KL, Anseth KS. Encapsulating chondrocytes in degrading PEG hydrogels with high modulus: engineering gel structural changes to facilitate cartilaginous tissue production. Biotechnol Bioeng. 2004;30:747-55.

Cairns DB, Armes SP, Chehimi MM, Perruchot C, Delamer M. X-ray photoelectron specstroscopy characterization of submicrometer-sized polypyrrole-polystyrene composites. *Langmuir* 1999;15:8059-66.

Campbell TE, Hodgson AJ, Wallace GG. Incorporation of Erythrocytes into Polypyrrole to Form the Basis of a Biosensor to Screen for Rhesus (D) Blood Groups and Rhesus (D) Antibodies. *Electroanalysis* 1999;11:215-222.

Carrion-Vazquez M, Marszalek PE, Oberhauser AF, Fernandez JM. Atomic force microscopy captures length phenotypes in single proteins. *Proc. Natl. Acad. Sci. USA* 1999;96:11288-292.

Castano H, O'Rear EA, McFetridge PS, Sikavitsas VI. Polypyrrole thin films formed by admicellar polymerization support the osteogenic differentiation of mesenchymal stem cells. *Macromol Biosci* 2004;4:785-94.

Chen CS, Mrksich M, Suang S, Whitesides GM, Ingber, DE. Geometric control of cell life and death. Science 1997;276:1425-1528.

Chyla AT, Ryley S, Walton DJ, Liu X, Chetwynd, DG. Effect of dopant counter-anion on tribological properties of polypyrrole. *Adv Mat Opt Electron* 1998;8:87-91.

Clausen-Schaumann H, Rief M, Tolksdorf C, Gaub HE. Mechanical stability of single DNA molecules. *Biophys. J.* 2000;78:1997-2007.

Collier JH, Camp, JP, Hudson TW, Schmidt CE. Synthesis and characterization of polypyrrole-hyaluronic acid composite biomaterials for tissue engineering applications. *J. Biomed. Mater. Res,* 2000;50:574-84.

Cook AD, Pajvani UB, Hrkach JS, Cannizzaro SM, Langer R. Colorimetric analysis of surface reactive amino groups on poly(lactic acid-co-lysine):poly(lactic acid) blends. *Biomaterials* 1997;18(21):1417-24.

Cui X, Hetke JF, Wiler JA, Anderson DJ, Martin DC. Electrochemical deposition and characterization of conducting polymer polypyrrole/PSS on multichannel neural probes. *Sensors and Actuators A: Physical* 2001;93:8-18.

Cutright DE, Beasley JD, Perez B. Histologic comparison of polylactic and polyglycolic acid sutures. Oral Surg. 1971;32:165.

Dammer U, Hegner M, Anselmetti D, Wagner P, Dreier M, Huber W, Guntherodt HJ. Specific antigen/antibody interactions measured by force microscopy. *Biophys. J.* 1996;70:2437-41.

Das GS, Rao GH, Wilson RF, Chandy T. Colchicine encapsulation within poly(ethylene glycol)-coated poly(lactic acid)/poly(epsilon-caprolactone) microspheres-controlled release studies. Drug Deliv. 2000;7:129-38.

Devlin JJ, Panganiban LC, Devlin PE. Random peptide libraries: a source of specific protein binding molecule*s. Scienc*e 1990;249:404-6.

Diaz AF, Castillo JA, Logan JA, Lee WY. Electrochemistry of conductive polypyrrole films. *J Electroanal Chem* 1981;129:115–132.

Doorbar J, Winter G. Isolation of a peptide antagonist to the thrombin receptor using phage displa*y. J Mol Biol* 1994;244:361-9.

Evan E. Probing the relation between foce-liftime-and chemistry in single molecular bonds. *Annu. Rev. Biophys. Biomol. Struct*. 2001;30:105-28.

Evans E, Ritchie K. Dynamic strength of molecular adhesion bonds. *Biophys. J.* 1997;72:1541-55.

Evans GRD. Peripheral nerve injury: A review and approach to tissue engineering constructs. *The Anatomical Record.* 2001;263:396-404

Evans E. Introductory Lecture: Energy landscapes of biomolecular adhesion and receptor anchoring at interfaces explored with dynamic force spectroscopy. *Faraday Discuss* 1998;111:1-16.

Fine EG, Decosterd I, Papaloizos M, Zurn AD, Aebischer P. GDNF and NGF released by synthetic guidance channels support sciatic nerve regeneration across a long gap. *Eur J Neurosci.* 2002;15:589-601.

Fisher JP, Jo S, Mikos AG, Reddi AH. Thermoreversible hydrogel scaffolds for articular cartilage engineering. J Biomed Mater Res A. 2004;71:268-74.

Flynn CE, et al. Synthesis and organization of nanoscale II VI semiconductor materials using evolved peptide specificity and viral capsid assembly. *J Mater Chem* 2003;13:2414-21.

Furnish EJ, Schmidt, CE. Tissue engineering of the peripheral nervous system. In: Patrick CW Jr., editor. *Frontiers in Tissue Engineerin*g: New York; 1998.

Garner B, Georgevich B, Hodgson AJ, Liu L, Wallace GG. Polypyrrole-heparin composites as stimulus-responsive substrates for endothelial cell growth. *J Biomed Mater Res* 1999;44:121-29.

Gaskin DJH, Starck K, Vulfson EN. Identification of inorganic crystal-specific seqeunces using phage display combinatorial library of short peptides:A feasibility study. *Biotech. Lett.* 2000;22:1211–16.

Genies EM, Marchesiello M, Bidan G. Preparation and properties of polypyrrole made in the presence of biological buffers. *Electrochim Acta* 1992;37:1015-20.

George PM, Lyckman AW, LaVan DA, Hedge A, Leung, Y, Avasare R, et al. Fabrication and biocompatibility of polypyrrole implants suitable for neural prosthetics. *Biomaterials* 2005; 26:3511-19.

Gerard, M.; Chaubey, A.; Malhotra, B.D. *Biosensors & Bioelectronics* 2002;17:345-359.

Grandbois M, Beyer M, Rief M, Clausen-Schaumann H, Gaub HE. How strong is a covalent bond? *Science* 1999;283:1727-30.

Grubmuller H, Heymann B, Tavan P. Ligand binding: molecular mechanics calculation of the streptavidin-biotin rupture force. *Science* 1996;271:997-99.

Healy K. Molecular engineering of materials for bioeactivity. *Curr. Opn. Sol. Sta. & Mater. Sci*. 1999;4:381-387.

Healy KE, Rezania A, Stile RA. Designing biomaterials to direct biological responses. *Ann N Y Acad Sci* 1999;875:24-35.

Hersel, U., Dahmen, C., Kessler, H. RGD modified polymers: biomaterials for stimulated cell adhesion and beyond. *Biomaterials* 2003;24:4385-4415.

Hinterdorfer P, Gruber HJ, Schilcher K, Baumgartner W, Haselgruebler T, Schinler H. Antibody-antigen unbinding forces measured by force microscopy using antibodies bound to AFM tips via a specifically designed flexible crosslinker. *Biophys. J.* 1995;68:139a.

Hirano BY, Mooney DJ. Peptide and protein presenting materials for tissue engineering. *Advanced Materials* 2004;16(1):17-25.

Hoerstrup, SP, Lu L, Lysaght, MJ, Mikos AG, Rein D, Schoen FJ. Et al. Tissue engineering, In: Ratner BD, Hoffman AS, Schoen FJ, Lemons JE, editors. *Biomaterials science: an introduction to materials science in medicine*. 2004, Academic Press: Boston.

http://www.ptei.org/techniques.asp. (*accessed* March 2005).

Huang S, Ingber DE. Shape-dependent control of cell growth, differentiation, and apoptosis: switching between atractors in cell regulatory network. Exp Cell Res 2000;261:91-103.

Hudson T, Evans GR, Schmidt C. Engineering strategies for peripheral nerve repair. *Clinics in Plastic Surgery* 1999;*26*(4):617-28.

Ikada Y, Shikinami Y, Hara Y, Tagawa M, Fukada E. *Journal of Biomedical Materials Research* 1996;30:553-58.

Jiao YY, Ubrich N, Marchand-Arvier M, Vigneron C, Hoffman M, Maincent P. Preparation and in vitro evaluation of heparin-loaded polymeric nanoparticles. Drug Deliv. 2001;8:135-41.

Jozefonvicz J, Jozefowicz M. Review: Interactions of biospecific functional polymers with blood proteins and cells. *J. Biomater. Sci.: Polymer Ed.* 1990;1:147-65.

Kassim A, Basar ZB, Mahmud HNME. Effects of preparation temperature on the conductivity of polypyrrole conducting polymer. *Proc. Indian Acad. Sci*., 2002;114:155-62.

Kimura K, Yanagida Y, Haruyama T, Kobatake E, Aizawa M. Electrically induced neurite outgrowth of PC12 cells on the electrode surface. *Med Biol Eng Comput.* 1998;36:493-8

Konturri K, Pentti P, Sundholm G. Polypyrrole as a model membrane for drug delivery. *J Electroanal Chem* 1998;453:231-38.

Korri-Youssoufi, H.; Barnier, F.: Srivastava, P.; Godillot, P; Yassar, A. *J. Am. Chem. Soc.* 1997;119:7388-89.

Kotwal A.Schmidt CE. *Biomaterials* 2001;22:1055-64.

Kubies D, Rypacek F, Kovarova J, Lednicky F. Microdomain structure in polylactide-block-poly(ethylene oxide) copolymer films. *Biomaterials* 2000;21(5):529-36.

Langer R, Vacanti JP. Tissue engineering. *Science* 1993; 260:920-6.

Lanza RP. *Principles of tissue engineering.* 2000, Academic Press: San Diego.

Lee GU, Chris LA, Colton RJ. Direct measurement of the forces between complementary strands of DNA. *Science* 1994;266:771-73.

Lee GU, Kidwell DA, Colton RJ. Sensing discrete streptavidin-biotin interactions with atomic force microscopy. *Lanmuir* 1994;10:354-57.

Lee WS, Mao C, Flynn CE, Belcher AM. Ordering quantum dots using genetically engineered viruses. *Science* 2002;296:892–95.

Lévy, R., and M. Maaloum. Measuring the spring constant of atomic force microscope cantilevers: thermal fluctuations and other methods. *Nanotechnology* 2002;13:33-37.

Li H, Rief M, Oesterhelt F, Gaub HE. Single-molecule force spectroscopy on xanthan by AFM. *Adv. Materials* 1998;10:316-19.

Li HC, Khor E. A collagen-polypyrrole hybrid: influence of 3-butanesulfonate substitution. *Macromol. Chem. Phys.* 1995;196;1801-12.

Li LH, Kong YM, Kim HW, Kim YW, Kim HE, Heo SJ, Koak JY. Improved biological performance of Ti implants due to surface modification by micro-arc oxidation. *Biomaterials*. 2004;25:2867-75.

Makowski M, Chmurzynski L. Ab initio study of the energetics of molecular heteroconjugation reactions in systems modeling side chains of biomolecules. *Theochem* 2004;672:183-190.

Mao C, *et al.* Viral assembly of oriented quantum dot nanowires. *Proc Natl Acad Sci* 2003;12: 6946-51.

Mao C, Zhu JJ, Hu YF, Ma QQ, Qiu YZ, Zhu AP, Zhao WB, Shen J. Surface modification using photocrosslinkable chitosan for improving hemocompatibility. Colloids Surf B Biointerfaces. 2004;10:47-53.

Massia, S.P., Hubbel, J.A. Covalently attached GRGD on polymer surfaces promotes biospecific adhesion of mammalian cells. *Ann. N.Y. Acad. Sci.* 1988;589:261-70.

Merkel R, Nassoy P, Leung A, Ritchie K, Evans E. Energy landscapes of receptor-ligand bonds explored with dynamic force spectroscopy. *Nature* 1999;397:50-53.

Mori T. Cancer-specific ligands identified from screening of peptide-display libraries. *Curr. Pharm. Des.* 2004;19:2335-43.

Mousa WF, Kobayashi M, Shinzato S, Kamimura M, Neo M, Yoshihara S, Nakamura T. Biological and mechanical properties of PMMA-based bioactive bone cements.*Biomaterials* 2000;21:2137-46.

Moy VT, Florin EL, Gaub HE. Intermolecular forces and energies between ligands and receptors. *Science* 1994;266:257-59.

Naik RR, Brott L, Carlson SJ, Stone MO. Silica precipitating peptides isolated from a combinatorial phage display libraries. *J. Nanosci. Nanotechno*l. 2002;2:1–6.

Naik, R. R., Stringer, S. J, Agarwal, G., Jones, S. E. & Stone, M. O. Biomimetic synthesis and patterning of silver nanoparticles. *Nature Mater.* 2002;1:169–72.

Nakamura, C. et al. Mechanical force analysis of peptide interactions using atomic force microscopy. *Biopoly. (Peptide Sci.)* 2004;76:48-54.

Parmley SF, Smith GP. Antibody-selectable filamentous fd phage vectors: affinity purification of target gene*s. Gen*e 1988;73:305-18.

Pernaut, J.M.; Reynolds, J. R. *Journal of Physical Chemistry B* 2000;104:4080-90.

Pfluger P, Krounbi M, Street GB, Weiser G. The chemical and physical properties of pyrrole-based conducting polymers: the oxidation of neutral polypyrrole. *Journal of Chemical Physics* 1983;78:3212-18.

Ph.D.^{TM} Phage Display Peptide Library Kits; Technical Bulletin E8100, E8110, E8120; New England Biolabs: Cambridge MA, 2004; 1-4.

Pierschbacher, M.D., Ruoslahti, E. Cell attachment activity of fibronectin can be duplicated by small synthetic fragments of the molecule. *Nature* 1984;309:30-33.

Pires NM, van der Hoeven BL, de Vries MR, Havekes LM, van Vlijmen BJ, Hennink WE, Quax PH, Jukema JW. Local perivascular delivery of anti-restenotic agents from a drug-eluting poly(epsilon-caprolactone) stent cuff. Biomaterials. 2005;26:5386-94.

Prabhu S, Sullivan JL, Betageri GV. Comparative assessment of in vitro release kinetics of calcitonin polypeptide from biodegradable microspheres. Drug Deliv. 2002;9:195-8.

Prezyna LA, Qiu Y-J, Reynolds JR, Wnek GE. Interaction of cationic polypeptides with electroactive polypyrrole/poly(styrenesulfonate) and poly(N-methylpyrrole)/ poly(styrenesulfonate) films. *Macromolecules* 1991;24:5283-87.

Queiroz AC, Santos JD, Vilar R, Eugenio S, Monteiro FJ. Laser surface modification of hydroxyapatite and glass-reinforced hydroxyapatite. *Biomaterials* 2004;25:4607-14.

Quirk R, Chan W, Davies M, Tendler S, Shakesheff K. Poly(L-lysine)- GRGDS as a biomimetic surface modifier for poly(lactic acid). *Biomaterials* 2001;22:865-72.

Rakovic D. Structure and properties of conducting polymers. *Mat Sci Forum* 1996;214:139-146.

Ratner BD. Surface modification of polymers: chemical, biological and surface analytical challenges. *Biosensors & Bioelectronics* 1995;10:797-804.

Ratner BD, Bryant SJ. Biomaterials: where we have been and where we are going. *Annu Rev Biomed Eng* 2004;6:41-75.

Ratner, B.D., Castner, D.G. Electron spectroscopy for chemical analysis. In: Vickerman, J.C., editor. *Surface analysis: the principle techniques*: New York; 1997.

Ratner BD, Hoffman AS, Schoen FJ, Lemons JE. *Biomaterials science: an introduction to materials science in medicine*. 2004, Academic Press: Boston.

Rief J, Fernandez JM, Gaub HE. Elastically coupled two-level systems as a model for biopolymer extensibility. *Phys. Rev. Lett.* 1998;81:4764-67.

Rief M, Gautel M, Schemmel A, Gaub HE. The mechanical stability of immunoglobulin and fibronectin III domains in the muscle protein titin measured by atomic force microscopy. *Biophys. J.* 1998;75:3008-14.

Rivers TJ, Hudson TW, Schmidt CE. Synthesis of a novel, biodegradable electrically conducting polymer for biomedical applications. *Advanced Functional Materials* 2002;12:33-7.

Rowley MJ, O'connor K, Wijeyewickrema L. Phage display for epitope determination: A paradigm for identifying receptor-ligand interactions. *Biotechnol. Annu. Rev.* 2004;10:151-88.

Sahota TS, Latham RK, Linford RG, Taylor PM. *Drug Development and Industrial Pharmacy* 2000;26:1039-44.

Saltzman MW. *Tissue engineering: principles for the design of replacement organs and tissues*. 2004, Oxford University Press: New York.

Sanghvi AB, Murray JL, Schmidt CE. Tissue engineering of peripheral nerve. In: Wnek GE, Bowlin, GL., editors. *Encyclopedia of biomaterials and biomedical engineering*: New York: 2004.

Sano K, Shiba K. A hexapeptide motif that electrostatically binds to the surface of titanium. J *Am Chem Soc* 2003;125: 14234-35.

Sano K, Shiba K. A hexapeptide motif that electrostatically binds to the surface of titanium. J. *Am. Chem. Soc.* 2003;125:14234-35.

Sarikaya M, Tamerler C, Jen AK, Schulten K, Baneyx F. Molecular biomimetics: nanotechnology through biology. *Nat. Mater*. 2003;2:577-85.

Sarikaya M, Tamerler C, Schwartz DT, Baneyx F. Materials assembly and formation using engineered polypeptides *Annu Rev Mater Res* 2004;34:373–408.

Scembri MA, Kjaergaard K, Klemm P. Bioaccumulation of heavy metals by fimbrial designer adhesions. *FEMS Microbial. Lett.* 1999;170:363–71.

Schmidt CE, Shastri VR, Vacanti JP, Langer R. Stimulation of neurite outgrowth using an electrically conducting polymer. *Proc Nat Acad Sci US*A 1997;94(17):8948-53.

Schwesinger F, Ros R, Strunz T, Anselmetti D, Guntherodt HJ, et al. Unbinding forces of single antibody-antigen complexes correlate with their thermal dissociation rates. *PNAS* 2000;97:9972-77.

Scott JK, Hoess R, Jackson S, Degrado W. Bioactive peptides identification by panning against immobilized purified receptors. *Proc Natl Acad Sci* 1992;89:5398-5402.

Seal BL, Otero TC, Panitch A. Review: polymeric biomaterials for tissue and organ regeneration. *Materials Science and Engr*. 2001;34:147-230.

Shakesheff K, Cannizzaro S, Langer R. Creating biomimetic micro-environments with synthetic polymer-peptide hybrid molecules. *J Biomater Sci Polym Ed* 1998;9:507-18.

Sheu MS, Hoffman AS, Feijen J. A glow discharge process to immobilize PEO/PPO surfactants for wettable and nonfouling biomaterials. J. Adhes. Sci. Technol. 1992;6:995-1101.

Siegers C, Biesalski M, Haag R. Self-assembled monolayers of dendritic polyglycerol derivatives on gold that resist the adsorption of proteins. Chemistry. 2004;10:2831-8.

Silk T, Hong Q, Tamm J, Compton RG. AFM studies of polypyrrole film surface morphology I. The influence of film thickness and dopant nature. *Syn Metals* 1998;93:59-64.

Silk T, Tamm J. Voltammetric study of the influence of cations on the redox-switching process of halogenide-doped polypyrrole. *Electrochimica Acta.*1996;41:1883-85.

Silk, T., Hong, Q., Tamm, J. & Compton, R.G. AFM studies of polypyrrole film surface morphology II. Roughness characterization by the fractal dimension analysis. *Syn. Met.* 1998;93:65-71.

Skotheim TA. Editor, The Handbook of Conducting Polymers, vol 1. Marcel Dekker, New York (1986).

Smith MM, Shi L, Navre M. Rapid identification of highly active and selective substrates for stromelysin and matrilysin using bacteriophage peptide display libraries. *J Biol Chem* 1995;270:6440-9.

Strunz T, Oroszlan K, Schafer R, Guntherodt HJ. Dynamic force spectroscopy of single DNA molecules. *Proc. Natl. Acad. Sci. USA* 1999;96:11277-282.

Suh KY, Seong J, Khademhosseini A, Laibinis PE, Langer R. A simple soft lithographic route to fabrication of poly(ethylene glycol) microstructures for protein and cell patterning.Biomaterials. 2004;25:557-63.

Supronowicz PR, Ajayau PM, Ullmann, K. R.; Arulanandam, B. P.; Metzger, D. W.; Bizios, R. *Journal of Biomedical Materials Research* 2002;59:499-506.

Tamm J, Hallik A, Alumaa A, Sammelselg V. Electrochemical properties of polypyrrole/sulphate films. *Electrochimica Acta.* 1997;42:2929-34.

Tong YW, Shoichet MS. Peptide surface modification of poly(tetrafluoroethylene-co-hexafluoropropylene) enhances its interaction with central nervous system neurons. *J Biomed Mat Res* 1998;42(1):85-95.

Undenfriend, S., Stein, S., Bohlen, P., Dairman, W. Fluorescamine: A reagent for assay of amino acids, peptides, proteins, and primary amines in the picomole range. *Science* 1972;172:871-72.

Valentini RF, Vargo TG, Gardella JA, Aebischer P. Electrically conductive polymeric susbtrates enhance nerve fibre outgrowth in vitro. *Biomaterials* 1992;13:183-190.

Vidal JC, Garcia E, Castillo JR. In situ preparation of a cholesterol biosensor: entrapment of cholesterol oxidase in an overoxidized polypyrrole film electrodeposited in a flow system: Determination of total cholesterol in serum. *Anal. Chim. Acta.* 1999;385:213-222.

Vork FTA, Schuermans BCAM, Barendrecht E. Influence of inserted anions on the properties of polypyrrole. *Electrochim. Acta.* 1990;35:567-75.

Wang LF, Wei YH, Chen KY, Lin JC, Kuo JF. Properties of phospholipid monolayer deposited on a fluorinated polyurethane. J Biomater Sci Polym Ed. 2004;15:957-69.

Wang X, Gu X, Yuan C, Chen S, Zhang P, Zhang T, Yao J, Chen F, Chen G. Evaluation of biocompatibility of polypyrrole in vitro and in vivo. *J Biomed Mater Res A.* 2004;68:411-22.

Whaley SR, English DS, Hu EL, Barbara PF, Belcher AM. Selection of peptides with semiconductor binding specificity for directed nanocrystal assembly. *Nature* 2000;405:665-68.

Willemsen OH, Snel MME, van der Werf KO, de Grooth BG, Greve J, Hinterdorfer P, et al. Simultaneous height and adhesion imaging of antibody-antigen interactions by atomic force microscopy. *Biophys. J.* 1998;75:2220-228.

Wong JY, Langer R, Ingber DE. Electrically conducting polymers can noninvasively control the shape and growth of mammalian cells. *Proc Natl Acad Sci U S A.* 1994;91:3201-4.

Xiao SJ, Textor M, Spencer N. Covalent attachment of cell-adhesive, (Arg-Gly Asp)-containing peptides to titanium surfaces. *Langmuir* 2000;14(19):5507-16.

Yang G, Cecconi C, Baase WA, Vetter IR, Breyer WA, Haack JA, et al. Solid-state synthesis and mechanical unfolding of polymers of T4 lysozyme. *Proc. Natl. Acad. Sci. USA* 2000;97:139-44.

Yang J, Marin DC. *Sensors and Actuators* 2004;113:204-211.

Yuan C, Chen A, Kolb P, Moy VT. Energy landscape of streptavidin-biotin complexes measured by atomic force microscopy. *Biochemistry* 2000;39:10219-23.

Zhang S, Altman M. Peptide self-assembly in functional polymer science and engineering. *Reac & Func Polym* 1999;41:91-102.

Zhang T, Gu M, Yu X. Degradation and drug delivery properties of poly(1,4-cyclohexanedicarboxylicanhydride). J Biomater Sci Polym Ed. 2001;12:491-501.

Vita

Archit Bharat Sanghvi was born to Bharat Shantilal Sanghvi and Kanchan Bharat Sanghvi in Naroda, Ahmedabad, India on February 13, 1978. The family, including his younger sister, Mitali Sanghvi, immigrated to the United States in 1988. He received his high school degree from Osbourn High School in Manassas, Virginia. From 1996-2000, Archit attended the University of Virginia in Charlottesville, Virginia, where he received his undergraduate bachelor's in Engineering Science with a concentration in Biomedical Engineering. The interest in biomedical engineering was initiated during his undergraduate career where he completed three summer internships at the National Institutes of Health and took various classes in biomaterials and tissue engineering.

For his doctoral studies in Biomedical Engineering, Archit attended the University of Texas at Austin, Austin, Texas from 2000-2005. During this time, he completed his Master's degree in Biomedical Engineering (2003) and with an initial research experience with Microfab Technologies Inc. in Plano Texas, where he worked with David Silva and Dr. Donald Hayes. Archit presented his research at various annual meetings including Materials Research Society and the Biomedical Engineering Society. Archit wrote two first-author publications and was a contributor to two other articles. During the year of 2003, Archit met his wife, Meera Sanghvi, who was an undergraduate student at the University of Texas at Austin.

Permanent Address: 3010 Heathmount Dr. Cedar Park, Texas 78613

This dissertation was typed by the author.